

# Koopman Operators with Intrinsic Observables in Rigged Reproducing Kernel Hilbert Spaces

Isao Ishikawa<sup>\*1,3</sup>, Yuka Hashimoto<sup>†2,3</sup>, Masahiro Ikeda<sup>‡3</sup>, and Yoshinobu Kawahara<sup>§4,3</sup>

<sup>1</sup>Ehime University

<sup>2</sup>NTT Corporation

<sup>3</sup>RIKEN

<sup>4</sup>Osaka University

## Abstract

This paper presents a novel approach for estimating the Koopman operator defined on a reproducing kernel Hilbert space (RKHS) and its spectra. We propose an estimation method, what we call *Jet Dynamic Mode Decomposition (JetDMD)*, leveraging the intrinsic structure of RKHS and the geometric notion known as jets to enhance the estimation of the Koopman operator. This method refines the traditional Extended Dynamic Mode Decomposition (EDMD) in accuracy, especially in the numerical estimation of eigenvalues. This paper proves JetDMD’s superiority through explicit error bounds and convergence rate for special positive definite kernels, offering a solid theoretical foundation for its performance. We also delve into the spectral analysis of the Koopman operator, proposing the notion of extended Koopman operator within a framework of rigged Hilbert space. This notion leads to a deeper understanding of estimated Koopman eigenfunctions and capturing them outside the original function space. Through the theory of rigged Hilbert space, our study provides a principled methodology to analyze the estimated spectrum and eigenfunctions of Koopman operators, and enables eigendecomposition within a rigged RKHS. We also propose a new effective method for reconstructing the dynamical system from temporally-sampled trajectory data of the dynamical system with solid theoretical guarantee. We conduct several numerical simulations using the van der Pol oscillator, the Duffing oscillator, the Hénon map, and the Lorenz attractor, and illustrate the performance of JetDMD with clear numerical computations of eigenvalues and accurate predictions of the dynamical systems.

**Keywords**— Koopman operator, composition operator, dynamical system, dynamic mode decomposition, Gelfand triple, rigged Hilbert space, reproducing kernel Hilbert space

## 1 Introduction

The Koopman operator is “linearization” of a dynamical system introduced in [43] for analyzing a nonlinear dynamical system as a linear transform on a function space. In recent years, Koopman operator has significantly

---

\*ishikawa.isao.zx@ehime-u.ac.jp

†yuka.hashimoto@ntt.com

‡masahiro.ikeda@riken.jp

§kawahara@ist.osaka-u.ac.jp

evolved as a method in the data-driven analysis of dynamical system, pioneered by [52, 55] (see [11] for the recent review). The Koopman operator is also known as the *composition operator* and has developed at the interface of operator theory and analytic function theory, originated from [62, 58]. Over the past few decades, research has spanned various fields in analysis in mathematics, including real analysis, complex analysis, and harmonic analysis.

Dynamic Mode Decomposition (DMD) has been actively studied as a data-driven estimation method for the Koopman operator. DMD is originally introduced as a numerical method to factorize a complex dynamics into the simple and essential components in fluid dynamics [64, 65], and then has been discussed about the connection with the Koopman operator [61]. Since DMD can be considered as a finite-dimensional approximation of the Koopman operator, linear algebraic operations such as eigendecomposition of the approximation matrix enable the decomposition of a dynamical system into sums of simple components and the extraction of an essential component governing its complex behavior. As a result, DMD and Koopman analysis have been attracting attention in recent years as a data-driven analysis method for dynamical systems, leading to a vast number of applications across a wide range of fields, for example, fluid dynamics [25, 65, 61, 53], epidemiology [60], neuroscience [10, 2], plasma physics [76, 37], quantum physics [39], finance [46], robotics [4, 1, 9, 8], the power grid [70, 69], and machine learning [38, 74, 75, 73, 72, 45, 5, 51, 59, 24]. See [66] for recent overview of variants of DMD.

Among the many extensions of DMD, Extended DMD (EDMD) [77] is known as one of the most general and basic extensions of DMD and provides a foundation for various DMD-based methods. EDMD can be described as a method for estimating the Koopman operator based on a set of observables with trajectory data from a dynamical system, and the Koopman operator is approximated through simple linear algebraic operations using the observables and the trajectory data. Here, it is important to note that, in estimating the Koopman operator, at least implicitly, one function space containing the observables is fixed, and the Koopman operator is considered to be defined on the fixed function space.

A problem lies in the fact that, for a given set of observables, there may exist (infinitely) many function spaces that can include these observables, while the mathematical properties of the Koopman operator can drastically differ depending on the function space where it acts. For example, on  $L^2$ -spaces with invariant measures, that act as unitary operators, whereas on other spaces, that might not even be bounded operators. As mentioned above, the Koopman operator has been extensively studied in mathematical literature. For example, there exist many studies on the operators' fundamental properties such as boundedness (see, for example, [80, 17, 35, 36, 68] and references therein). These studies also have shown that the properties of Koopman operators drastically change depending on the choice of function spaces. That is, EDMD actually capture information of the Koopman operator on a specific function space determined by the chosen observables. This problem is continuous with the major challenges faced by DMD-based methods, such as spectral pollution, invariant subspaces, continuous spectrum, and the treatment of chaotic dynamics, as mentioned in [15, 16]. Therefore, we require a detailed analysis of both observables and function spaces. However, in previous studies, the relationship between observables and function spaces has not been sufficiently discussed.

In this paper, we focus on the Koopman operator defined on a reproducing kernel Hilbert space (RKHS) and propose a fundamental solution to the significant challenge on the estimation of the Koopman operator by mathematically analyzing the relationship between the function spaces and observables. An RKHS is formally defined as a Hilbert space composed of functions where any point evaluation is a continuous linear functional. RKHS provides a general and effective theoretical framework through functional analysis, establishing a solid field in mathematics [63] and machine learning [31], with applications for various problems within each domain. The Koopman operator on RKHS has been studied in complex analysis, and rapidly developed and extended in machine learning and data analysis in recent years [38, 28, 18, 40, 27, 34, 29, 45, 5, 51, 59, 21].

The core notion we introduced is the space of *intrinsic observables* for estimating the Koopman operator in RKHS, constructed utilizing a geometric structure called jet on a fixed point of the dynamical system. Jet is a geometric formulation of the Taylor expansion, providing a geometrically canonical object on a manifold as a higher-order counterpart of the tangent bundle (see, for example, [41, Section 4]).

Leveraging the intrinsic observables, we propose a new estimation method, referred to as *Jet Dynamic Mode Decomposition (JetDMD)*, that provides refinement of a special class of EDMDs, such as EDMD with monomials, and significantly improves the estimation performance of the Koopman operator (see also Section 7

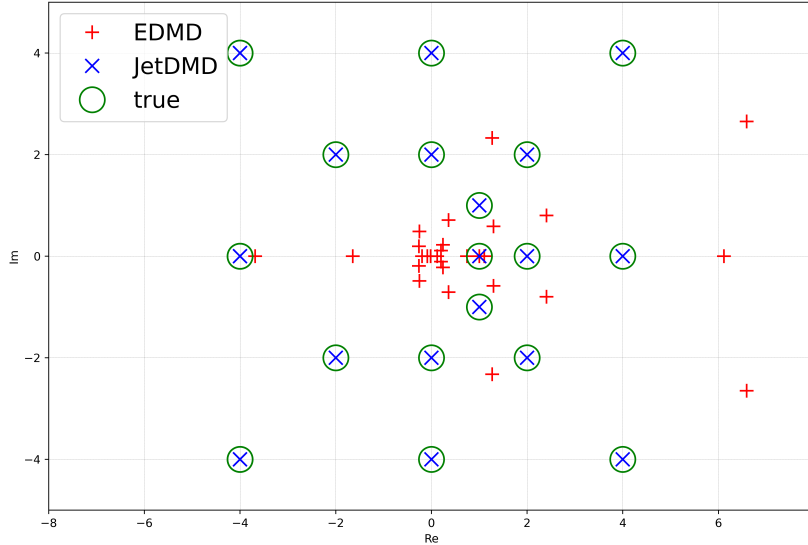


Figure 1: The comparison of the computed eigenvalues of the dynamical system  $f(x,y) := (x^2 - y^2 + x - y, 2xy + x + y)$  on  $\mathbb{R}^2$  using data of 100 pairs of sample from the uniform distribution on  $[-1, 1]^2$  and their images under  $f$ . The red +’s indicate the eigenvalues computed via EDMD using monomials of degree up to 10. The blue x’s indicate the estimated eigenvalues with JetDMD. The green circles indicate set  $\{\lambda_+^m \lambda_-^n\}_{m+n \leq 5}$ , where  $\lambda_{\pm} = 1 \pm i$  are the eigenvalues of the Jacobian matrix of  $f$  at the origin.

for its detailed algorithms and numerical results). For instance, JetDMD provides much more precise depiction in numerical estimation of eigenvalues than EDMD as shown in Figure 1. It is also noteworthy that we obtain a new interpretation of EDMD within the framework of JetDMD. For example, EDMD using monomials can be rephrased as “JetDMD without truncation using an exponential kernel for a dynamical system with a fixed point at the origin.”

Furthermore, we elucidate the mathematical machinery behind the performance of JetDMD as described in Figure 1. In fact, the superior performance of JetDMD is achieved through the surprisingly simple operation of the “truncation to a leading principal submatrix”, and our paper clarifies the reason why this works. We provide an explicit error bound for JetDMD, and for the Gaussian kernel and the exponential kernel, we prove the convergence of JetDMD with explicit convergence rate. As a result, we show that eigenvalues and eigenvectors estimated by JetDMD actually converge to the corresponding theoretical counterparts. It implies that JetDMD provides an alternative solution for the spectral pollution that always appears in the estimation the Koopman operator. We also emphasize that we do not impose the boundedness of the Koopman operator, and our proofs are based on a detailed mathematical analysis in RKHS. Although some convergence results for EDMD proved in [44], their results do not cover ours because they essentially impose the boundedness on the Koopman operator and basically obtain a weak convergence of eigenvectors and eigenvalues.

In addition, JetDMD provides a novel interpretation for the “Koopman eigenfunctions” estimated using observables and rigorous eigendecomposition of the “extended” Koopman operator. In DMD-based methods including EDMD, the interpretation of the estimated eigenvalues and eigenfunctions has always been a significant issue, and it is essential element in extracting quantitative information from complex and chaotic dynamical systems. When the Koopman operator does not preserve the space of observables, the question of what the eigenfunctions estimated by EDMD represent has always been a problem. As an answer to this problem, we show that the “Koopman eigenfunctions” generally exist outside the function space and that the space to which they truly belong can be captured using the theory of rigged Hilbert space. The rigged Hilbert space is defined as a Hilbert space equipped with a dense linear subspace with a finer topology and embedded into the dual

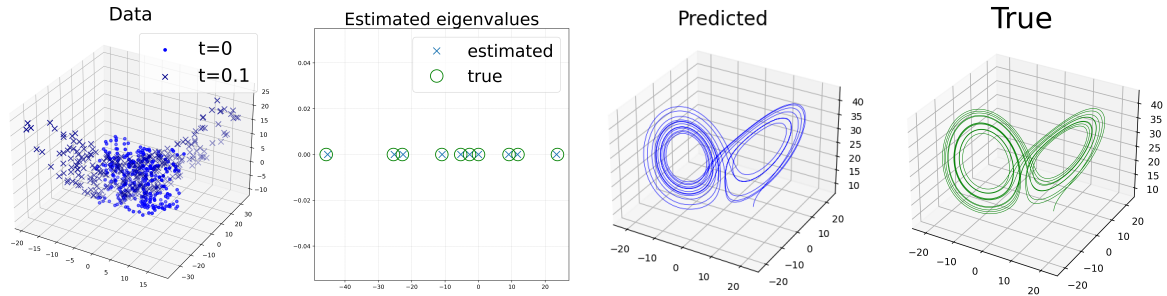


Figure 2: Illustration of the data-driven reconstruction of the Lorenz system with Algorithm 7, corresponding to the right images of Figure 16. The leftmost figure illustrates the data used for estimation, that is composed of the pairs of 300 samples from the uniform distribution on  $[-10, 10]^3$  and their images under the flow map at time 0.1. The left-center figure shows the estimated and theoretical eigenvalues of the generator of the Koopman operator. The center-right is the trajectory of the dynamical system reconstructed by our method, and the rightmost figure is the true trajectory.

space of the dense subspace. The triple composed of the Hilbert space, the dense linear subspace, and its dual space is referred to the Gelfand triple. For more detail of the accurate formulation and application, see Section 4, [6, 13, 22, 23, 14] and references therein.

More precisely, we show that JetDMD actually approximates the “extended” Koopman operator, not Koopman operator itself, in the rigged RKHS defined by a Gelfand triple constructed from the space of intrinsic observables and its dual space. This “extended” Koopman operator is defined as the dual operator of the Perron-Frobenius operator on the space of the observables, inducing a continuous linear map on a linear topological space (not function space) that includes the original RKHS, and its eigenvectors are not necessarily functions. Our framework provides a theoretical methodology to deal with the estimated “Koopman eigenfunctions” using the observables as the approximation of the eigenvector of the “extended” Koopman operator in the rigged RKHS whether Koopman operator preserves the space of observables or not. We also note that considering the Koopman operators as the dual of Perron-Frobenius operator also appears in [67] and they have rigorous convergence result for EDMD for analytic maps on the circle. Although the spectrum of the original Koopman operator on RKHS is quite complicated and can include continuous spectrum, the spectrum of the “extended” Koopman operator is much simpler and clearer, and it is possible to prove the Jordan-Chevalley decomposition and the eigendecomposition of the “extended” Koopman operator in the dual space of the observables. Therefore, our framework provides a effective approach to analyze the estimated eigenvectors and the spectrum of the Koopman operators via the theory of rigged Hilbert space.

As an application of JetDMD, we propose a method for reconstructing the original dynamical system from temporally-sampled trajectory data or vector field data of the dynamical system. As shown in Figure 2, our method is capable of accurately reconstructing the chaotic system such as the Lorenz attractor from temporally-sampled trajectory data. Our method also significantly generalizes the lifting method proposed in [48] based on JetDMD, and we theoretically prove the reconstruction capability of a broad class of analytic dynamical systems with arbitrary precision if we have sufficient number of samples and computational resources.

The structure of this paper is as follows: In Section 2, we introduce the notion of jet, construct the canonical invariant subspaces in RKHS, and prove their basic properties. In Section 3, we provide several theoretical results for data-driven estimation of Perron-Frobenius operator and show the error bound in the general setting. In Section 4, we introduce the notion of Gelfand triple and rigged Hilbert space. We define the extended Koopman operator  $C_f^\times$  and prove the Jordan-Chevalley decomposition of the extended Koopman operator. We also show the eigendecomposition of the extended Koopman operator under mild condition. In Section 5, we provide the framework for estimating the generator of the Koopman operator using discrete data of vector fields. We also show the corresponding result for continuous dynamical systems to those in the previous sections. In Section 6, we focus on the specific positive definite kernel, the Gaussian kernel and exponential kernel,

respectively. We provide sufficient conditions for the technical assumptions for the convergence results in the previous sections, and we also present more explicit error bounds. In Section 7, we propose JetDMD and provide its algorithm and perform numerical simulations. We illustrate the estimated eigenvalues for the van der Pol oscillator, the Duffing oscillator, and Hénon map, and depict the approximated eigenfunctions of the extended Koopman operators. Furthermore, we describe an application of JetDMD for data-driven reconstruction of dynamical systems. We also provide the theoretical guarantee of the algorithms as well and include discussion on the comparison of JetDMD with other popular methods, EDMD and Kernel DMD.

## 1.1 Notation

We denote the set of the real (resp. complex) numbers by  $\mathbb{R}$  (resp.  $\mathbb{C}$ ). We denote by  $i \in \mathbb{C}$  the imaginary unit. We denote the set of integers by  $\mathbb{Z}$ . For any subset of  $S \subset \mathbb{R}$ , we denote by  $S_{>0}$  (resp.  $S_{\geq 0}$ ) the set of positive (resp. non-negative) elements of  $S$ . We denote by  $\partial_{x_j}$  the partial derivative with respect to the  $j$ -th variable of a differentiable function on an open set of  $\mathbb{R}^d$ . We denote by  $dx$  the Lebesgue measure on  $\mathbb{R}^d$ .

We denote by  $\mathbb{R}^{m \times n}$  (resp.  $\mathbb{C}^{m \times n}$ ) the set of real (resp. complex)  $m \times n$  matrices. We define the Frobenius norm and the operator norm of the matrix as  $\|\cdot\|$  and  $\|\cdot\|_{\text{op}}$ , respectively. We usually regard  $x \in \mathbb{C}^d$  as an element of  $\mathbb{C}^{d \times 1}$  and describe the Euclidean norm by  $\|x\|$ . We always use the bold uppercase letters to describe the matrices, like  $\mathbf{A}$ ,  $\mathbf{B}$ ,  $\mathbf{C}$ . For a matrix  $\mathbf{A}$ , we denote the transpose (resp. adjoint) matrix of  $\mathbf{A}$  by  $\mathbf{A}^\top$  (resp.  $\mathbf{A}^* := \overline{\mathbf{A}}^\top$ ). We denote the identity matrix and the zero matrix of size  $n$  by  $\mathbf{I}_n$  and  $\mathbf{O}_n$ , respectively.

For any subset  $S \subset V$  of a complex vector space  $V$ , we denote by  $\text{span}(S)$  the linear subspace generated by  $S$ .

For a function  $h : X \rightarrow \mathbb{C}$  on a topological space  $X$ , we define  $\text{supp}(h)$  the closure of the set  $\{x \in X : h(x) \neq 0\}$ .

We basically use the multi-index notation. For example, for  $\alpha = (\alpha_1, \dots, \alpha_d) \in \mathbb{Z}_{\geq 0}^d$  and  $z = (z_1, \dots, z_d) \in \mathbb{C}^d$ , we write  $z^\alpha := z_1^{\alpha_1} \dots z_d^{\alpha_d}$ . We also define  $|\alpha| := \sum_{i=1}^d \alpha_i$ ,  $\partial_x^\alpha := \partial_{x_1}^{\alpha_1} \dots \partial_{x_d}^{\alpha_d}$ , and  $\alpha! := \prod_{i=1}^d \alpha_i!$  for  $\alpha = (\alpha_1, \dots, \alpha_d) \in \mathbb{Z}_{\geq 0}^d$ .

For an open subset  $\Omega \subset \mathbb{R}^d$ , we denote by  $\mathcal{E}(\Omega)$  (resp.  $\mathfrak{H}(\Omega)$ ) the space of  $\mathbb{C}$ -valued infinitely differentiable functions (resp. real analytic functions) on  $\Omega$ . The topology of  $\mathcal{E}(\Omega)$  is the uniform convergence topology of the higher derivatives on the compact subsets (see [79, p.26–27]). The topology of  $\mathfrak{H}(\Omega)$  is the inductive limit topology of  $\varinjlim \mathfrak{H}(U)$ . Here, we denote by  $\mathfrak{H}(U)$  the space of holomorphic function on an open subset  $U \subset \mathbb{C}^d$ , equipped with the uniform convergence topology on the compact subsets, and  $\mathfrak{H}(U)$ 's constitute the inductive system via the restriction maps and  $U$  varies over the open subset of  $\mathbb{C}^d$  such that  $U \cap \mathbb{R} = \Omega$  (see [47] for details).

For a topological vector space  $V$ , we denote the dual space with the strong topology by  $V'$ . For  $\mu \in V'$  and  $h \in V$ , we denote  $\mu(h)$  by  $\langle \mu | h \rangle$ . For a continuous linear map  $L : V_1 \rightarrow V_2$  between topological vector spaces  $V_1$  and  $V_2$ , we denote by  $L'$  the dual linear operator  $L' : V_2' \rightarrow V_1'$ .

For a set  $X$  and  $a, b \in X$ , we define the Kronecker delta by

$$\delta_{a,b} = \begin{cases} 1 & \text{if } a = b, \\ 0 & \text{otherwise.} \end{cases}$$

For a family of real number  $\{a_\lambda\}_{\lambda \in \Lambda}$ , we denote by  $a_\lambda \lesssim b_\lambda$  if there exists  $C > 0$  independent of  $\lambda \in \Lambda$  such that  $a_\lambda \leq C b_\lambda$  for all  $n$ .

## 1.2 Summary of main results and their implications

In the following, we overview our main results for the convenience of the readers. We introduce minimal notation and describe the essence of our main results. Here, although we only consider the discrete dynamical system, we have corresponding results to the continuous dynamical system, and provide a theoretical framework for estimating the generator using discrete data of vector fields. See Section 5 for details. We will use notation described in Section 1.1.

Let  $\Omega \subset \mathbb{R}^d$  be a connected open subset and let  $p \in \Omega$ . Let  $f : \Omega \rightarrow \Omega$  be a map of class  $C^\infty$ . Let  $\lambda_1, \dots, \lambda_d$  be the eigenvalues (with multiplicity) of the Jacobian matrix  $df_p$  at  $p$  and let  $\lambda = (\lambda_1, \dots, \lambda_d)$ . In this paper, as the function space where the Koopman operator acts, we always consider the RKHS  $H$  associated with a positive definite kernel  $k : \Omega \times \Omega \rightarrow \mathbb{C}$  of class  $C^\infty$ . Readers should refer to, for example, [63] for the general theory of RKHS.

**Example 1.1.** Let  $\Omega = \mathbb{R}^d$  and  $k(x, y) = e^{x^\top y}$ , the RKHS  $H$  associated with  $k$  is explicitly described as follows:

$$H = \left\{ h|_{\mathbb{R}^d} : h \text{ is holomorphic on } \mathbb{C}^d \text{ and } \int_{\mathbb{R}^d \times \mathbb{R}^d} |h(x + yi)|^2 e^{-\|x\|^2 - \|y\|^2} dx dy < \infty \right\}.$$

This space is usually called the Fock space [81] and recently treated in the context of the Koopman operator [54].

We define the *Koopman operator*  $C_f : H \rightarrow H$  by the linear operator defined by  $C_f h := h \circ f$  with domain  $D(C_f) := \{h \in H : h \circ f \in H\}$ . We assume that  $C_f$  is densely defined on  $H$ , namely,  $D(C_f)$  is a dense subspace of  $H$ . We denote the Perron–Frobenius operator, that is the adjoint operator of  $C_f$ , by  $C_f^*$ .

An important fact here is that the RKHS associated with the positive definite kernel  $k$  of class  $C^\infty$  is characterized as a Hilbert space satisfying the following two conditions: it is included in the space  $\mathfrak{E}(\Omega)$  of the functions of class  $C^\infty$  and the inclusion map

$$\iota : H \hookrightarrow \mathfrak{E}(\Omega)$$

is continuous [3, Theorem 2.6]. In the function space  $\mathfrak{E}(\Omega)$ , we can naturally define the continuous linear map  $f^* : \mathfrak{E}(\Omega) \rightarrow \mathfrak{E}(\Omega)$ ;  $h \mapsto h \circ f$ , known as the pull-back, equivalent notion of the Koopman operator. Since RKHS is a subspace of  $\mathfrak{E}(\Omega)$ , the Koopman operator  $C_f$  on  $H$  can be regarded as the restriction of the pull-back  $f^*$  to  $H$ . In terms of category theory, the functor  $M \mapsto \mathfrak{E}(M)$  from the category of smooth manifolds to the category of  $\mathbb{C}$ -algebras is fully faithful [57], and the pull-back  $f^*$  (equivalently, Koopman operator) on  $\mathfrak{E}(\Omega)$  provides an algebraic counterpart that is entirely equivalent to the dynamical system on  $\Omega$ . Therefore, RKHS naturally appears as a machinery for numerically handling the universal object  $f^* : \mathfrak{E}(\Omega) \rightarrow \mathfrak{E}(\Omega)$ , and provides a general theoretical framework for numerical treatments. In this sense, JetDMD can be described as a method for data-driven estimation of the pull-back  $f^*$  on  $\mathfrak{E}(\Omega)$  using RKHS.

Let us introduce *jet*. The space  $\mathfrak{J}_{p,n}$  of  $n$ -jet at  $p \in \Omega$  is defined as the quotient space  $\mathfrak{E}(\Omega) / \sim$ , where the equivalence relation  $\sim$  is defined as  $h \sim g$  if and only if the  $\partial^\alpha h(p) = \partial^\alpha g(p)$  for  $|\alpha| \leq n$ , where we use the multi-index notation. We denote the natural surjection  $\mathfrak{E}(\Omega) \rightarrow \mathfrak{J}_{p,n}$  by  $j_{p,n}$ . We note that the space of  $n$ -jets at  $p$  is geometrically canonical object, namely, it is invariant under the change of coordinate.

Let  $p \in \Omega$ . For each integer  $n \geq 0$ , we introduce a finite-dimensional subspace  $V_{p,n} \subset H$  as follows:

$$V_{p,n} = \sum_{|\alpha| \leq n} \mathbb{C} \cdot \partial_x^\alpha k(x, \cdot)|_{x=p},$$

$$V_p = \bigcup_{n \geq 0} V_{p,n} = \sum_{\alpha \in \mathbb{Z}_{\geq 0}^d} \mathbb{C} \cdot \partial_x^\alpha k(x, \cdot)|_{x=p}.$$

This space  $V_p$  is what we call the space of *intrinsic observables*. We note that we can intrinsically define  $V_{p,n}$  as the image under the dual map of the composition of continuous linear maps  $H \xrightarrow{\iota} \mathfrak{E}(\Omega) \xrightarrow{j_{p,n}^*} \mathfrak{J}_{p,n}$  (see Section 2 for details). Originally,  $V_{p,n}$  is introduced in [36] as a key notion for connecting the boundedness of Koopman operators with the behavior of dynamical systems. For special RKHSs, the equivalent notion is considered in [33] as a machinery for proving the linearity of dynamical systems with bounded Koopman operators.

As in the following proposition, the union of  $V_{p,n}$  for  $n \geq 0$  constitutes a dense subspace of  $H$  and, if  $p$  is a fixed point of  $f$ ,  $V_{p,n}$  is invariant under the Perron–Frobenius operator  $C_f^*$  for all  $n \geq 0$  (Theorem 2.12 and Proposition 2.14):

**Proposition 1.2.** The space  $V_p$  is dense in  $H$ . Moreover, if  $p$  satisfies  $f(p) = p$ , we have  $C_f^*(V_{p,n}) \subset V_{p,n}$  for any  $n \geq 0$ . In addition, if  $f(p) = p$  and the dual map  $\iota'$  of  $\iota$  is injective on the image of  $j'_{p,n}$ , the set of eigenvalues of  $C_f^*|_{V_{p,n}}$  coincides with

$$\left\{ \lambda^\alpha : |\alpha| \leq n, \alpha \in \mathbb{Z}_{\geq 0}^d \right\}.$$

We note that RKHSs of the Gaussian kernel and the exponential kernel, mainly treated in this paper, satisfies the condition of the injectivity of  $\iota'$  on the image of  $j'_{p,n}$ .

Now, we describe the JetDMD (see Section 7 for details). As seen below, Jet DMD provides a refinement of EDMD with the intrinsic observables. Let  $r_n := \dim V_{p,n}$ . Let  $\{v_i\}_{i=1}^\infty$  be an orthonormal basis of  $V_p$  such that  $\{v_1, \dots, v_{r_n}\}$  constitutes a basis of  $V_{p,n}$ . Then, for  $x \in \Omega$ , we define a vector of length  $r_n$  by

$$\mathbf{v}_n(x) := \left( \overline{v_i(x)} \right)_{i=1}^{r_n}.$$

For  $X = (x_1, \dots, x_N) \in \Omega^N$ , we define a matrix of size  $r_n \times N$  by

$$\mathbf{V}_n^X := (\mathbf{v}_n(x_1), \dots, \mathbf{v}_n(x_N)). \quad (1.1)$$

Let  $m \leq n$ . Let  $y_i = f(x_i)$  for  $i = 1, \dots, N$  and define  $Y := (y_1, \dots, y_N)$ . Then, we consider the matrix  $\widehat{\mathbf{C}}_{m,n,N} \in \mathbb{C}^{r_m \times r_m}$  defined by the leading principal submatrix of order  $r_m$  of  $\mathbf{V}_n^Y (\mathbf{V}_n^X)^\dagger$ , namely,

$$\mathbf{V}_n^Y (\mathbf{V}_n^X)^\dagger = \begin{pmatrix} \widehat{\mathbf{C}}_{m,n,N} & * \\ * & * \end{pmatrix},$$

where  $(\cdot)^\dagger$  is the Moore-Penrose pseudo-inverse. We remark that EDMD corresponds to the case of  $m = n$ . According to the following example, EDMD with monomials is recovered in JetDMD with exponential kernel:

**Example 1.3.** Let  $\Omega = \mathbb{R}^d$  and let  $k(x, y) = e^{x^\top y}$ . Then, we can take the following set of polynomials of degree up to  $n$

$$\left\{ 1, x_1, \dots, x_d, \dots, \frac{x_1^{\alpha_1} \dots x_d^{\alpha_d}}{\sqrt{\alpha_1! \dots \alpha_d!}}, \dots, \frac{x_d^n}{\sqrt{n!}} \right\}$$

as the orthonormal basis of  $V_{0,n}$  (here, we take  $p = 0$ ) and we have  $r_n = \binom{n+d}{d}$ . Figure 1 actually describes the computational result in this setting. Using this orthonormal basis, the matrix  $\mathbf{V}_n^Y (\mathbf{V}_n^X)^\dagger$  essentially coincides with the one considered in EDMD with monomials. In Figure 1, we considered  $f(x, y) := (x^2 - y^2 + x - y, 2xy + x + y)$ , and performed the calculation using  $x_1, \dots, x_{100}$  from the uniform distribution on  $[-1, 1]^2$ . The red  $+$ 's indicates the eigenvalues of  $\widehat{\mathbf{C}}_{n,n,N}$  for  $n = 10$ , corresponding to EDMD, and the blue  $\times$ 's indicates those of  $\widehat{\mathbf{C}}_{m,n,N}$  for  $(m, n) = (5, 10)$ , corresponding to JetDMD.

When we take  $N \rightarrow \infty$  and  $n \rightarrow \infty$ , the matrix  $\widehat{\mathbf{C}}_{m,n,N}$  with JetDMD actually converges to the correct target  $C_f^*|_{V_{p,m}}$ , more precisely, we have the following theorem (Theorem 3.5 and Theorem 6.13 for the general and precise statements):

**Theorem 1.4.** Let  $m \leq n$ . Let  $\Omega = \mathbb{R}^d$  and let  $p \in \Omega$ . Let  $k(x, y) = e^{(x-p)^\top (y-p)}$  or  $k(x, y) = e^{-|x-y|^2/2\sigma^2}$ . Let  $f = (f_1, \dots, f_d) : \mathbb{R}^d \rightarrow \mathbb{R}^d$  be a map such that  $f(p) = p$  and  $V_p \subset D(C_f)$ . Let  $x_1, \dots, x_N$  be i.i.d random variables of the distribution with compactly supported density function  $\rho$  such that  $\text{ess. inf}_{x \in U} \rho(x) > 0$  for some open subset  $U \subset \mathbb{R}^d$ . Let  $y_i = f(x_i)$  for  $i = 1, \dots, N$ . Then, there exist  $b_m > 0$  and  $R > 0$  such that we have

$$\begin{aligned} \lim_{N \rightarrow \infty} \left\| \widehat{\mathbf{C}}_{m,n,N} - \mathbf{C}_{f,m}^* \right\| &\leq \|C_f|_{V_{p,m}}\|_{\text{op}} \cdot b_m n^m \cdot \frac{R^n}{\sqrt{n!}} \quad \text{a.e.} \\ &\xrightarrow[n \rightarrow \infty]{} 0 \quad \text{a.e.} \end{aligned} \quad (1.2)$$

where  $\mathbf{C}_{f,m}^* \in \mathbb{C}^{r_m \times r_m}$  is the representation matrix of  $C_f^*|_{V_{p,m}}$  with respect to the orthonormal basis  $\{v_1, \dots, v_{r_m}\}$ .

This theorem clearly explains why the step of “truncating  $\mathbf{V}_n^Y(\mathbf{V}_n^X)^\dagger$  to a leading principal submatrix” is inevitable. From the proofs of Theorem 3.5 and Theorem 6.13, in (1.2), the constant  $\|C_f|_{V_{p,p}}\|_{\text{op}}$  arises from extracting the first  $r_m$  rows of the matrix  $\mathbf{V}_n^Y(\mathbf{V}_n^X)^\dagger$ , while the constant  $b_m n^m$  appears as a result of extracting the first  $r_m$  columns. Since  $V_p$  is dense in  $H$ , we easily see that the sequence  $\{\|C_f|_{V_{p,m}}\|_{\text{op}}\}_{m \geq 0}$  is bounded if and only if the Koopman operator  $C_f$  is a bounded linear operator on  $H$ . However, according to [12] and [33], no nonlinear dynamics induces a bounded Koopman operator on  $H$ . Thus, we have the divergence  $\|C_f|_{V_{p,n}}\|_{\text{op}} \rightarrow \infty$  as  $n \rightarrow \infty$  for the nonlinear dynamical system  $f$ . This fact implies the difficulty of analyzing EDMD, corresponding to JetDMD with  $m = n$ , and it generally suggests that EDMD fails to estimate the target operator since the term  $\|C_f|_{V_{p,n}}\|_{\text{op}} \cdot b_n n^n$  will rapidly diverge if we take  $n \rightarrow \infty$ . We also emphasize that here we prove this theorem under the assumption that  $C_f$  is densely defined, but we do not assume its boundedness.

As explained above, the matrix  $\widehat{\mathbf{C}}_{m,n,N}$  produced by JetDMD is capable of approximating the Perron-Frobenius operator  $C_f^*|_{V_{p,m}}$  restricted to  $V_{p,m}$ . Thus, by considering the adjoint of  $\widehat{\mathbf{C}}_{m,n,N}$  in  $V_{p,m}$ , we can estimate the adjoint linear map  $(C_f^*|_{V_{p,m}})^*$  on  $V_{p,m}$  (note that the first “\*” means the adjoint in  $H$ , but the second one means the adjoint in  $V_{p,m}$ ). While it seems that the limit of  $(C_f^*|_{V_{p,m}})^*$  along  $m$  becomes the Koopman operator  $C_f$  on  $H$ , it actually converges not to the Koopman operator itself, but to the “extended” Koopman operator defined through the Gelfand triple.

Since a rigorous explanation of the Gelfand triple and the extended Koopman operator is provided in Section 4, here we will explain the “extended” Koopman operator in a somewhat rough manner. Let  $\Phi := V_p$ . We equip  $\Phi$  with the inductive limit topology. Then,  $(\Phi, H, \Phi')$  determine the Gelfand triple and satisfies the inclusion relation  $\Phi \subset H = H' \subset \Phi'$ , where  $(\cdot)'$  indicates the dual space with the strong topology, and we identify  $H$  with its dual via the Riesz representation theorem. We usually call a Hilbert space equipped with a Gelfand triple the *rigged Hilbert space*. The Gelfand triple is introduced for further investigation of the spectrum of linear operators, and it has been well studied in quantum mechanics. For more detail of the mathematical formulation and applications, see [6, 13, 22, 23] and references therein. Since  $C_f^*(\Phi) \subset \Phi$  by Proposition 1.2, the dual operator of  $C_f^*|_{\Phi}$  induces a continuous linear operator on  $\Phi'$ . We denote this induced continuous linear operator by  $C_f^\times := (C_f^*|_{\Phi})' : \Phi' \rightarrow \Phi'$  and call it the *extended Koopman operator*. It can be shown that  $C_f^\times$  is actually the extension of Koopman operator, namely, it satisfies  $C_f^\times|_H = C_f$  on the domain of  $C_f$  (Proposition 4.3) and is regarded as the limit of  $(C_f^*|_{V_{p,n}})^*$ . Moreover, we can prove the Jordan–Chevalley decomposition of  $C_f^\times$  on  $\Phi'$  (Theorem 4.7) and the eigendecomposition of  $C_f^\times$  on  $\Phi'$  under mild conditions as follows:

**Theorem 1.5.** Assume that  $\iota'$  is injective on the image of  $j'_{p,n}$  and that  $\lambda^\alpha \neq \lambda^\beta$  for  $\alpha, \beta \in \mathbb{Z}_{\geq 0}^d$  with  $\alpha \neq \beta$ . Then, there exist families of vectors  $\{w_\alpha\}_{\alpha \in \mathbb{Z}_{\geq 0}^d} \subset \Phi$  and  $\{u_\alpha\}_{\alpha \in \mathbb{Z}_{\geq 0}^d} \subset \Phi'$  such that

$$\begin{aligned} C_f^\times u_\alpha &= \lambda^\alpha u_\alpha, \\ \langle u_\alpha | w_\beta \rangle &= \delta_{\alpha,\beta} \end{aligned}$$

for all  $\alpha, \beta \in \mathbb{Z}_{\geq 0}^d$ , where  $\delta_{\alpha,\beta}$  is the Kronecker delta, and

$$C_f^\times u = \sum_{\alpha \in \mathbb{Z}_{\geq 0}^d} \lambda^\alpha \langle w_\alpha | u \rangle u_\alpha.$$

for  $u \in \Phi'$  and  $w \in \Phi$ .

It is worth noting that the eigenvectors of the extended Koopman operator  $C_f^\times$  can be interpreted as eigenfunctions of the Koopman operator in a weak sense (see Proposition 4.10), but they are not eigenfunctions in the usual sense. An important consequence derived from the usage of Gelfand triple is that what is estimated using a family of observables is not the Koopman operator itself, but the extended Koopman operator defined on the space of functional of the intrinsic observables. Therefore, the estimated eigenvectors with the observables are strictly those of the extended Koopman operator and, unless the Koopman operator preserves the space of the observables, they are generally not eigenfunctions of the Koopman operator. According to the numerical experiment in Section 7, the eigenvectors of the extended Koopman operator capture some important characteristics



of the dynamical system. However, the extended Koopman operator and its eigenvectors remain abstract and are not fully understood. Their mathematical properties and their relation with the behavior of the dynamical system are crucial research topics for the future.

## Acknowledgement

II, MI, YK acknowledge support from the Japan Science and Technology Agency (JST) under CREST grant JPMJCR1913. YK acknowledges support from the Japan Society of Promotion of Science (JSPS) under KAK-ENHI Grant Number JP22H05106. II acknowledges support from the JST under ACT-X grant JPMJAX2004.

## 2 Intrinsic observables and jets

Here, we describe the core notion of this paper, the space of the intrinsic observables. We introduce the notion of jet and the space of the intrinsic observables, and show their basic properties. Let  $\Omega \subset \mathbb{R}^d$  be an open subset.

### 2.1 Jets and derivatives of Dirac deltas

Let  $\mathfrak{P}_n \subset \mathfrak{E}(\Omega)$  be the set of polynomial functions of degree less than or equal to  $n$ :

$$\mathfrak{P}_n := \left\{ x \mapsto \sum_{|\alpha| \leq n} a_\alpha x^\alpha : a_\alpha \in \mathbb{C} \text{ for } \alpha \text{ with } |\alpha| \leq n \right\}.$$

For  $p \in \Omega$  and non-negative integer  $n \geq 0$ , we define

$$\tau_{p,n} : \mathfrak{E}(\Omega) \rightarrow \mathfrak{P}_n; h \mapsto \sum_{|\alpha| \leq n} \frac{\partial_x^\alpha h(p)}{\alpha!} (x-p)^\alpha. \quad (2.1)$$

**Definition 2.1.** We define the set  $\mathfrak{J}_{p,n}$  of  $n$ -jets from  $\Omega$  to  $\mathbb{C}$  at  $p$  by the quotient space

$$\mathfrak{J}_{p,n} := \mathfrak{E}(\Omega) / \text{Ker}(\tau_{p,n}). \quad (2.2)$$

We denote by  $j_{p,n}$  the natural map  $j_{p,n} : \mathfrak{E}(\Omega) \rightarrow \mathfrak{J}_{p,n}$ .

By definition,  $\tau_{p,n}$  induces the isomorphism from  $\mathfrak{J}_{p,n}$  to  $\mathfrak{P}_n$ . We note that the notion of the jet is a mathematically canonical object on a smooth manifold (not depending on the choice of coordinate systems). For details of the theory of jets, see, for example, [41, Section 4].

Using the jets, we define subspaces of the dual space  $\mathfrak{E}(\Omega)'$  by

$$\begin{aligned} \mathfrak{D}_{p,n} &:= j'_{p,n}(\mathfrak{J}'_{p,n}), \\ \mathfrak{D}_p &:= \bigcup_{n \geq 0} \mathfrak{D}_{p,n}. \end{aligned}$$

We also define  $\mathfrak{D}_{p,-1} := \{0\}$ . We note that  $\dim \mathfrak{D}_{p,n}$  coincides with  $\binom{n+d}{d}$ . For  $\alpha \in \mathbb{Z}_{\geq 0}^d$  and  $p \in \Omega$ , let  $\delta_p^{(\alpha)}$  be the  $\alpha$ -th derivative of the Dirac delta at  $p$ , that is defined by

$$\delta_p^{(\alpha)}(h) := \partial_x^\alpha h(p)$$

for  $h \in \mathfrak{E}(\Omega)$ . As in the following proposition,  $\mathfrak{D}_{p,n}$  coincides with the derivatives of the Dirac deltas:

**Proposition 2.2** (Alternative definition of  $\mathfrak{D}_{p,n}$ ). For any  $n \geq 0$ , we have

$$\mathfrak{D}_{p,n} = \sum_{|\alpha| \leq n} \mathbb{C} \delta_p^{(\alpha)}.$$

To show this proposition, we prove the following lemma:

**Lemma 2.3.** The set

$$\left\{ \delta_p^{(\alpha)} : p \in \Omega, \alpha \in \mathbb{Z}_{\geq 0} \right\}$$

is linearly independent.

*Proof.* Let  $p_1, p_2, \dots, p_r \in \Omega$  be distinct points. For each  $i = 1, \dots, r$ , let

$$D_i := \sum_{\alpha} c_{i,\alpha} \delta_{p_i}^{(\alpha)}.$$

Here, we assume that  $c_{i,\alpha} = 0$  for all but finitely many  $i$ 's and  $\alpha$ 's. It suffices to show that  $c_{i,\alpha} = 0$  for  $i = 1, \dots, r$  and  $\alpha \in \mathbb{Z}_{\geq 0}^d$  if  $\sum_{i=1}^r D_i = 0$ . Let  $\phi_i \in \mathfrak{C}(\Omega)$  such that  $\phi(p_i) = 1$  and  $p_j \notin \text{supp}(\phi_i)$  for  $j \neq i$ . Then, for any  $\alpha$ ,

$$\left( \sum_{k=1}^r D_k \right) ((x - p_i)^\alpha \phi_i) = D_i ((x - p_i)^\alpha \phi_i) = \alpha! c_{i,\alpha} = 0.$$

Thus, we have  $c_{i,\alpha} = 0$ . □

*Proof of Proposition 2.2.* Since  $\tau'_{p,n}(\mathfrak{P}_n) = j'_{p,n}(\mathfrak{J}'_{p,n})$ , we prove  $\tau'_{p,n}(\mathfrak{P}_n) = \mathfrak{D}_{p,n}$ . For  $\beta \in \mathbb{Z}_{\geq 0}^d$  with  $|\beta| \leq n$ , let  $\ell_\beta \in \mathfrak{P}'_n$  be the linear function of  $\mathfrak{P}_n$  defined by  $\ell_\beta(\sum_{\alpha} a_{\alpha} x^{\alpha}) := \beta! a_{\beta}$ . Then, for any  $h \in \mathfrak{C}(\Omega)$ , we have

$$\langle \tau'_{p,n}(\ell_\beta) | h \rangle = \partial_x^\beta h|_{x=p} = \langle \delta_p^{(\beta)} | h \rangle.$$

Thus, we conclude that the image of  $\tau'_{p,n}$  includes  $\mathfrak{D}_{p,n}$ . Since  $\tau_{p,n}$  is surjective, the dual map  $\tau'_{p,n}$  is injective, thus the dimension of the image of  $\tau'_{p,n}$  coincides with that of  $\mathfrak{P}_n$ . On the other hand, the dimension of  $\mathfrak{D}_{p,n}$  is the same as  $\dim \mathfrak{P}_n$  by Lemma 2.3. Therefore, the image of  $\tau'_{p,n}$  coincides with  $\mathfrak{D}_{p,n}$ . □

For a map  $f = (f_1, \dots, f_d) : \Omega \rightarrow \Omega$  of class  $C^\infty$ , let  $f^* : \mathfrak{C}(\Omega) \rightarrow \mathfrak{C}(\Omega)$  be the *pull-back* (Koopman operator) on  $\mathfrak{C}(\Omega)$ , that allocates  $h \circ f \in \mathfrak{C}(\Omega)$  to  $h \in \mathfrak{C}(\Omega)$ , and let  $f_* := (f^*)' : \mathfrak{C}(\Omega)' \rightarrow \mathfrak{C}(\Omega)'$  be the *push-forward*, that is the dual map of  $f^*$ . Let  $\mathbb{C}[X_1, \dots, X_d]_n$  be the space of homogeneous polynomials of degree equal to  $n$ :

$$\mathbb{C}[X_1, \dots, X_d]_n := \left\{ \sum_{|\alpha|=n} a_{\alpha} X_1^{\alpha_1} \cdots X_d^{\alpha_d} : a_{\alpha} \in \mathbb{C} \text{ for } \alpha \text{ with } |\alpha| = n \right\}.$$

Then, by Lemma 2.3, we have the linear isomorphism

$$\rho_n : \mathfrak{D}_{p,n} / \mathfrak{D}_{p,n-1} \longrightarrow \mathbb{C}[X_1, \dots, X_d]_n$$

defined by  $\rho \left( \delta_p^{(\alpha)} + \mathfrak{D}_{p,n-1} \right) := X_1^{\alpha_1} \cdots X_d^{\alpha_d}$  for  $\alpha$  with  $|\alpha| = n$ . Then, we have the following statements:

**Proposition 2.4.** (1) For each integer  $n \geq -1$ , we have  $f_*(\mathfrak{D}_{p,n}) \subset \mathfrak{D}_{f(p),n}$ .

(2) Let  $\text{gr}_{f_*}^n : \mathfrak{D}_{p,n} / \mathfrak{D}_{p,n-1} \rightarrow \mathfrak{D}_{f(p),n} / \mathfrak{D}_{f(p),n-1}$  be the linear map induced  $f_*$  via (1). Then, we have

$$\text{gr}_{f_*}^n = \rho_n^{-1} \circ S_n(df_p) \circ \rho_n, \tag{2.3}$$

where  $S_n(df_p) \in \mathbb{C}^{d \times d}$  is the  $n$ -th symmetric product of the Jacobian matrix  $df_p$ , that is the linear map on  $\mathbb{C}[X_1, \dots, X_d]_n$  defined by

$$S_n(df_p)(Q(X_1, \dots, X_d)) := Q \left( (X_1, \dots, X_d)^\top \cdot df_p \right)$$

for  $Q(X_1, \dots, X_d) \in \mathbb{C}[X_1, \dots, X_d]_n$ .

- (3) Let  $\mathbf{C}_{f,n}^* \in \mathbb{C}^{\binom{n+d}{d} \times \binom{n+d}{d}}$  be the representation matrix of  $f_*|_{\mathfrak{D}_{p,n}} : \mathfrak{D}_{p,n} \rightarrow \mathfrak{D}_{f(p),n}$  with respect to the basis  $\{\delta_p^{(\alpha)} : |\alpha| \leq n\}$  and  $\{\delta_{f(p)}^{(\alpha)} : |\alpha| \leq n\}$ . Then,  $\mathbf{C}_{f,n}^*$  is in the form of

$$\mathbf{C}_{f,n}^* = \begin{pmatrix} 1 & * & * & * \\ 0 & \mathbf{J}_{p,1} & * & * \\ \vdots & \ddots & \ddots & \vdots \\ 0 & \cdots & 0 & \mathbf{J}_{p,n} \end{pmatrix}, \quad (2.4)$$

where  $\mathbf{J}_{p,i}$  is the representation matrix of  $S_i(df_p)$  with respect to the basis  $\{X_1^{\alpha_1} \cdots X_d^{\alpha_d} : |\alpha| = i\} \subset \mathbb{C}[X_1, \dots, X_d]$  for  $i = 1, \dots, n$ .

- (4) Let  $\lambda_1, \dots, \lambda_d$  be the eigenvalues (with multiplicity) of the Jacobian matrix  $df_p$  and let  $\lambda := (\lambda_1, \dots, \lambda_d)$ . Then, the set of eigenvalues of  $f_*|_{\mathfrak{D}_{p,n}}$  is  $\{\lambda^\alpha : |\alpha| \leq n\}$ .

*Proof.* The statements (1) and (2) are direct consequences of [36, Lemma 2.2]. The formula (2.4) follows from (2). The statement (4) immediately follows from (2.4).  $\square$

## 2.2 Construction of the space of intrinsic observables in reproducing kernel Hilbert spaces

Let  $H \subset \mathfrak{E}(\Omega)$  be a Hilbert space with inner product  $\langle \cdot, \cdot \rangle_H$ . We denote the inclusion map by

$$\iota : H \hookrightarrow \mathfrak{E}(\Omega). \quad (2.5)$$

We always assume the following assumption:

**Assumption 2.5.** The inclusion map  $\iota$  is continuous.

What is important here is that such a Hilbert space is captured in the framework reproducing kernel Hilbert space (RKHS). First, we provide the definition of RKHS:

**Definition 2.6.** Let  $X$  be a set and let  $H$  be a Hilbert space composed of maps from  $X$  to  $\mathbb{C}$  with inner product  $\langle \cdot, \cdot \rangle_H$ . We say that  $H$  is a *reproducing kernel Hilbert space (RKHS)* on  $X$  if the point evaluation map  $h \mapsto h(x)$  from  $H$  to  $\mathbb{C}$  is a continuous linear map for any  $x \in X$ .

Let  $H$  be an RKHS on a set  $X$ . Then, for each  $x \in X$ , by the Riesz representation theorem, there uniquely exists  $k_x \in H$  satisfying

$$\langle h, k_x \rangle_H = h(x).$$

We define  $k(x, y) := \langle k_x, k_y \rangle$  for  $x, y$  in  $X$ . Then,  $k$  is a positive definite kernel on  $X$ . Here we say a map  $k : X \times X \rightarrow \mathbb{C}$  is positive definite kernel on  $X$  if the matrix  $(k(x_i, x_j))_{i,j=1,\dots,r}$  is a Hermitian positive semi-definite matrix for any finite elements  $x_1, \dots, x_r \in X$ . Conversely, for a positive definite kernel  $k$  on  $X$ , there uniquely exists an RKHS on  $X$  (see [3, Theorem 2.2], for example). Thus, we have an one-to-one correspondence between the RKHSs on  $X$  and the positive definite kernels on  $X$ . In the remainder of this paper, we always consider  $X = \Omega$ .

Under Assumption 2.5,  $H$  is an RKHS on  $\Omega$  since the point evaluation map at  $x \in \Omega$  coincides with  $\delta_x \circ \iota$ . We note that the associated positive definite kernel  $k$  of  $H$  is a function of class  $C^\infty$ . Conversely, as in the following proposition, the RKHS on  $\Omega$  of a positive definite kernel of class  $C^\infty$  is continuously included in  $\mathfrak{E}(\Omega)$ . Moreover, if the positive definite kernel  $k$  satisfies  $k_x \in \mathfrak{H}(\Omega)$  for all  $x \in \Omega$ ,  $H$  is continuously included in the space of real analytic functions.

**Proposition 2.7.** The correspondence  $H \mapsto k$  induces an one-to-one correspondence between the Hilbert spaces  $H \subset \mathfrak{E}(\Omega)$  (resp.  $\mathfrak{H}(\Omega)$ ) with continuous inclusions and the continuous positive definite kernels  $k$  such that  $k_x \in \mathfrak{E}(\Omega)$  (resp.  $\mathfrak{H}(\Omega)$ ) for all  $x \in \Omega$ .

*Proof.* It follows from [3, Theorems 2.6 and 2.7].  $\square$

We define

$$\tau : H' \longrightarrow H \quad (2.6)$$

be the anti-linear isomorphism such that  $\langle \ell | \cdot \rangle = \langle \cdot, \tau(\ell) \rangle_H$  for  $\ell \in H'$  by the Riesz representation theorem. Now, we define the space of the intrinsic observables as follows:

**Definition 2.8** (Intrinsic observables). For  $p \in \Omega$  and  $n \geq 0$ , we define a finite dimensional subspace of  $H$  by

$$V_{p,n} := (\tau \circ \iota')(\mathfrak{D}_{p,n}).$$

We denote the orthogonal projection to  $V_{p,n}$  by

$$\pi_n : H \rightarrow V_{p,n} \quad (2.7)$$

and define

$$V_p := \bigcup_{n \geq 0} V_{p,n}$$

We remark that we can explicitly describe  $(\tau \circ \iota')(\delta_p^{(\alpha)}) \in H$  using  $k$  as follows:

**Proposition 2.9.** For  $\alpha \in \mathbb{Z}_{\geq 0}^d$  and  $p \in \Omega$ , we have

$$(\tau \circ \iota')(\delta_p^{(\alpha)}) = \partial_x^\alpha k(x, \cdot)|_{x=p}. \quad (2.8)$$

*Proof.* Let  $y \in \Omega$  be an arbitrary point. Then, it follows from the following computation:

$$\begin{aligned} (\tau \circ \iota')(\delta_p^{(\alpha)})(y) &= \langle \tau \iota' \delta_p^{(\alpha)}, k_y \rangle_H = \overline{\langle k_y, \tau \iota' \delta_p^{(\alpha)} \rangle} = \overline{\partial_x^\alpha k_y(x)|_{x=p}} \\ &= \partial_x^\alpha k(x, y)|_{x=p}. \end{aligned}$$

$\square$

We introduced the space of intrinsic observables in  $H$  via the space of jets  $\mathfrak{J}_{p,n}$  and the continuous inclusion  $\iota : H \subset \mathfrak{E}(\Omega)$ . This definition is mathematically canonical, but is a little abstract and not explicit as well. As an immediate conclusion of Proposition 2.9, the space  $V_{p,n}$  has an alternative explicit expression:

**Corollary 2.10.** For  $p \in \Omega$  and  $n \geq 0$ , we have

$$V_{p,n} = \sum_{|\alpha| \leq n} \mathbb{C} \cdot \partial_x^\alpha k(x, \cdot)|_{x=p} \quad (2.9)$$

Now, let us introduce the Koopman operator on the RKHS and consider the relation between the intrinsic observables and the Koopman operator. For a map  $f = (f_1, \dots, f_d) : \Omega \rightarrow \Omega$  of class  $C^\infty$ , let  $C_f$  be the Koopman operator, that is a linear operator defined by  $C_f h := h \circ f$  with domain  $D(C_f) = \{h \in H : h \circ f \in H\}$ . When  $C_f$  is densely defined, we can define the adjoint operator  $C_f^* : H \rightarrow H$ , that is known as the Perron–Frobenius operator. For Koopman operators with dense domain, the Perron–Frobenius operator on  $H$  is compatible with the push-forward:

**Proposition 2.11.** Assume that  $C_f$  is densely defined. For any  $\ell \in \mathfrak{E}(\Omega)$ ,  $(\tau \circ \iota')(\ell) \in D(C_f^*)$  and  $C_f^* \circ (\tau \circ \iota') = (\tau \circ \iota') \circ f_*$  holds.

*Proof.* Since  $f^*$  is a continuous linear map on  $\mathfrak{E}(\Omega)$ , we see that  $\langle C_f h, \tau'(\ell) \rangle_H = (\ell \circ f^* \circ \iota)(h)$  is also continuous on  $h \in D(C_f)$ , proving the first statement. As for the second statement, since  $\tau(\ell \circ f^* \circ \iota) = \tau' f_*(\ell)$ , we have  $\langle h, \tau' f_*(\ell) \rangle_H = \langle h, C_f^* \tau'(\ell) \rangle_H$ . Thus, we have the second statement.  $\square$

Then, we have the following theorem:

**Theorem 2.12.** Let  $p$  a point  $p$  such that  $f(p) = p$ . Assume that  $C_f$  is densely defined. Then, we have the following statements:

- (1)  $C_f^*(V_{p,n}) \subset V_{p,n}$  for all  $n \geq 0$ .
- (2) Assume that  $\iota'|_{\mathfrak{D}_p} : \mathfrak{D}_p \rightarrow H'$  is injective. Then, the set of the eigenvalues of  $C_f^*$  is

$$\{\lambda^\alpha : |\alpha| \leq n\},$$

where  $\lambda := (\lambda_1, \dots, \lambda_d)$  and  $\lambda_1, \dots, \lambda_d$  are the eigenvalues (with multiplicity) of the Jacobian matrix  $df_p$ .

*Proof.* It follows from Proposition 2.4 and Proposition 2.11.  $\square$

The assumption of the injectivity of  $\iota'|_{\mathfrak{D}_p} : \mathfrak{D}_p \rightarrow H$  of (2) in Theorem 2.12 holds in typical RKHSs used in the applications, for example, the exponential kernel  $k(x, y) = e^{(x-b)^\top(y-b)/\sigma^2}$  and the Gaussian kernel  $e^{-|x-y|^2/2\sigma^2}$ . We provide more theoretical results for these two kernels in Section 6.

We end this section with several special properties of the space of intrinsic observables when the positive definite kernel  $k$  has a real analyticity. We consider the following assumption:

**Assumption 2.13.** The open set  $\Omega$  is connected and  $k$  is continuous on  $\Omega \times \Omega$ , satisfying  $k_x \in \mathfrak{H}(\Omega)$  for any  $x \in \Omega$ .

Then, we have the following proposition:

**Proposition 2.14.** Under Assumption 2.13,  $V_p$  is dense in  $H$ .

*Proof.* Let  $h \in (V_p)^\perp$ . Then,  $\langle h, (\tau \circ \iota') \delta_p^{(\alpha)} \rangle_H = \partial_x^\alpha h(p) = 0$  for any  $\alpha \in \mathbb{Z}_{\geq 0}^d$ . Thus,  $h$  is zero on a neighborhood of  $p$ , and thus  $h = 0$  since  $h$  is real analytic and  $\Omega$  is connected. Therefore, we have  $(V_p)^\perp = \{0\}$  and  $V_p$  is dense in  $H$ .  $\square$

For  $x \in \Omega$ , we introduce the minimal approximation error for between  $k_x$  and the elements of  $V_{p,n}$  as follows:

$$\mathcal{E}_{p,n}(x) := \min_{v \in V_{p,n}} \|k_x - v\|_H = \|k_x - \pi_n k_x\|_H, \quad (2.10)$$

where  $\pi_n : H \rightarrow V_{p,n}$  is the orthogonal projection of (2.7). Proposition 2.14 implies that using elements of  $V_{p,n}$  for sufficiently large  $n$ , we can approximate the family  $\{k_x\}_{x \in K}$  with arbitrary precision for any compact set  $K$ :

**Proposition 2.15.** Suppose Assumption 2.13 holds. Let  $K \subset \Omega$  be a compact set. Then,  $\sup_{x \in K} \mathcal{E}_{p,n}(x) \rightarrow 0$  as  $n \rightarrow \infty$ .

*Proof.* By definition, for each  $x \in \Omega$ , we have  $\mathcal{E}_{p,n}(x) \geq \mathcal{E}_{p,n+1}(x)$  for all  $n \geq 0$  and  $\mathcal{E}_{p,n}(x) \rightarrow 0$  as  $n \rightarrow \infty$ . Since  $\mathcal{E}_{p,n}(x)$  is continuous, by Dini's theorem,  $\mathcal{E}_{p,n}(x)$  uniformly converges to 0 on  $K$ , namely,  $\lim_{n \rightarrow \infty} \sup_{x \in K} \mathcal{E}_{p,n}(x) \rightarrow 0$ .  $\square$

Then, we have the following lemma, that will play a main role in the theoretical results for the reconstruction of dynamical systems in Section 7:

**Lemma 2.16.** Assume  $C_f$  is densely defined. Let  $B \subset D(C_f)$  be a subset such that  $C_f(B)$  is a bounded subset in  $H$ . Then, for any compact set  $K \subset \Omega$ , we have

$$\sup_{\substack{x \in K \\ h \in B}} |\langle k_{f(x)} - C_f^* \pi_n k_x, h \rangle| \leq \sup_{x \in K} \mathcal{E}_{p,n}(x) \cdot \sup_{h \in B} \|C_f h\|_H.$$

Moreover, if we further assume Assumption 2.13, we have

$$\sup_{\substack{x \in K \\ h \in B}} |\langle k_{f(x)} - C_f^* \pi_n k_x, h \rangle| \rightarrow 0$$

as  $n \rightarrow \infty$ .

*Proof.* The first statement follows from  $|\langle k_{f(x)} - C_f^* \pi_n k_x, h \rangle| \leq \mathcal{E}_{p,n}(x) \|C_f h\|_H$  using the Cauchy–Schwarz inequality and the formula  $C_f^* k_x = k_{f(x)}$ . The second statement follows from the first statement with Proposition 2.15.  $\square$

### 3 Estimation of Perron–Frobenius operators

Here, we provide the key error bound for the estimation of the Perron–Frobenius operator using the intrinsic observables. In this section, we always assume  $C_f$  is densely defined and consider the following assumptions:

**Assumption 3.1** (Existence of a fixed point).  $p$  is a fixed point of  $f$ , namely,  $f(p) = p$ .

**Assumption 3.2** (Domain condition for  $C_f$ ).  $V_p \subset D(C_f)$ .

We note that Assumptions 2.13 and 3.2 imply that  $C_f$  is densely defined by Proposition 2.14. As for the dynamical system  $f$ , although we are only assuming that  $f$  is  $C^\infty$ , if we further impose Assumption 3.2 on  $f$ , then  $f$  is automatically has a stronger analytic property than mere smoothness. We also note that we have more specific sufficient condition of Assumption 3.2 for the exponential kernel and the Gaussian kernel (see Section 6.3).

#### 3.1 Error analysis

Let  $r_n := \dim V_{p,n}$ . We fix a basis  $\mathcal{B}_p = \{v_n\}_{n \geq 0}$  of  $V_p$  such that  $\mathcal{B}_{p,n} = \{v_i\}_{i=1, \dots, r_n}$  constitutes a basis of  $V_{p,n}$ . Then, we define

$$\mathbf{v}_n(x) := \left( \overline{v_i(x)} \right)_{i=1}^{r_n}, \quad (3.1)$$

$$\mathbf{G}_n := (\langle v_i, v_j \rangle_H)_{i,j=1, \dots, r_n}. \quad (3.2)$$

For  $X = (x_1, \dots, x_N) \in \Omega^N$ , we define

$$\mathbf{V}_n^X := (\mathbf{v}_n(x_1), \dots, \mathbf{v}_n(x_N)). \quad (3.3)$$

We have an explicit description of the coefficients of the basis  $\mathcal{B}_{p,n}$  for the minimizer that attains the minimization problem (2.10):

**Proposition 3.3.** Let  $x \in \Omega$ . Let  $\pi_n k_x = \sum_{i=1}^{r_n} c_i^*(x) v_i$ . Then,  $c_i^*(x)$  satisfies

$$\mathbf{G}_n \cdot (c_i^*(x))_{i=1}^{r_n} = \mathbf{v}_n(x). \quad (3.4)$$

*Proof.* Let  $k_x = v' + \sum_{i=1}^{r_n} c_i^*(x) v_i$ , where  $v' \in V_{p,n}^\perp$ . Then, considering  $\langle v_j, k_x \rangle_H$  for each  $j$ , we have the identity (3.4).  $\square$

**Example 3.4.** Assume that  $\iota'|_{\mathfrak{D}_p}$  is injective. We fix a numbering of  $\mathbb{Z}_{\geq 0}^d$  such that  $\mathbb{Z}_{\geq 0}^d = \{\alpha^{(i)}\}_{i=1}^\infty$  and  $|\alpha^{(i)}| \leq |\alpha^{(j)}|$  if  $i \leq j$ . Then, if we take  $\partial_x^{\alpha^{(i)}} k(x, \cdot)|_{x=p}$  as  $v_i$ , we have

$$\mathbf{v}_n(x) = (\partial_x^{\alpha^{(i)}} k(x, p))_{i=1}^{r_n}, \quad \mathbf{G}_n = \left( \partial_x^{\alpha^{(i)}} \partial_y^{\alpha^{(j)}} k(p, p) \right)_{i,j=1,\dots,r_n}.$$

Then, we have the following theorem:

**Theorem 3.5.** Let  $p \in \Omega$ . Let  $m, n \geq 0$  be integers with  $m \leq n$ . Let  $\mathbf{C}_{f,m}^*$  be the representation matrix of  $C_f^*|_{V_{p,m}}$  with respect to  $\mathcal{B}_{p,m}$ . Let  $X_N := (x_1, \dots, x_N) \in \Omega^N$  and  $Y_N := (y_1, \dots, y_N) \in \Omega^N$  such that  $f(x_i) = y_i$  for  $i = 1, \dots, N$ . We assume Assumption 2.13,  $r_n \leq N$ ,  $\text{span}(\{\pi_n k_{x_1}, \dots, \pi_n k_{x_N}\}) = V_{p,n}$ , and that  $p$  satisfies Assumptions 3.1 and 3.2. We define the square matrices  $\widehat{\mathbf{C}}_{m,n,N}$  and  $\mathbf{E}_{m,n}^{X_N}$  of size  $r_m$  by the leading principal minor matrix of order  $r_m$  such that

$$\mathbf{G}_m^{-1} \mathbf{V}_m^{Y_N} (\mathbf{V}_n^{X_N})^\dagger \mathbf{G}_n = \begin{pmatrix} \widehat{\mathbf{C}}_{m,n,N} & * \\ & * \end{pmatrix}, \quad (3.5)$$

$$\mathbf{G}_n (N^{-1} \mathbf{V}_n^{X_N} (\mathbf{V}_n^{X_N})^*)^{-1} \mathbf{G}_n = \begin{pmatrix} \mathbf{E}_{m,n}^{X_N} & * \\ * & * \end{pmatrix}. \quad (3.6)$$

Then, we have

$$\left\| \mathbf{C}_{f,m}^* - \mathbf{G}_m \widehat{\mathbf{C}}_{m,n,N} \right\| \leq \|C_f|_{V_{p,m}}\|_{\text{op}} \|\mathbf{G}_m^{-1/2}\|_{\text{op}} \|\mathbf{E}_{m,n}^{X_N}\|_{\text{op}}^{1/2} \sqrt{\frac{1}{N} \sum_{i=1}^N \mathcal{E}_{p,n}(x_i)^2}. \quad (3.7)$$

*Proof.* Let  $\mathbf{P}_m := (\mathbf{G}_m^{-1} \quad \mathbf{O}_{r_n-r_m}) \mathbf{G}_n$  be the representation matrix of  $\pi_m|_{V_{p,n}} : V_{p,n} \rightarrow V_{p,m}$  with respect to the basis  $\mathcal{B}_{p,n}$  and  $\mathcal{B}_{p,m}$ . We denote by  $\mathbf{P}_m^\diamond := (\mathbf{I}_{r_m} \quad \mathbf{O}_{r_n-r_m})^\top$  the representation matrix of the adjoint operator of  $\pi_m|_{V_{p,n}}$ . Then, we have

$$\begin{aligned} \widehat{\mathbf{C}}_{m,n,N} &= \mathbf{P}_m \mathbf{G}_n^{-1} \mathbf{V}_n^{Y_N} (\mathbf{V}_n^{X_N})^\dagger \mathbf{G}_n \mathbf{P}_m^\diamond, \\ \mathbf{C}_{f,m}^* &= \mathbf{P}_m \mathbf{C}_{f,n}^* \mathbf{P}_m^\diamond. \end{aligned}$$

By the assumption that  $\pi_n k_{x_1}, \dots, \pi_n k_{x_N}$  span  $V_{p,n}$ , we have  $\mathbf{V}_n^{X_N} (\mathbf{V}_n^{X_N})^\dagger = \mathbf{I}_{r_n}$ . Therefore, we see that

$$\left\| \mathbf{C}_{f,m}^* - \widehat{\mathbf{C}}_{m,n,N} \right\| \leq \|\mathbf{G}_m^{-1/2}\|_{\text{op}} \|\mathbf{G}_m^{1/2} \mathbf{P}_m \mathbf{C}_{f,n}^* \mathbf{G}_n^{-1} \mathbf{V}_n^{X_N} - \mathbf{G}_m^{1/2} \mathbf{P}_m \mathbf{G}_n^{-1} \mathbf{V}_n^{Y_N}\| \cdot \|(\mathbf{V}_n^{X_N})^\dagger \mathbf{G}_n \mathbf{P}_m^\diamond\|_{\text{op}}. \quad (3.8)$$

By [26], we have

$$((\mathbf{V}_n^{X_N})^\dagger)^* (\mathbf{V}_n^{X_N})^\dagger = (\mathbf{V}_n^{X_N} (\mathbf{V}_n^{X_N})^*)^{-1}.$$

Thus,

$$\|(\mathbf{V}_n^{X_N})^\dagger \mathbf{G}_n \mathbf{P}_m^\diamond\|_{\text{op}} = N^{1/2} \|\mathbf{E}_{m,n}^{X_N}\|_{\text{op}}^{1/2}. \quad (3.9)$$

By Proposition 3.3, we see that

$$\begin{aligned} (\pi_m C_f^* \pi_n k_{x_1}, \dots, \pi_m C_f^* \pi_n k_{x_N}) &= (v_i)_{i=1}^{r_m} \mathbf{P}_m \mathbf{C}_{f,n}^* \mathbf{G}_n^{-1} \mathbf{V}_n^{X_N}, \\ (\pi_m \pi_n k_{y_1}, \dots, \pi_m \pi_n k_{y_N}) &= (v_i)_{i=1}^{r_m} \mathbf{P}_m \mathbf{G}_n^{-1} \mathbf{V}_n^{Y_N}. \end{aligned}$$

Thus, we have

$$\|\mathbf{G}_m^{1/2} \mathbf{P}_m \mathbf{C}_{f,n}^* \mathbf{G}_n^{-1} \mathbf{V}_n^{X_N} - \mathbf{G}_m^{1/2} \mathbf{P}_m \mathbf{G}_n^{-1} \mathbf{V}_n^{Y_N}\|^2 = \sum_{i=1}^N \|\pi_m C_f^* \pi_n k_{x_i} - \pi_m \pi_n k_{y_i}\|_H^2.$$

Since  $\pi_m \pi_n k_{y_i} = \pi_m k_{y_i} = \pi_m C_f^* k_{x_i}$ , we have

$$\begin{aligned} \|\pi_m C_f^* \pi_n k_{x_i} - \pi_m \pi_n k_{y_i}\| &\leq \|\pi_m C_f^* (\pi_n k_{x_i} - k_{x_i})\|_H \\ &\leq \|\pi_m C_f^*\|_{\text{op}} \|\pi_n k_{x_i} - k_{x_i}\|_H \\ &= \|\pi_m C_f^*\|_{\text{op}} \mathcal{E}_{p,n}(x_i). \end{aligned} \quad (3.10)$$

By Assumption 3.2, the linear map  $C_f|_{V_{p,m}} : V_{p,m} \rightarrow H$  is automatically bounded, and its adjoint coincides with  $\pi_m C_f^*$ . Thus, we have  $\|\pi_m C_f^*\|_{\text{op}} = \|C_f|_{V_{p,m}}\|_{\text{op}} < \infty$ . Therefore, combining the inequality (3.8) with (3.9) and (3.10), we have (3.7).  $\square$

This theorem describes the essence of the truncating process in JetDMD as mentioned in the following remark of Theorem 1.4 in Section 1. The presence of the constant  $\|C_f|_{V_{p,m}}\|_{\text{op}}$  arises from extracting the first  $r_m$  rows of the matrix, while the constant  $\|\mathbf{E}_{m,n}^{X_N}\|_{\text{op}}$  appears as a result of extracting the first  $r_m$  columns. Estimating the growth rate of those constants  $\|C_f|_{V_{p,m}}\|_{\text{op}}$  and  $\|\mathbf{E}_{m,n}^{X_N}\|_{\text{op}}$  as  $m$  and  $n$  increase is extremely challenging, and it is generally expected that they will grow rapidly with  $m$  and  $n$ . This indicates the difficulty of analyzing EDMD, corresponding the case of  $m = n$ , and generally suggests that the estimation with EDMD is likely to fail. In contrast, if we fix  $m$ , then  $\|C_f|_{V_{p,m}}\|_{\text{op}}$  becomes just a constant and the behavior of  $\|\mathbf{E}_{m,n}^{X_N}\|_{\text{op}}$  along  $n$  gets much tamer and more controllable. As a result, we have rigorous convergence results in some specific RKHSs (see Section 6).

**Remark 3.6.** It is easy to show that  $C_f$  is bounded on  $H$  if and only if  $\{\|C_f|_{V_{p,n}}\|_{\text{op}}\}_{n=1}^\infty$  is a bounded sequence since  $V_p = \cup_n V_{p,n}$  is dense in  $H$ . However, some theoretical results show the dynamical system becomes linear when the Koopman operator is bounded on specific RKHSs corresponding to a certain important kernels such as the exponential kernel [12] and the Gaussian kernel [33] (we will use them in the numerical simulation). Moreover, it is also show that the dynamical system is never chaotic if the Koopman operator is bounded [36]. Thus, in the context of nonlinear analysis, we cannot expect that Koopman operator on RKHS is bounded, namely, we should assume that  $\|C_f|_{V_{p,n}}\|_{\text{op}} \rightarrow \infty$  as  $n \rightarrow \infty$ , in many cases.

We will use the following corollary for further investigation of (3.8) when the sample number  $N$  goes to infinity:

**Corollary 3.7.** We use the notation and assume the assumptions in Theorem 3.5. Let  $\mu$  be a Borel probability measure on  $\Omega$ . Let  $\nu$  be an arbitrary  $\sigma$ -finite Borel measure absolutely continuous with respect to  $\mu$  on  $\Omega$ . Suppose that  $x_1, \dots, x_N$  be the i.i.d. random variables with respect to  $\mu$ . Assume that the Radon-Nikodym derivative  $\partial_\mu \nu$  of  $\nu$  is an element of  $L^\infty(\mu)$ . We further assume that  $\mathcal{B}_{p,n}$  constitutes an orthogonal system in  $H$  and that  $V_{p,n} \subset L^2(\mu)$  (more precisely, any element of  $V_{p,n}$  is square integrable with respect to  $\mu$  and the natural map  $V_{p,n} \rightarrow L^2(\mu)$  is injective). Let  $\{u_i\}_{i=1}^{r_n}$  be an orthonormal basis of  $V_{p,n}$  in  $L^2(\nu)$ . We define  $\{q_{ij}\}_{i,j=1,\dots,r_n}$  by the complex numbers satisfying

$$u_i = \sum_{j=1}^{r_n} q_{ij} \nu_j.$$

For  $k, \ell \geq 0$ , let

$$\mathbf{Q}_{k,\ell}(\nu) := (q_{ij})_{i \leq r_k, j \leq r_\ell}.$$

Then, we have

$$\limsup_{N \rightarrow \infty} \left\| \mathbf{C}_{f,m}^* - \widehat{\mathbf{C}}_{m,n,N} \right\| \leq L_m \|\mathcal{E}_{p,n}\|_{L^2(\mu)} \|\mathbf{Q}_{n,m}(\nu)\|_{\text{op}} \quad \text{a.e.}, \quad (3.11)$$

where

$$L_m := \|\partial_\mu \nu\|_{L^\infty(\mu)} \|\mathbf{G}_m\|_{\text{op}} \|\mathbf{G}_m^{-1/2}\|_{\text{op}} \|C_f|_{V_{p,m}}\|_{\text{op}}.$$



*Proof.* We put  $\mathbf{Q}_{k,\ell} := \mathbf{Q}_{k,\ell}(\mathbf{v})$ . By definition of  $\mathbf{Q}_{n,n}$ , we have

$$\mathbf{I}_n = \mathbf{Q}_{n,n} \left( \langle v_i, v_j \rangle_{L^2(\mathbf{v})} \right)_{i,j=1,\dots,r_n} \mathbf{Q}_{n,n}^*.$$

Thus, we have

$$\mathbf{G}_n \left( \langle v_i, v_j \rangle_{L^2(\mathbf{v})} \right)_{i,j=1,\dots,r_n}^{-1} \mathbf{G}_n = \mathbf{G}_n \mathbf{Q}_{n,n}^* \mathbf{Q}_{n,n} \mathbf{G}_n.$$

By the law of large number, we have

$$\mathbf{G}_n (N^{-1} \mathbf{V}_n^{X_N} (\mathbf{V}_n^{X_N})^*)^{-1} \mathbf{G}_n \longrightarrow \left( \langle v_i, v_j \rangle_{L^2(\mu)} \right)_{i,j=1,\dots,r_n}^{-1} \quad \text{a.e.} \quad (3.12)$$

as  $N \rightarrow \infty$ . Since  $\mathbf{G}_n$  is a diagonal matrix, and the following matrix

$$\left( \|\partial_\mu \mathbf{v}\|_{L^\infty(\mu)} \langle v_i, v_j \rangle_{L^2(\mu)} - \langle v_i, v_j \rangle_{L^2(\mathbf{v})} \right)_{i,j=1,\dots,r_n}$$

is a positive semi-definite matrix by the assumption, we have

$$\lim_{N \rightarrow \infty} \|\mathbf{E}_{m,n}^{X_N}\|_{\text{op}}^{1/2} \leq \|\partial_\mu \mathbf{v}\|_{L^\infty(\mu)} \|\mathbf{G}_m \mathbf{Q}_{n,m}^* \mathbf{Q}_{n,m} \mathbf{G}_m\|_{\text{op}}^{1/2} \leq \|\mathbf{G}_m\|_{\text{op}} \|\partial_\mu \mathbf{v}\|_{L^\infty(\mu)} \cdot \|\mathbf{Q}_{n,m}\|_{\text{op}} \quad \text{a.e.}$$

by the convergence (3.12). Therefore, the inequality (3.11) follows from Theorem 3.5.  $\square$

**Remark 3.8.** Theorem 3.5 and Corollary 3.7 are equivalent (up to constant). In fact, Theorem 3.5 corresponds to Corollary 3.7 in the case of  $\mu = \mathbf{v} = \frac{1}{N} \sum_{i=1}^N \delta_{x_i}$

## 3.2 Several analysis with bounded Koopman operators

Here, we provide several results when  $C_f$  is bounded. Unfortunately, the Koopman operator on an RKHS is not necessarily bounded and only linear dynamical system can induce bounded Koopman operators in some cases, for example, on the RKHS of the Gaussian kernel [33] and the exponential kernel [12]. We can also show that a dynamical system around the fixed point is stable if the Koopman operator is bounded and any chaotic dynamical system is out of scope in the Koopman analysis on RKHS with boundedness [36]. However, there many examples and studies of bounded Koopman operators in the fields of complex analysis as well (see [80, 17, 68] and reference therein). It will be worth providing several results when the Koopman operator is bounded.

We show that the level sets of an eigenvector of  $C_f^*|_{V_{p,n}}$  for sufficiently large  $n$  provide invariant subsets, more generally, we have the following theorem:

**Proposition 3.9.** We assume that  $C_f$  is bounded on  $H$  and  $t'|_{\mathfrak{D}_p}$  is injective. Let  $\lambda_1, \dots, \lambda_d$  be the eigenvalues (with multiplicity) of the Jacobian matrix  $df_p$  and write  $\lambda := (\lambda_1, \dots, \lambda_d)$ . Let  $u_{\alpha,n} \in V_{p,n}$  be a unit eigenvector of  $C_f^*|_{V_{p,n}}$  associated with  $\lambda^\alpha$  for  $\alpha \in \mathbb{Z}_{\geq 0}^d$ . Then, for  $x \in \Omega$ , we have

$$|u_{\alpha,n}(f(x)) - \lambda^\alpha u_{\alpha,n}(x)| \leq \|C_f - \lambda^\alpha\|_{\text{op}} \mathcal{E}_{p,n}(x).$$

Moreover, for any compact subset  $K \subset \Omega$ ,

$$\sup_{x \in K} |u_{\alpha,n}(f(x)) - \lambda^\alpha u_{\alpha,n}(x)| \rightarrow 0$$

as  $n \rightarrow \infty$ .

*Proof.* Let  $x \in \Omega$  and let  $\tilde{v}_x := \pi_n k_x \in V_{n,p}$ . We have

$$\begin{aligned} u_{\alpha,n}(f(x)) &= \langle u_{\alpha,n}, C_f^* k_x \rangle_H \\ &= \langle C_f u_{\alpha,n}, k_x \rangle_H \\ &= \langle C_f u_{\alpha,n}, \tilde{v}_x \rangle + \langle C_f u_{\alpha,n}, k_x - \tilde{v}_x \rangle. \end{aligned}$$

Since

$$\langle C_f u_{\alpha,n}, \tilde{v}_x \rangle_H = \langle C_f^*|_{V_{n,p}}^* u_{\alpha,n}, \tilde{v}_x \rangle_H = \lambda^\alpha \langle u_{\alpha,n}, \tilde{v}_x \rangle_H,$$

combining with the Cauchy–Schwarz inequality, we have

$$|u_{\alpha,n}(f(x)) - \lambda^\alpha u_{\alpha,n}(x)| \leq \|(C_f - \lambda^\alpha)u_{\alpha,n}\|_H \mathcal{E}_{p,n}(x) \leq \|C_f - \lambda^\alpha\|_H \mathcal{E}_{p,n}(x).$$

The second statement follows from Proposition 2.15.  $\square$

Let  $\mu$  be a probability measure on  $\Omega$  and assume that  $\int_\Omega \sqrt{k(x,x)} d\mu < \infty$ . Let  $\Phi(\mu) \in H$  be the kernel mean embedding of  $\mu$ , that is the unique element such that  $\langle h, \Phi(\mu) \rangle = \int_\Omega h(x) d\mu(x)$  for all  $h \in H$ . For details of the theory for kernel mean embedding, see [56]. We define

$$\mathcal{E}_{p,n}(\mu) := \min_{v \in V_{p,n}} \|\Phi(\mu) - v\|_H.$$

For an integer  $m \geq 0$ , we define

$$\widehat{\Phi}_n^m(\mu) := C_{f^m}^* \pi_n \Phi(\mu).$$

Then,  $\widehat{\Phi}_n^m(\mu)$  will provide a prediction of the push-forward measure of  $\mu$  by  $f^m$  as follows:

**Proposition 3.10.** Assume that  $C_f$  is bounded on  $H$  and  $\int_\Omega \sqrt{k(x,x)} d\mu < \infty$ . Then, we have

$$\|\Phi(f_* \mu) - \widehat{\Phi}_n^m(\mu)\|_H \leq \|C_{f^m}\|_{\text{op}} \mathcal{E}_{p,n}(\mu).$$

*Proof.* Since  $\Phi_n^0(\mu)$  is the orthonormal projection of  $\Phi(\mu)$  to  $V_{p,n}$ , we see that

$$\mathcal{E}_{p,n}(\mu) = \|\Phi_n^0(\mu) - \Phi(\mu)\|.$$

Then, the statement follows since  $\Phi_n^m(\mu) = C_{f^m}^* \Phi_n^0(\mu)$  and  $C_{f^m}^* \Phi(\mu) = \Phi(f_*^m \mu)$ .  $\square$

## 4 Extended Koopman operators and rigged Hilbert spaces

Here, we explain the theory of rigged Hilbert space with the Gelfand triple. Then, we introduce the extended Koopman operator and show its Jordan–Chevalley decomposition and eigendecomposition. In this section, we always assume Assumption 2.13. We denote by  $\tau : H' \rightarrow H$  the anti-linear isomorphism of (2.6).

### 4.1 Rigged Hilbert spaces

First, we introduce the notion of the Gelfand triples. We explicitly describe some natural identifications appearing in typical description of the theory of Gelfand triple, and our definition is slightly different from the usual one.

**Definition 4.1.** Let  $H$  be a Hilbert space. Let  $\Phi$  and  $\Phi^*$  be locally convex Hausdorff topological spaces over  $\mathbb{C}$  equipped with a continuous pairing

$$\langle \cdot, \cdot \rangle : \Phi \times \Phi^* \longrightarrow \mathbb{C} \tag{4.1}$$

such that

$$\begin{aligned} \langle f, a\mu + b\xi \rangle &= \bar{a}\langle f, \mu \rangle + \bar{b}\langle f, \xi \rangle \\ \langle af + bg, \mu \rangle &= a\langle f, \mu \rangle + b\langle g, \mu \rangle \end{aligned}$$

for  $a, b \in \mathbb{C}$ ,  $f, g \in \Phi$ , and  $\mu, \xi \in \Phi^*$ . Assume that there exist injective continuous linear maps  $i : \Phi \rightarrow H$  and  $j : H \rightarrow \Phi^*$ . We call the triplet  $(\Phi, H, \Phi^*)$  with continuous injections  $i : \Phi \rightarrow H$  and  $j : H \rightarrow \Phi^*$  the *Gelfand triple* if the following conditions hold:

- (1)  $i(\Phi)$  is a dense subset of  $H$ ,
- (2) the natural anti-linear map  $\mathfrak{s} : \Phi^* \rightarrow \Phi'$ ;  $\mu \mapsto \langle \cdot, \mu \rangle$  is a bijective homeomorphism,
- (3) the pairing  $\langle \cdot, \cdot \rangle$  is compatible with the bilinear form  $\langle \cdot | \cdot \rangle$ , namely, for  $g \in \Phi$  and  $\mu \in \Phi^*$ ,

$$\langle g, \mu \rangle = \langle \mathfrak{s}(\mu) | g \rangle. \quad (4.2)$$

- (4) the pairing  $\langle \cdot, \cdot \rangle$  is compatible with the inner product  $\langle \cdot, \cdot \rangle_H$ , namely, for any  $g \in \Phi$ ,  $h \in H$ ,

$$\langle g, j(h) \rangle = \langle i(g), h \rangle_H. \quad (4.3)$$

We also call the Hilbert space equipped with the Gelfand triple *the rigged Hilbert space*.

The Gelfand triplet is introduced for further investigation of the spectrum of linear operators. We usually refer to the point spectrum computed via the ‘‘analytic continuation’’ with the Gelfand triplet as the resonance, the resonance poles, or the generalized eigenvalue, and they have been well studied in quantum mechanics. For more details of the mathematical formulation and application based on the Gelfand triplet, see [6, 13, 22, 23, 14] and references therein.

Using the Gelfand triple, we can define an extension of a linear operator, that will be used for defining the extended Koopman operator.

**Definition 4.2.** Let  $(\Phi, H, \Phi^*)$  be the Gelfand triple of a Hilbert space  $H$ . Let  $T : H \rightarrow H$  be a densely defined linear operator. Assume that the adjoint operator  $T^*$  satisfies  $T^*(i(\Phi)) \subset i(\Phi)$  and  $T^*|_{\Phi} := i^{-1}T^*i : \Phi \rightarrow \Phi$  is continuous. We define the continuous linear map  $T^\times : \Phi^* \rightarrow \Phi^*$  by the unique linear map satisfying

$$\langle f, T^\times \mu \rangle = \langle T^*|_{\Phi} f, \mu \rangle$$

for any  $\mu \in \Phi^*$  and  $f \in \Phi$ , equivalently,

$$T^\times := \mathfrak{s}^{-1}(T^*|_{\Phi})' \mathfrak{s}. \quad (4.4)$$

As in the following proposition, we may actually regard  $T^\times$  as an extension of  $T$  to  $\Phi^*$ .

**Proposition 4.3.** Let  $T : H \rightarrow H$  be a linear map with a dense domain  $D(T)$ . For  $h \in D(T)$ , we have  $jTh = T^\times jh$ .

*Proof.* It suffices to show that  $\mathfrak{s}jT = (T^*|_{\Phi})' \mathfrak{s}j$ . Let  $g \in \Phi$  be an arbitrary element. By direct computation, we have

$$\langle \mathfrak{s}jT(h) | g \rangle = \langle i(g), Th \rangle_H = \langle T^*i(g), h \rangle_H = \langle \mathfrak{s}j(h) | T^*(g) \rangle = \langle (T^*|_{\Phi})' \mathfrak{s}j(h) | g \rangle.$$

Thus,  $\mathfrak{s}jT = (T^*|_{\Phi})' \mathfrak{s}j$ . □

## 4.2 Extended Koopman operators

Here, we will define  $\Phi$  and  $\Phi^*$  to be the space of observables and a ‘‘limit’’ of the space of observables, respectively. Then, we will define the extended Koopman operator on  $\Phi^*$ .

Let  $f : \Omega \rightarrow \Omega$  be a map. Assume that Assumption 2.13 holds, that  $C_f : H \rightarrow H$  is densely defined, and that there exist  $p_1, \dots, p_r \in \Omega$  satisfying Assumption 3.1. Let

$$\Lambda := \{p_1, \dots, p_r\} \subset \Omega.$$

We define

$$V_{\Lambda, n} := \sum_{i=1}^r V_{p_i, n} \subset H. \quad (4.5)$$

Let  $\iota_{n,n+1} : V_{\Lambda,n} \rightarrow V_{\Lambda,n+1}$  be the inclusion map. We regard  $(V_{\Lambda,n}, \iota_{n,n+1})_n$  as an inductive system and define a locally convex space as the inductive limit of  $(V_{\Lambda,n}, \iota_{n,n+1})_n$ :

$$\Phi := \varinjlim V_{\Lambda,n}. \quad (4.6)$$

Namely, the space  $\Phi$  coincides  $\sum_{p \in \Lambda} V_p$  as a set and its topology is the strongest topology such that the inclusion map  $\iota_n : V_{\Lambda,n} \hookrightarrow \Phi$  is continuous for any  $n \geq 0$ . We define the injection  $i : \Phi \rightarrow H$  as the inclusion map.

Let  $\pi_{n+1,n} : V_{\Lambda,n+1} \rightarrow V_{\Lambda,n}$  be the orthogonal projection. Then,  $(V_{\Lambda,n}, \pi_{n+1,n})$  constitutes a projective system. Then, we define  $\Phi^*$  as the projective limit  $\varprojlim V_{\Lambda,n}$ , that is defined within the direct product of  $V_{\Lambda,n}$ 's as follows:

$$\Phi^* := \varprojlim V_{\Lambda,n} := \left\{ (\mu_n)_n \in \prod_{n=0}^{\infty} V_{\Lambda,n} : \pi_{n+1,n}(\mu_{n+1}) = \mu_n \right\} \subset \prod_{n=0}^{\infty} V_{\Lambda,n}. \quad (4.7)$$

Recall  $\pi_n : H \rightarrow V_{p,n}$  is the orthogonal projection (2.7). Then, we define the injection  $j : H \rightarrow \Phi^*$  by  $j(h) := (\pi_n(h))_{n=0}^{\infty}$ . We define a pairing

$$\langle \cdot, \cdot \rangle : \Phi \times \Phi^* \longrightarrow \mathbb{C}; (h, (g_n)_n) \mapsto \lim_{n \rightarrow \infty} \langle h, g_n \rangle_H. \quad (4.8)$$

Then, we have the following proposition:

**Proposition 4.4.** The triplet  $(\Phi, H, \Phi^*)$  defined as above is a Gelfand triple.

*Proof.* The condition (1) follows from Proposition 2.14. Regarding the condition (2), by [42, Theorem 12], the natural map  $\Phi' \rightarrow \varprojlim V'_{\Lambda,n}$ ;  $\mu \mapsto (\mu|_{V_{\Lambda,n}})_n$  induces an isomorphism. Since the inner product induces an anti-linear isomorphism  $V_{\Lambda,n} \cong V'_{\Lambda,n}$ , we have the isomorphism  $\mathfrak{s}$  in (2) as the composition of the above isomorphisms. Other two conditions are obvious.  $\square$

By (1) of Theorem 2.12,  $C_f^*(\Phi) \subset \Phi$  holds. Thus, we define the *extended Koopman operator*

$$C_f^\times : \Phi^* \rightarrow \Phi^* \quad (4.9)$$

by Definition 4.2. If a family of linear maps  $\{A_n : V_{\Lambda,n} \rightarrow V_{\Lambda,n}\}_{n=0}^{\infty}$  satisfies  $A_n \pi_{n+1,n} = \pi_{n+1,n} A_{n+1}$ , we can define the continuous linear map

$$\lim A_n : \Phi^* \rightarrow \Phi^*; (g_n) \rightarrow (A_n g_n).$$

Using this notation, the extended Koopman operator  $C_f^\times$  has an explicit description:

**Proposition 4.5.** We regard  $C_f^*|_{V_{\Lambda,n}}$  as a linear map on  $V_{\Lambda,n}$  and denote its adjoint in  $V_{\Lambda,n}$  by  $(C_f^*|_{V_{\Lambda,n}})^*$ . Then, we have

$$C_f^\times = \lim (C_f^*|_{V_{\Lambda,n}})^* \quad (4.10)$$

*Proof.* Since  $(C_f^*|_{V_{\Lambda,n}})^* \pi_{n+1,n} = \pi_{n+1,n} (C_f^*|_{V_{\Lambda,n+1}})^*$ , it follows from the equivalent definition (4.4) of  $C_f^\times$ .  $\square$

Moreover, if  $C_f$  satisfies Assumption 3.2, we have a more explicit description as follows:

**Theorem 4.6.** Assume that  $C_f$  satisfies Assumption 3.2. Then, we have

$$(C_f^*|_{V_{\Lambda,n}})^* = \pi_n C_f \iota_n. \quad (4.11)$$

In particular,

$$C_f^\times = \lim \pi_n C_f \iota_n. \quad (4.12)$$

*Proof.* The second statement follows from Proposition 4.5. We prove the first statement. It suffices to show that  $\langle (C_f^*|_{V_{\Lambda,n}})^* g, h \rangle_H = \langle \pi_n C_f g, h \rangle_H$  for any  $g, h \in V_{\Lambda,n}$ . It is proved via the direct calculation as follows:

$$\langle (C_f^*|_{V_{\Lambda,n}})^* g, h \rangle_H = \langle g, C_f^*|_{V_{\Lambda,n}} h \rangle_H = \langle C_f g, h \rangle_H = \langle \pi_n C_f g, h \rangle_H.$$

□

Each map  $\pi_n C_f \iota_n$  in Theorem 4.6 is known as a finite approximation through projection into a finite dimensional subspace, that always appears when approximating the Koopman operator. Theorem 4.6 provides a crucial fact that  $\pi_n C_f \iota_n$ 's form a projective system, meaning that they are commutative with projections:

$$\pi_{n+1,n}(\pi_{n+1} C_f \iota_{n+1}) = (\pi_n C_f \iota_n) \pi_{n+1,n}.$$

This fact is important as they give not only the approximation of the extended Koopman operator, but also the consistent family of eigenvectors. Moreover, according to Theorem 3.5,  $\pi_n C_f \iota_n$  is the adjoint of a matrix that can be estimated in a data-driven manner. In this sense, the spaces  $V_{\Lambda,n}$ 's of the intrinsic observables constructed from the jets provide an appropriate series of subspaces that enables the correct finite approximation of the Koopman operators.

### 4.3 Eigendecomposition of the extended Koopman operators

We use the same notation as in Section 4.2. First, we describe the ‘‘Jordan–Chevalley decompositions’’ of the Perron–Frobenius operator  $C_f^*|_{\Phi}$  and the extended Koopman operator  $C_f^\times$ :

**Theorem 4.7.** Suppose that Assumption 2.13 holds and that  $C_f$  is densely defined. Let  $r_n := \dim V_{\Lambda,n}$ . Then, there exist continuous linear operators  $S_f^\times, N_f^\times : \Phi^* \rightarrow \Phi^*$  and  $S_f, N_f : \Phi \rightarrow \Phi$  such that

$$\begin{aligned} C_f^\times &= S_f^\times + N_f^\times, \\ C_f^*|_{\Phi} &= S_f + N_f, \end{aligned}$$

with the following properties:

- (1) there exist a family of complex numbers  $\{\gamma_i\}_{i=1}^\infty$  and those of vectors  $\{w_i\}_{i=1}^\infty \subset \Phi$  and  $\{u_i\}_{i=1}^\infty \subset \Phi^*$  such that  $\{w_i\}_{i=1}^{r_n}$  constitutes a basis of  $V_{\Lambda,n}$ , and

$$\begin{aligned} S_f^\times u_i &= \gamma_i u_i, \\ S_f w_i &= \bar{\gamma}_i w_i, \\ \langle u_i, w_j \rangle &= \delta_{i,j} \end{aligned}$$

for positive integers  $i, j \geq 1$ , and

$$\begin{aligned} S_f^\times u &= \sum_{i=1}^\infty \gamma_i \langle w_i, u \rangle u_i, \\ S_f w &= \sum_{i=1}^\infty \bar{\gamma}_i \langle w, u_i \rangle w_i \end{aligned}$$

hold for  $u \in \Phi^*$  and  $w \in \Phi$ , where the two convergence on the right hand sides are in the topologies of  $\Phi^*$  and  $\Phi$ , respectively,

- (2) for each  $u \in \Phi^*$ ,  $(N_f^\times)^n u \rightarrow 0$  as  $n \rightarrow \infty$ ,  
(3) for each  $w \in \Phi$ , there exists  $n \geq 0$  such that  $N_f^n w = 0$ ,  
(4)  $S_f N_f = N_f S_f$  and  $S_f^\times N_f^\times = S_f^\times N_f^\times$ .

*Proof.* Let  $C_f^*|_{V_{\Lambda,n}} = S_{f,n} + N_{f,n}$  be the Jordan–Chevalley decomposition (see, for example, [7, Proposition 4.2]), namely,  $S_{f,n} : V_{\Lambda,n} \rightarrow V_{\Lambda,n}$  is diagonalizable,  $N_{f,n} : V_{\Lambda,n} \rightarrow V_{\Lambda,n}$  is nilpotent, and  $S_{f,n}N_{f,n} = N_{f,n}S_{f,n}$ . Then, by the uniqueness of the Jordan–Chevalley decomposition, we have  $S_{f,n+1}|_{V_{\Lambda,n}} = S_{f,n}$  and  $N_{f,n+1}|_{V_{\Lambda,n}} = N_{f,n}$ . We define  $S_f, N_f : \Phi \rightarrow \Phi$  by the linear map such that  $S_{fg} := S_{f,n}g$  and  $N_{fg} := N_{f,n}g$  for  $g \in V_{p,n}$ . Since  $S_{f,n}^*$ 's and  $N_{f,n}^*$ 's constitute projective systems, they induce linear maps  $S_f^\times := \lim S_{f,n}^*$  and  $N_f^\times := \lim N_{f,n}^*$  on  $\Phi^*$ . By definition, the linear maps satisfy (2), (3), and (4).

Since each  $S_{f,n}$  is diagonalizable and  $S_{f,n+1}|_{V_{\Lambda,n}} = S_{f,n}$ , there exist  $\{\gamma_i\}_{i=1}^\infty \subset \mathbb{C}$  and  $\{w_i\}_{i=1}^\infty \subset \Phi$  such that the set  $W_n := \{w_i\}_{i=1}^n$  spans  $V_{\Lambda,n}$  for any  $n \geq 0$  and

$$S_f w_i = \bar{\gamma}_i w_i \quad (4.13)$$

holds. Let  $i \leq r_n$  be an arbitrary positive integer. Since the orthogonal complement of  $W_n \setminus \{w_i\}$  in  $V_{\Lambda,n}$  is 1-dimensional, there uniquely exists  $u_{i,n} \in V_{\Lambda,n}$  such that

$$\langle w_i, u_{i,n} \rangle_H = 1.$$

Since  $\langle w_i, S_{f,n}^* u_{i,n} - \gamma_i u_{i,n} \rangle_{V_{\Lambda,n}} = 0$  for all  $j = 1, \dots, r_n$ , we see that  $S_{f,n}^* u_{i,n} - \gamma_i u_{i,n}$  is orthogonal to all the elements of  $W_n$ , resulting in  $S_{f,n}^* u_{i,n} = \gamma_i u_{i,n}$ . Thus, for any  $i, j \leq r_n$ , we have  $\langle \pi_{n+1,n} u_{i,n+1}, w_j \rangle_H = \langle u_{i,n}, w_j \rangle_H = \delta_{i,j}$ , thus  $\pi_{n+1,n} u_{i,n+1} = u_{i,n}$ . Therefore,  $u_i := (u_{i,n})_{n=1}^\infty$  determines an element of  $\Phi^*$  and satisfies

$$\begin{aligned} S_f^\times u_i &= \gamma_i u_i, \\ \langle w_i, u_j \rangle &= \delta_{i,j}. \end{aligned}$$

for all  $i, j \in \mathbb{Z}_{\geq 0}$ . By combining this with (4.13), we have the first statement of (1). The second statement of (1) is obvious.  $\square$

**Remark 4.8.** Let  $\lambda_{i,1}, \dots, \lambda_{i,d}$  be the eigenvalues (with multiplicity) of the Jacobian matrix  $df_{p_i}$  at the fixed point  $p_i$ . Let  $\lambda_i := (\lambda_{i,1}, \dots, \lambda_{i,d})$ . Assume that  $l'|_{\sum_{i=1}^r \mathfrak{D}_{p_i}} : \sum_{i=1}^r \mathfrak{D}_{p_i} \rightarrow H'$  is injective. Then,  $\{\lambda_i^\alpha : i = 1, \dots, r, \alpha \in \mathbb{Z}_{\geq 0}^d\}$  coincides with the family  $\{\gamma_i\}_{i=1}^\infty$  of complex numbers introduced in Theorem 4.7.

The extended Koopman operator  $C_f^\times$  are diagonalizable if the multiplications of the eigenvalues of the Jacobian of  $f$  at  $p_i$  are distinct for each fixed point  $p_i$ , the Perron–Frobenius operator  $C_f^*|_\Phi$  as in the following corollary:

**Corollary 4.9.** Let  $\lambda_{i,1}, \dots, \lambda_{i,d}$  be the eigenvalues (with multiplicity) of the Jacobian matrix  $df_{p_i}$  at the fixed point  $p_i$ . Let  $\lambda_i := (\lambda_{i,1}, \dots, \lambda_{i,d})$ . Assume that  $l'|_{\sum_{i=1}^r \mathfrak{D}_{p_i}} : \sum_{i=1}^r \mathfrak{D}_{p_i} \rightarrow H'$  is injective and that  $\lambda_i^\alpha \neq \lambda_i^\beta$  for  $\alpha, \beta \in \mathbb{Z}_{\geq 0}^d$  with  $\alpha \neq \beta$ . Then, there exist families of vectors  $\{w_{i,\alpha}\}_{i \in \{1, \dots, r\}, \alpha \in \mathbb{Z}_{\geq 0}^d} \subset \Phi$  and  $\{u_{i,\alpha}\}_{i \in \{1, \dots, r\}, \alpha \in \mathbb{Z}_{\geq 0}^d} \subset \Phi^*$  such that

$$\begin{aligned} C_f^\times u_{i,\alpha} &= \lambda_i^\alpha u_{i,\alpha}, \\ C_f^* w_{i,\alpha} &= \bar{\lambda}_i^\alpha w_{i,\alpha}, \\ \langle u_{i,\alpha}, w_{j,\beta} \rangle &= \delta_{(i,\alpha),(j,\beta)} \end{aligned}$$

for all  $i, j \in \{1, \dots, r\}$ ,  $\alpha, \beta \in \mathbb{Z}_{\geq 0}^d$ , and

$$\begin{aligned} C_f^\times u &= \sum_{i \in \{1, \dots, r\}, \alpha \in \mathbb{Z}_{\geq 0}^d} \lambda_i^\alpha \langle w_{i,\alpha}, u \rangle u_{i,\alpha}, \\ C_f^* w &= \sum_{i \in \{1, \dots, r\}, \alpha \in \mathbb{Z}_{\geq 0}^d} \bar{\lambda}_i^\alpha \langle w, u_{i,\alpha} \rangle w_{i,\alpha} \end{aligned}$$

for  $u \in \Phi^*$  and  $w \in \Phi$ , where the two convergence on the right hand sides are in  $\Phi^*$  and  $\Phi$ , respectively.

*Proof.* It follows from Theorem 4.7.  $\square$

According to Corollary 4.9, the extended Koopman operator  $C_f^\times$  has eigenvectors under fairly mild conditions. However, it is important to emphasize that these eigenvectors are not the eigenfunctions of the Koopman operator  $C_f$  itself. Nevertheless, as shown in the following proposition, they can be considered as eigenvectors approximately.

**Proposition 4.10.** Assume that  $C_f$  satisfies Assumption 3.2. Let  $(g_n)_n \in \Phi^*$  be an eigenvector of the eigenvalue  $\lambda$  of  $C_f^\times$ . Then,  $C_f g_n - \lambda g_n \in V_{\Lambda, n}^\perp$ .

*Proof.* Let  $h \in V_{\Lambda, n}$ . By Proposition 4.11, we have  $\pi_n C_f g_n = \lambda g_n$ . Thus, we have

$$\langle C_f g_n - \lambda g_n, h \rangle_H = \langle \pi_n C_f g_n - \lambda g_n, h \rangle_H = 0.$$

Therefore,  $C_f g_n - \lambda g_n \in V_{\Lambda, n}^\perp$ .  $\square$

## 5 Corresponding results to continuous dynamical systems

Here, we explain the corresponding theory for continuous dynamical systems, and derive the results on the generator of Koopman operators. As the Koopman operators for the flow maps of a continuous dynamical system constitute a semigroup, we can consider the derivative of the Koopman operators at time 0. We define the generator of the Koopman operator as the derivative of the Koopman operators at time 0. The behavior of the generator of the Koopman operators is generally tamer and more controllable than that of the Koopman operators. Moreover, we may reconstruct the Koopman operators as the image of the generator under the exponential map. Therefore, the elucidating the mathematical properties of the generators is a significant issue as well as the Koopman operators in the context of continuous dynamical system.

We use the notation introduced in Section 2. Let  $F = (F_1, \dots, F_d) : \Omega \rightarrow \mathbb{R}^d$  be a map of class  $C^\infty$ . We consider the ordinary differential equation:

$$\frac{dz}{dt} = F(z). \quad (5.1)$$

For  $x \in \Omega$  and an element  $t$  of an open interval containing 0, we denote  $z(t)$  with  $z(0) = x$  by  $\phi^t(x)$ . We will assume the following assumption for some  $p \in \Omega$ :

**Assumption 5.1.**  $p \in \Omega$  is an equilibrium point of  $F$ , namely  $F(p) = 0$ .

### 5.1 The generator of Koopman operators on the canonical invariant subspaces

We define the continuous linear map  $\mathcal{A}_F : \mathfrak{E}(\Omega) \rightarrow \mathfrak{E}(\Omega)$  by

$$\mathcal{A}_F(h) := \lim_{t \rightarrow 0} \frac{h \circ \phi^t - h}{t} = \sum_{i=1}^d F_i \frac{\partial h}{\partial x_i} = F^\top \nabla h. \quad (5.2)$$

Then, we have the corresponding statements to Proposition 2.4:

**Proposition 5.2.** (1) For each  $n \geq 0$ ,  $\mathcal{A}_F^n(\mathfrak{D}_{p, n}) \subset \mathfrak{D}_{p, n}$ .

(2) Let  $\text{gr}_{\mathcal{A}_F}^n : \mathfrak{D}_{p, n} / \mathfrak{D}_{p, n-1} \rightarrow \mathfrak{D}_{p, n} / \mathfrak{D}_{p, n-1}$  be the linear map induced by  $\mathcal{A}_F^n$  via (1). Then, we have

$$\text{gr}_{\mathcal{A}_F}^n = \rho_n^{-1} \circ T_n(dF_p) \circ \rho_n, \quad (5.3)$$

where  $T_n(dF_p)$  is the linear map on  $\mathbb{C}[X_1, \dots, X_d]_n$  defined by

$$T_n(dF_p)(Q(X_1, \dots, X_d)) := (X_1, \dots, X_d) \cdot dF_p \cdot \nabla Q(X_1, \dots, X_d)$$

- (3) Let  $\mathbf{A}_{F,n}^* \in \mathbb{C}^{\binom{n+d}{d} \times \binom{n+d}{d}}$  be the representation matrix of  $\mathcal{A}'_F|_{\mathfrak{D}_{p,n}} : \mathfrak{D}_{p,n} \rightarrow \mathfrak{D}_{p,n}$  with respect to the basis  $\{\delta_p^{(\alpha)} : |\alpha| \leq n\}$ . Then,  $\mathbf{A}_{F,n}^*$  is in the form of

$$\mathbf{A}_{F,n}^* = \begin{pmatrix} 1 & * & * & * \\ 0 & \mathbf{K}_{p,1} & * & * \\ \vdots & \ddots & \ddots & \vdots \\ 0 & \cdots & 0 & \mathbf{K}_{p,n} \end{pmatrix}, \quad (5.4)$$

where  $\mathbf{K}_{p,i}$  is the representation matrix of  $T_i(dF_p)$  with respect to the basis  $\{X_1^{\alpha_1} \cdots X_d^{\alpha_d} : |\alpha| = i\} \subset \mathbb{C}[X_1, \dots, X_d]$ .

- (4) Let  $\mu_1, \dots, \mu_d$  be the eigenvalues (with multiplicity) of the Jacobian matrix  $dF_p$  and let  $\mu := (\mu_1, \dots, \mu_d)$ . Then, the set of eigenvalues of  $\mathcal{A}'_F|_{\mathfrak{D}_{p,n}}$  is

$$\{\alpha^\top \mu : |\alpha| \leq n\}.$$

*Proof.* We only give the proof of (1) as the other statements are proved in the same way as in the proof of Proposition 2.4. By Proposition 2.2, it suffices to show that  $\mathcal{A}'_F \delta_p^{(\alpha)} \in \mathfrak{D}_{p,n}$ . Let  $h \in \mathfrak{E}(\Omega)$ . Then, by direct calculation, we have

$$\langle \mathcal{A}'_F \delta_p^{(\alpha)} | h \rangle = \langle \delta_p^{(\alpha)} | F \cdot \nabla h \rangle = F(p)^\top \nabla (\partial_x^\alpha h)(p) + \langle D | h \rangle$$

for some  $D \in \mathfrak{D}_{p,n}$ . Since  $F(p) = 0$ , we have  $D = \mathcal{A}'_F \delta_p^{(\alpha)} \in \mathfrak{D}_{p,n}$ .  $\square$

## 5.2 The generators of the Koopman operators on reproducing kernel Hilbert spaces

Here, we use the same notation as those in Sections 3, 5.1, and 5.2. Let  $H \subset \mathfrak{E}(\Omega)$  be a Hilbert space and assume that Assumption 2.5 holds. We denote the corresponding positive definite kernel by  $k \in \mathfrak{E}(\Omega \times \Omega)$ . We define the linear operator  $A_F : H \rightarrow H$  by

$$A_F(h) := \sum_{i=1}^d F_i \frac{\partial h}{\partial x_i} = F^\top \nabla h. \quad (5.5)$$

First, we state the corresponding results to Proposition 2.11 and Theorem 2.12. We omit the proofs of these statements as they are the same as the corresponding ones.

**Proposition 5.3.** Assume that  $A_F$  is densely defined. Then, for any  $\ell \in \mathfrak{E}(\Omega)$ , we have  $(\tau \circ \iota')(\ell) \in D(A_F^*)$ . In particular,  $V_p \subset D(A_F^*)$ .

**Theorem 5.4.** Assume that Assumption 5.1 for some  $p \in \Omega$  holds and  $A_F$  is densely defined. Then, we have the following statement:

- (1)  $A_F^*(V_{p,n}) \subset V_{p,n}$  for all  $n \geq 0$ .
- (2) Assume that  $(\tau \circ \iota')|_{\mathfrak{D}_p} : \mathfrak{D}_p \rightarrow H$  is injective. Then, the set of the eigenvalues of  $A_F^*$  is

$$\{\alpha^\top \mu : |\alpha| \leq n\},$$

where  $\mu_1, \dots, \mu_d$  are the eigenvalues (with multiplicity) of the Jacobian matrix  $dF_p$  and let  $\mu := (\mu_1, \dots, \mu_d)$ .

We note the relation between  $A_F$  and  $C_{\phi^t}$  as in the following proposition:

**Proposition 5.5.** Let  $t \geq 0$ . Assume that  $\phi^t(x)$  exists for any  $x$  (meaning the ODE (5.1) can be solved until the time  $t$  for any initial point). Assume that  $A_F$  is densely defined. Then, for any integer  $n \geq 0$ , we have

$$C_{\phi^t}^*|_{V_{p,n}} = \exp(tA_F^*|_{V_{p,n}}). \quad (5.6)$$



*Proof.* Since  $p$  is the fixed point of  $\phi^s$  for all  $0 \leq s \leq t$ ,  $C_{\phi^t}^*$  and  $A_F^*$  induce the linear map on the finite dimensional subspace  $V_{p,n}$ . The statement follows from the following ordinary differential equation:

$$\frac{d}{dt} C_{\phi^t}^*|_{V_{p,n}} = A_F^*|_{V_{p,n}} C_{\phi^t}^*|_{V_{p,n}}$$

□

### 5.3 Estimation of the generators

We use the same notation and assumptions as those in Section 3 and the previous sections. We will further assume the following condition:

**Assumption 5.6** (Domain condition for  $A_F$ ).  $V_p \subset D(A_F)$ .

We provide a useful sufficient condition for Assumption 5.6 as in the following proposition.

**Proposition 5.7.** Assume that  $V_p$  is closed under differential operators and  $F_i h \in H$  for any  $h \in V_p$  for  $i = 1, \dots, d$ . Then, the domain of  $A_F$  contains  $V_p$ .

*Proof.* Since each component of  $F_i \partial_{x_i} h$  is in  $H$  for any  $h \in V_p$  and  $i = 1, \dots, d$  by the assumptions, it follows from (5.5). □

We have more detailed sufficient condition for Assumption 5.6 for special positive definite kernels in Section 6.3.

**Remark 5.8.** Since the multiplication map  $h \mapsto F_i h$  is a closed operator, the condition  $F_i h \in H$  for all  $h \in H$  is equivalent to the boundedness of  $h \mapsto F_i h$ .

As in Section 3.1, let  $r_n := \dim V_{p,n}$ . We fix a basis  $\mathcal{B}_p = \{v_n\}_{n \geq 0}$  of  $V_p$  such that  $\mathcal{B}_{p,n} = \{v_i\}_{i=1, \dots, r_n}$  constitutes a basis of  $V_{p,n}$ . Then, for  $x \in \Omega$  and  $X = (x_1, \dots, x_N) \in \Omega^N$ , we define

$$\mathbf{v}_n(x) := \left( \overline{v_i(x)} \right)_{i=1}^{r_n}, \quad \mathbf{G}_n := (\langle v_i, v_j \rangle_H)_{i,j=1, \dots, r_n}, \quad \mathbf{V}_n^X := (\mathbf{v}_n(x_1), \dots, \mathbf{v}_n(x_N)).$$

We also define

$$\mathbf{W}_m^{X_N, F(X_N)} := \sum_{i=1}^d (F_i(x_1) \partial_{x_i} \mathbf{v}_n(x_1), \dots, F_i(x_N) \partial_{x_i} \mathbf{v}_n(x_N)). \quad (5.7)$$

Then, we have the corresponding results to Theorem 3.5 and Corollary 3.7 (we omit the proofs of these results as they are proved in the same way):

**Theorem 5.9.** Let  $p \in \Omega$ . Let  $m, n \geq 0$  be integers with  $m \leq n$ . Let  $\mathbf{A}_{F,m}^*$  be the representation matrix of  $A_F^*|_{V_{p,m}}$  with respect to  $\mathcal{B}_{p,m}$ . Let  $X_N := (x_1, \dots, x_N) \in \Omega^N$  and  $Y_N := (y_1, \dots, y_N) \in \Omega^N$  such that  $f(x_i) = y_i$  for  $i = 1, \dots, N$ . We assume Assumption 2.13,  $r_n \leq N$ ,  $\text{span}(\{\pi_n k_{x_1}, \dots, \pi_n k_{x_N}\}) = V_{p,n}$ , and that  $p$  satisfies Assumptions 5.1 and 5.6. We define the matrices  $\widehat{\mathbf{A}}_{m,n,N}$  and  $\mathbf{E}_{m,n}^{X_N}$  of size  $r_m$  by the leading principal minor matrices of order  $r_m$  as follows:

$$\begin{aligned} \mathbf{G}_m^{-1} \mathbf{W}_m^{X_N, F(X_N)} (\mathbf{V}_n^{X_N})^\dagger \mathbf{G}_n &= \begin{pmatrix} \widehat{\mathbf{A}}_{m,n,N} & * \\ & * \end{pmatrix}, \\ \mathbf{G}_n (N^{-1} \mathbf{V}_n^{X_N} (\mathbf{V}_n^{X_N})^*)^{-1} \mathbf{G}_n &= \begin{pmatrix} \mathbf{E}_{m,n}^{X_N} & * \\ * & * \end{pmatrix}. \end{aligned}$$

Then, we have

$$\left\| \mathbf{A}_{F,m}^* - \widehat{\mathbf{A}}_{m,n,N} \right\| \leq \|A_F|_{V_{p,m}}\|_{\text{op}} \|\mathbf{G}_m^{-1/2}\|_{\text{op}} \cdot \|\mathbf{E}_{m,n}^{X_N}\|_{\text{op}}^{1/2} \sqrt{\frac{1}{N} \sum_{i=1}^N \mathcal{E}_{p,n}(x_i)^2}. \quad (5.8)$$

**Corollary 5.10.** We use the same notation and assume the assumptions in Theorem 5.9. Let  $\mu$  be a Borel probability measure on  $\Omega$ . Let  $\nu$  be an arbitrary  $\sigma$ -finite Borel measure absolutely continuous with respect to  $\mu$  on  $\Omega$ . Suppose that  $x_1, \dots, x_N$  be the i.i.d. random variables with respect to  $\mu$ . Assume that the Radon-Nikodym derivative  $\partial_\mu \nu$  of  $\nu$  is an element of  $L^\infty(\mu)$ . We further assume that  $\mathcal{B}_{p,n}$  constitutes an orthogonal system in  $H$  and that  $V_{p,n} \subset L^2(\mu)$  (more precisely, any element of  $V_{p,n}$  is square integrable with respect to  $\mu$  and the natural map  $V_{p,n} \rightarrow L^2(\mu)$  is injective). We define  $\{q_{ij}\}_{i,j=1,\dots,r_n}$  by the complex numbers satisfying

$$u_i = \sum_{j=1}^{r_n} q_{ij} \nu_j.$$

For  $k, \ell \geq 0$ , let

$$\mathbf{Q}_{k,\ell}(\nu) := (q_{ij})_{i \leq r_k, j \leq r_\ell}.$$

Then, we have

$$\limsup_{N \rightarrow \infty} \left\| \mathbf{A}_{F,m}^* - \widehat{\mathbf{A}}_{m,n,N} \right\| \leq L_m \|\mathcal{E}_{p,n}\|_{L^2(\mu)} \|\mathbf{Q}_{n,m}(\nu)\|_{\text{op}} \quad \text{a.e.}, \quad (5.9)$$

where

$$L_m := \|\partial_\mu \nu\|_{L^\infty(\mu)} \|\mathbf{G}_m\|_{\text{op}} \|\mathbf{G}_m^{-1/2}\|_{\text{op}} \|A_F|_{V_{p,m}}\|_{\text{op}}.$$

## 5.4 Eigendecompositions of the generator of Koopman operators

Here, we use the notation introduced in Section 4. We assume that Assumption 2.13 holds and that there exist  $p_1, \dots, p_r \in \Omega$  satisfying Assumption 3.1 and define  $\Lambda := \{p_1, \dots, p_r\} \subset \Omega$ . The corresponding results to Theorem 4.7 and Corollary 4.9 are as follows:

**Theorem 5.11.** Suppose that Assumption 2.13 holds and that  $A_F$  is densely defined. Let  $r_n := \dim V_{\Lambda,n}$ . Then, there exist continuous linear operators  $S_F^\times, N_F^\times : \Phi^* \rightarrow \Phi^*$  and  $S_F, N_F : \Phi \rightarrow \Phi$  such that

$$\begin{aligned} A_F^\times &= S_F^\times + N_F^\times, \\ A_F^*|_\Phi &= S_F + N_F, \end{aligned}$$

with the following properties:

- (1) there exist a family of complex numbers  $\{\gamma_i\}_{i=1}^\infty$  and those of vectors  $\{w_i\}_{i=1}^\infty \subset \Phi$  and  $\{u_i\}_{i=1}^\infty \subset \Phi^*$  such that  $\{w_i\}_{i=1}^{r_n}$  constitutes a basis of  $V_{\Lambda,n}$ , and

$$\begin{aligned} S_F^\times u_i &= \gamma_i u_i, \\ S_F w_i &= \bar{\gamma}_i w_i, \\ \langle u_i, w_j \rangle &= \delta_{i,j} \end{aligned}$$

for positive integers  $i, j \geq 1$ , and

$$\begin{aligned} S_F^\times u &= \sum_{i=1}^{\infty} \gamma_i \langle w_i, u \rangle u_i, \\ S_F w &= \sum_{i=1}^{\infty} \bar{\gamma}_i \langle w, u_i \rangle w_i \end{aligned}$$

for  $u \in \Phi^*$  and  $w \in \Phi$ , where the convergences on the right hand sides are in the topologies of  $\Phi^*$  and  $\Phi$ , respectively,

- (2) for each  $u \in \Phi^*$ ,  $(N_F^\times)^n u \rightarrow 0$  as  $n \rightarrow \infty$ ,  
(3) for each  $w \in \Phi$ , there exists  $n \geq 0$  such that  $N_F^n w = 0$ ,

(4)  $S_F N_F = N_F S_F$  and  $S_F^\times N_F^\times = N_F^\times S_F^\times$ .

**Corollary 5.12.** Let  $\mu_{i,1}, \dots, \mu_{i,d}$  be the eigenvalues (with multiplicity) of the Jacobian matrix  $dF_{p_i}$  at the equilibrium point  $p_i$ . Let  $\mu_i := (\mu_{i,1}, \dots, \mu_{i,d})$ . Assume that  $\mu_i^\top \alpha \neq \mu_i^\top \beta$  for  $\alpha, \beta \in \mathbb{Z}_{\geq 0}^d$  satisfying  $\alpha \neq \beta$ . Then, there exists a family of vectors  $\{w_{i,\alpha}\}_{i \in \{1, \dots, r\}, \alpha \in \mathbb{Z}_{\geq 0}^d} \subset \Phi$  and  $\{u_{i,\alpha}\}_{i \in \{1, \dots, r\}, \alpha \in \mathbb{Z}_{\geq 0}^d} \subset \Phi^*$  such that

$$\begin{aligned} A_F^\times u_\alpha &= \mu_i^\top \alpha u_{i,\alpha}, \\ A_F w_\alpha &= \overline{\mu_i^\top \alpha} w_{i,\alpha}, \\ \langle u_{i,\alpha}, w_{j,\beta} \rangle &= \delta_{(i,\alpha),(j,\beta)} \end{aligned}$$

for all  $i, j \in \{1, \dots, r\}$ ,  $\alpha, \beta \in \mathbb{Z}_{\geq 0}^d$ , and

$$\begin{aligned} A_F^\times u &= \sum_{i \in \{1, \dots, r\}, \alpha \in \mathbb{Z}_{\geq 0}^d} \mu_i^\top \alpha \langle w_{i,\alpha}, u \rangle u_{i,\alpha}, \\ A_F w &= \sum_{i \in \{1, \dots, r\}, \alpha \in \mathbb{Z}_{\geq 0}^d} \overline{\mu_i^\top \alpha} \langle w, u_{i,\alpha} \rangle w_{i,\alpha} \end{aligned}$$

for  $u \in \Phi^*$  and  $w \in \Phi$ , where the convergences on the right hand sides are in  $\Phi^*$  and  $\Phi$ , respectively.

## 6 Estimations with the exponential kernels and Gaussian kernels

Here, we introduce the Gaussian kernel and the exponential kernel, where Assumption 2.13 trivially holds, and discuss their properties. We precisely estimate the right hand sides of Corollaries 3.7 and 5.10 and finally prove the explicit convergence rate for JetDMD. In this section, we will use the notation introduced in Section 3 and set  $\Omega = \mathbb{R}^d$ . We denote by  $L^2(\mathbb{R}^d)$  the  $L^2$ -space with respect to the Lebesgue measure on  $\mathbb{R}^d$  and define the Fourier transform  $\mathcal{F}[h]$  for  $h \in L^2(\mathbb{R}^d)$  by

$$\mathcal{F}[h](\xi) := \frac{1}{(2\pi)^{d/2}} \int_{\mathbb{R}^d} h(x) e^{-ix^\top \xi} dx. \quad (6.1)$$

### 6.1 Exponential kernels and Gaussian kernels

For  $\sigma > 0$  and  $b \in \mathbb{R}^d$ , we denote by  $H^e(\sigma, b)$  the RKHS associated with the *exponential kernel* defined by

$$k^e(x, y) = e^{\frac{(x-b)^\top (y-b)}{\sigma^2}}. \quad (6.2)$$

For  $\sigma > 0$ , we denote by  $H^g(\sigma)$  the RKHS associated with the *Gaussian kernel* defined by

$$k^g(x, y) = e^{-|x-y|^2/2\sigma^2}. \quad (6.3)$$

First, we provide the explicit description of the RKHS for each kernel as in the following propositions:

**Proposition 6.1** (RKHS of the exponential kernel). Let  $\sigma > 0$  and  $b \in \mathbb{R}^d$ . We define the Hilbert spaces  $H_0$  and  $H_1$  by

$$\begin{aligned} H_0 &:= \left\{ h(x) = \sum_{\alpha \in \mathbb{Z}_{\geq 0}^d} a_\alpha (x-b)^\alpha : \sum_{\alpha \in \mathbb{Z}_{\geq 0}^d} \sigma^{2|\alpha|} |\alpha|! |a_\alpha|^2 < \infty \right\}, \\ H_1 &:= \left\{ h|_{\mathbb{R}^d} : h \text{ is holomorphic on } \mathbb{C}^d \text{ and } \int_{\mathbb{R}^d \times \mathbb{R}^d} |h(x+iy)|^2 e^{-(\|x-b\|^2 + \|y\|^2)/\sigma^2} dx dy < \infty \right\}, \end{aligned}$$

equipped with the inner products

$$\begin{aligned}\langle h, g \rangle_{H_0} &:= \sum_{\alpha \in \mathbb{Z}_{\geq 0}^d} \sigma^{2|\alpha|} \alpha! a_\alpha \overline{b_\alpha}, \\ \langle h, g \rangle_{H_1} &:= \frac{1}{(\pi\sigma^2)^d} \int_{\mathbb{R}^d \times \mathbb{R}^d} h(x+yi) \overline{g(x+yi)} e^{-\frac{\|x-b\|^2 + \|y\|^2}{\sigma^2}} dx dy,\end{aligned}$$

where we put  $h(x) = \sum_\alpha a_\alpha (x-b)^\alpha$ ,  $g(x) = \sum_\alpha b_\alpha (x-b)^\alpha$  for the inner product of  $H_0$ . Then, we have  $H^e(\sigma, b) = H_0 = H_1$ .

*Proof.* As for  $H^e(\sigma, b) = H_0$ , it follows from the fact that  $k_x \in H_0$  and  $\langle h, k_x \rangle_{H_0} = h(x)$  for any  $x \in \mathbb{R}^d$ , and that the subspace generated by  $k_x$ 's for  $x \in \Omega$  is dense in  $H_0$ . As for  $H^e(\sigma, b) = H_1$ , see for example, [81, Chapter 2].  $\square$

**Proposition 6.2** (RKHS of the Gaussian kernel). Let  $\sigma > 0$ . We define the Hilbert spaces  $H_0$  and  $H_1$  by

$$\begin{aligned}H_0 &= \left\{ h \in L^2(\mathbb{R}^d) : \int_{\mathbb{R}^d} |\mathcal{F}[h](\xi)|^2 e^{\sigma^2|\xi|^2/2} d\xi < \infty \right\}, \\ H_1 &= \left\{ h|_{\mathbb{R}^d} : h \text{ is holomorphic on } \mathbb{C}^d \text{ and } \int_{\mathbb{R}^d \times \mathbb{R}^d} |h(x+yi)|^2 e^{-2\|y\|^2/\sigma^2} dx dy < \infty \right\},\end{aligned}$$

equipped with the inner products

$$\begin{aligned}\langle g, h \rangle_{H_0} &:= \frac{\sigma^d}{(2\pi)^{d/2}} \int_{\mathbb{R}^d} \mathcal{F}[g](\xi) \overline{\mathcal{F}[h](\xi)} e^{\sigma^2|\xi|^2/2} d\xi, \\ \langle g, h \rangle_{H_1} &:= \frac{1}{(\pi\sigma^2)^d} \int_{\mathbb{R}^d \times \mathbb{R}^d} g(x+yi) \overline{h(x+yi)} e^{-2\|y\|^2/\sigma^2} dx dy.\end{aligned}$$

Then, we have  $H^g(\sigma) = H_0 = H_1$

*Proof.* We show  $H^g(\sigma) = H_0$ . It suffices to show that  $\langle h, k_x \rangle_{H_1} = h(x)$  for  $h \in H_1$  and  $x \in \mathbb{R}^d$ . Since

$$\mathcal{F}[k_x](\xi) = \frac{1}{\sigma^d} e^{-ix^\top \xi} e^{-\sigma^2|\xi|^2/2},$$

we have

$$\langle \mathcal{F}[h], \mathcal{F}[k_x] \rangle_{H_1} = \frac{1}{\sigma^d} \mathcal{F}^{-1}[\mathcal{F}[h]](x) = h(x).$$

As for  $H^g(\sigma) = H_1$ , see [63, Theorem 1.17].  $\square$

We define

$$\mathfrak{m}_{\sigma, b} : H^e(\sigma, b) \rightarrow H^g(\sigma)$$

by  $(\mathfrak{m}_{\sigma, b} h)(x) := h(x) e^{-\|x-b\|^2/2\sigma^2}$ . Then,  $\mathfrak{m}_{\sigma, b}$  induces an isomorphism from  $H^e(\sigma, b)$  to  $H^g(\sigma)$  as in the following proposition:

**Proposition 6.3.** Let  $\sigma > 0$  and  $b \in \mathbb{R}^d$ . Then,  $\mathfrak{m}_{\sigma, b}$  induces the isomorphism of Hilbert spaces such that  $\mathfrak{m}_{\sigma, b} k_p^e = e^{\|p-b\|^2/2\sigma^2} k_p^g$  for all  $p \in \mathbb{R}^d$ .

*Proof.* It follows from the equalities  $H = H_1$  for both kernels in Propositions 6.1 and 6.2.  $\square$

## 6.2 Explicit description of the intrinsic observables

In this section, we denote  $r_n := \binom{n+d}{d}$  (eventually, it coincides with the dimension of the space of the intrinsic observables). Let  $\mathfrak{P}_n$  be the set of polynomial functions on  $\mathbb{R}^d$  of degree less than or equal to  $n$ . Then, we can determine the space of intrinsic observables  $V_{p,n}$  as follows:

**Proposition 6.4.** Let  $k$  be the exponential kernel (6.2) or the Gaussian kernel (6.3). Then,  $V_{p,n} = \{qk_p : q \in \mathfrak{P}_n\}$ .

*Proof.* It follows from Corollary 2.10.  $\square$

**Proposition 6.5.** Let  $\sigma > 0$  and  $b \in \mathbb{R}^d$ . We fix a numbering of  $\mathbb{Z}_{\geq 0}^d$  such that  $\mathbb{Z}_{\geq 0}^d = \{\alpha^{(i)}\}_{i=1}^\infty$  and  $|\alpha^{(i)}| \leq |\alpha^{(j)}|$  if  $i \leq j$ . Let

$$v_i^\varepsilon(x) := v_i^\varepsilon(x; \sigma, b) := \frac{(x-p)^{\alpha^{(i)}}}{\sigma^{|\alpha^{(i)}|}} e^{-\frac{(p-b)^\top(2x-p-b)}{2\sigma^2}}.$$

Then,  $\{v_i^\varepsilon\}_{i=1}^{r_n}$  is an orthogonal basis of  $V_{p,n}$  and the matrix  $\mathbf{G}_n$  of (3.2) is a diagonal matrix whose  $i$ -th diagonal component is  $\alpha^{(i)}$ !. In particular,  $\iota'$ , the dual map of  $\iota$  of (2.5) is injective on  $\sum_{p \in \mathbb{R}^d} \mathcal{D}_p$ .

*Proof.* By direct calculation, we have

$$v_i^\varepsilon(z) \overline{v_j^\varepsilon(z)} e^{-\|z-b\|^2/\sigma^2} = \sigma^{-|\alpha^{(i)}|-|\alpha^{(j)}|} (z-p)^{\alpha^{(i)}} (\bar{z}-p)^{\alpha^{(j)}} e^{-\|z-p\|^2/2\sigma^2}.$$

The first statement follows from the combination of the above equality with the identity  $H = H_1$  in Proposition 6.1 and [81, Proposition 2.1]. As for the second statement, let  $\mathcal{B}_{p,n} := \{v_i^\varepsilon\}_{i=1}^{r_n}$ . Then, by Lemma 2.3 and Proposition 2.2, it suffices to show the linear independence of  $\cup_{p \in \mathbb{R}^d} \mathcal{B}_{p,n}$  for all  $n \geq 0$ . We omit the proof as it is easily proved via the induction on  $n$  using the differential operator.  $\square$

**Proposition 6.6.** Let  $\sigma > 0$ . We fix a numbering of  $\mathbb{Z}_{\geq 0}^d$  such that  $\mathbb{Z}_{\geq 0}^d = \{\alpha^{(i)}\}_{i=1}^\infty$  and  $|\alpha^{(i)}| \leq |\alpha^{(j)}|$  if  $i \leq j$ . Let

$$v_i^g(x) := v_i^g(x; \sigma) := \frac{(x-p)^{\alpha^{(i)}}}{\sigma^{|\alpha^{(i)}|}} e^{-\frac{\|x-p\|^2}{2\sigma^2}}.$$

Then,  $\{v_i^g\}_{i=1}^{r_n}$  is an orthogonal basis of  $V_{p,n}$  and  $\mathbf{G}_n$  is a diagonal matrix whose  $i$ -th diagonal component is  $\alpha^{(i)}$ !. In particular,  $\iota'$  is injective on  $\sum_{p \in \mathbb{R}^d} \mathcal{D}_p$ .

*Proof.* Since

$$\mathfrak{m}_{\sigma,0}(v_i^g) = v_i^g,$$

it follows from Proposition 6.3.  $\square$

## 6.3 Validity of Assumptions 3.2 and 5.6

Here, we provide several sufficient conditions for Assumptions 3.2 and 5.6 to be satisfied.

First, we discuss the discrete case. Let  $f : \mathbb{R}^d \rightarrow \mathbb{R}^d$  be a map of class  $C^\infty$ . At present, we know the nontrivial results only for the RKHS with respect to the exponential kernel.

**Proposition 6.7.** Let  $\sigma > 0$  and  $p \in \mathbb{R}^d$ . Assume  $f(\cdot)^\alpha \in H^e(\sigma, p)$  for all  $\alpha \in \mathbb{Z}_{\geq 0}^d$ . Then, Assumption 3.2 for  $p \in \mathbb{R}^d$  holds for  $H^e(\sigma, p)$ .

*Proof.* Since  $V_p$  in  $H^e(\sigma, p)$  coincides with the space of polynomial functions, it follows from Proposition 6.1.  $\square$

For example, if we take  $f$  as the polynomial map,  $f(\cdot)^\alpha \in H^e(\sigma, p)$  always holds and thus Assumption 3.2 is satisfied. Here, we note that we assume  $b = p$  in Proposition 6.7, and this assumption is essential. We do not assume  $b = p$  although the class of the dynamical systems satisfying Assumption 3.2 is more restricted, in the following result:

**Proposition 6.8.** Let  $\sigma > 0$  and  $b \in \mathbb{R}^d$ . Assume that there exists  $\tilde{f} : \mathbb{C}^d \rightarrow \mathbb{C}^d$  and  $0 \leq \varepsilon < 1$  such that  $\tilde{f}|_{\mathbb{R}^d} = f$  and

$$\|\tilde{f}(z)\| \leq \varepsilon \|z\|^2 \quad (6.4)$$

for all  $z \in \mathbb{C}^d$ . Then, Assumption 3.2 for  $p \in \mathbb{R}^d$  holds for  $H^e(\sigma, b)$ .

*Proof.* It follows from Proposition 6.1.  $\square$

Next, we discuss the continuous case. In contrast to the discrete case, a quite general class of dynamical systems satisfies Assumption 5.6. Let  $F : \mathbb{R}^d \rightarrow \mathbb{R}^d$  be a  $C^\infty$  map and regard it as a vector field on  $\mathbb{R}^d$ . Regarding the continuous dynamical system of (5.1), we have the following propositions:

**Proposition 6.9.** Let  $\sigma > 0$  and  $b \in \mathbb{R}^d$ . Let  $k^e$  be the positive definite kernel for  $H^e(\sigma, b)$ . Let  $p \in \mathbb{R}^d$ . Assume that there exists  $\tilde{F} = (\tilde{F}_1, \dots, \tilde{F}_d) : \mathbb{C}^d \rightarrow \mathbb{C}^d$  such that  $\tilde{F}|_{\mathbb{R}^d} = F$  and that

$$\int_{\mathbb{R}^d \times \mathbb{R}^d} |(\tilde{F}_i P k_p^e)(x + yi)|^2 e^{-(\|x-b\|^2 + \|y\|^2)/\sigma^2} dx dy < \infty \quad (6.5)$$

for  $i = 1, \dots, d$  and any polynomial function  $P$ . Then, Assumption 5.6 for  $p \in \mathbb{R}^d$  holds for  $H^e(\sigma, b)$ .

*Proof.* By Proposition 6.4, it follows from the definition of  $A_F$ .  $\square$

**Proposition 6.10.** Let  $\sigma > 0$ . Let  $k^g$  be the positive definite kernel for  $H^g(\sigma)$ . Let  $p \in \mathbb{R}^d$ . Assume that there exists  $\tilde{F} : \mathbb{C}^d \rightarrow \mathbb{C}^d$  such that  $\tilde{F}|_{\mathbb{R}^d} = F$  and that

$$\int_{\mathbb{R}^d \times \mathbb{R}^d} |(F_i P k_p^g)(x + yi)|^2 e^{-\|y\|^2/\sigma^2} dx dy < \infty \quad (6.6)$$

for  $i = 1, \dots, d$  and any polynomial function  $P$ . Then, Assumption 5.6 for  $p \in \mathbb{R}^d$  holds for  $H^g(\sigma)$ .

*Proof.* By Proposition 6.4, it follows from the definition of  $A_F$ .  $\square$

## 6.4 Explicit convergence rates

**Proposition 6.11.** Let  $\sigma > 0$  and  $b \in \mathbb{R}^d$ . We consider  $\mathcal{E}_{p,n}$  of (2.10) for  $H^e(\sigma, b)$ . For any  $x \in \mathbb{R}^d$ , we have

$$\mathcal{E}_{p,n}(x) = e^{\frac{\|x-b\|^2 - \|x-p\|^2}{2\sigma^2}} \sqrt{\sum_{m=n+1}^{\infty} \frac{1}{m!} \left(\frac{\|x-p\|^2}{\sigma^2}\right)^m} \leq \frac{1}{\sqrt{(n+1)!}} \left(\frac{\|x-p\|}{\sigma}\right)^{n+1} e^{\|x-b\|^2/2\sigma^2}. \quad (6.7)$$

*Proof.* Let

$$v_\alpha(x) := \frac{(x-p)^\alpha}{\sqrt{\alpha! \sigma^{|\alpha|}}} e^{\frac{(p-b)^\top (2x-p-b)}{2\sigma^2}}.$$

Since  $v_\alpha$ 's constitutes an orthonormal basis of  $V_p$  by Proposition 6.5, we have

$$k(x, y) = \sum_{\alpha \in \mathbb{Z}_{\geq 0}^d} v_\alpha(x) v_\alpha(y).$$

Thus, we have

$$\mathcal{E}_{p,n}(x)^2 = e^{\frac{(p-b)^\top (2x-p-b)}{\sigma^2}} \sum_{m=n+1}^{\infty} \frac{1}{m!} \left(\frac{\|x-p\|^2}{\sigma^2}\right)^m.$$

Since  $(p-b)^\top (2x-p-b) = \|x-b\|^2 - \|x-p\|^2$ , we have the first equality. The second follows from the inequality:

$$\sum_{m=n+1}^{\infty} \frac{1}{m!} \left(\frac{\|x-p\|^2}{\sigma^2}\right)^m \leq \frac{1}{(n+1)!} e^{\frac{\|x-p\|^2}{\sigma^2}}.$$

$\square$

**Proposition 6.12.** Let  $\sigma > 0$ . We consider  $\mathcal{E}_{p,n}$  of (2.10) for  $H^g(\sigma)$ . For any  $x \in \mathbb{R}^d$ , we have

$$\mathcal{E}_{p,n}(x) = e^{-|x-p|^2/\sigma^2} \sqrt{\sum_{m=n+1}^{\infty} \frac{1}{m!} \left(\frac{|x-p|^2}{\sigma^2}\right)^m} \leq \frac{1}{\sqrt{(n+1)!}} \left(\frac{|x-p|}{\sigma}\right)^{n+1}. \quad (6.8)$$

*Proof.* It follows from the combination of Proposition 6.11 with Proposition 6.3.  $\square$

Then, we have a detailed result of Corollary 3.7 as follows:

**Theorem 6.13.** We use the same notation and assumptions as those in Corollary 3.7. Assume that  $H = H^e(\sigma, b)$  or  $H^g(\sigma)$ . Assume that  $\mu$  is compactly supported and absolutely continuous with respect to the Lebesgue measure, namely there exists a compactly supported non-negative measurable function  $\rho : \mathbb{R}^d \rightarrow \mathbb{R}_{\geq 0}$  such that  $\mu = \rho(x)dx$ . We assume that there exists a rectangle  $R(a, r) := \prod_{i=1}^d [a_i - r_i, a_i + r_i]$  for  $a_i \in \mathbb{R}$  and  $r_i \in \mathbb{R}_{>0}$  ( $i = 1, \dots, d$ ) such that  $\text{ess.inf}_{x \in R(a, r)} \rho(x) > 0$ . Let

$$B_1 := \sup_{x \in \text{supp}(\rho)} \|x - p\|,$$

$$B_2 := \sup_{i=1, \dots, d} \left(1 + \frac{|a_i - p_i|}{r_i}\right).$$

Then, there exists a constant  $C > 0$  independent of  $n$  such that

$$\limsup_{N \rightarrow \infty} \left\| \mathbf{C}_{f,m}^* - \widehat{\mathbf{C}}_{m,n,N} \right\| \leq \frac{Cn^{m+d}}{\sqrt{(n+1)!}} \left(\frac{2B_1 B_2}{\sigma}\right)^n \quad \text{a.e.} \quad (6.9)$$

*Proof.* First, we show the case of  $H = H^e(\sigma, b)$ . We note that  $\pi_n k_{x_1}, \dots, \pi_n k_{x_N}$  are linearly independent with probability 1 by the assumption  $\text{ess.inf}_{x \in R(a, r)} \rho(x) > 0$ . We define

$$\mathbf{v} := e^{-\frac{(p-b)^\top(2x-p-b)}{\sigma^2}} \mathbf{1}_{R(a, r)}(x) dx. \quad (6.10)$$

Now, we estimate  $\|\mathcal{E}_{p,n}\|_{L^2(\mu)}$ , and  $\|\mathbf{Q}_{n,m}(\mathbf{v})\|$  in Corollary 3.7. As for  $\|\mathcal{E}_{p,n}\|_{L^2(\mu)}$ , by Proposition 6.12, we immediately have

$$\|\mathcal{E}_{p,n}\|_{L^2(\mu)} \lesssim \frac{B_1^n}{\sigma^n \sqrt{(n+1)!}}. \quad (6.11)$$

Next, we estimate  $\|\mathbf{Q}_{n,m}(\mathbf{v})\|$ . Let  $\{P_n(t)\}_{n \geq 0}$  be the orthonormal polynomials in the  $L^2$ -space on  $\mathbb{R}$  associated with  $\mathbf{1}_{[-1,1]}(x)dx$  such that the degree of  $P_n$  coincides with  $n$ . Let  $\gamma_n$  be the leading coefficient of  $P_n(t)$  and let  $\omega_{n,1}, \dots, \omega_{n,n}$  be the roots (with multiplicity) of  $P_n(t)$ . Then, by [71, Theorem 12.7.1], the following inequality holds:

$$|\gamma_n| \lesssim 2^n. \quad (6.12)$$

We define

$$Q_\alpha(x) := e^{-\frac{(p-b)^\top(2x-p-b)}{2\sigma^2}} \prod_{i=1}^d \frac{1}{\sqrt{r_i}} P_{\alpha_i} \left(\frac{x_i - a_i}{r_i}\right).$$

Then,  $\{Q_\alpha(x)\}_{|\alpha| \leq n}$  constitutes an orthonormal basis of  $V_{p,n}$  in  $L^2(\mathbf{v})$ . Let

$$\frac{1}{\sqrt{r_i}} P_{\alpha_i} \left(\frac{x_i - a_i}{r_i}\right) = \sum_{j=0}^{\alpha_i} c_{\alpha_i, j} (x_i - p_i)^j$$

for some real numbers  $c_{\alpha_i, j} \in \mathbb{R}^d$ . By [71, Theorem 3.3.1], we have  $|\omega_{n,i}| \leq 1$  for  $i = 1, \dots, n$ . Thus, by

$$\frac{1}{\sqrt{r_i}} P_{\alpha_i} \left( \frac{x_i - a_i}{r_i} \right) = \frac{\gamma_{\alpha_i}}{r_i^{\alpha_i+1/2}} \prod_{j=1}^{\alpha_i} (x_i - p_i - (r_i \omega_{\alpha_i, j} + a_i - p_i)),$$

we have

$$\begin{aligned} |c_{\alpha_i, j}| &\leq \sum_{\substack{S \subset \{1, \dots, \alpha_i\} \\ |S| = \alpha_i - j}} \frac{\gamma_{\alpha_i}}{r_i^{\alpha_i+1/2}} \prod_{\ell \in S} |r_i \omega_{\alpha_i, \ell} + a_i - p_i| \\ &\leq \binom{\alpha_i}{j} \frac{\gamma_{\alpha_i}}{r_i^{\alpha_i+1/2}} (r_i + |a_i - p_i|)^{\alpha_i - j} \\ &\leq \binom{\alpha_i}{j} \frac{\gamma_{\alpha_i}}{r_i^{j+1/2}} \left( 1 + \frac{|a_i - p_i|}{r_i} \right)^{\alpha_i}. \end{aligned} \quad (6.13)$$

Let

$$q_{\alpha, \beta} := \prod_{i=1}^d c_{\alpha_i, \beta_i}.$$

Thus, combining this with (6.12), we have

$$|q_{\alpha, \beta}| \lesssim \frac{2^{|\alpha|}}{\min(r_1, \dots, r_d)^{|\beta|+d/2}} \left( 1 + \sup_{i=1, \dots, d} \frac{|a_i - p_i|}{r_i} \right)^{|\alpha|} \prod_{i=1}^d \alpha_i^{\beta_i}. \quad (6.14)$$

Since

$$\|\mathbf{Q}_{n,m}(\mathbf{v})\|_{\text{op}}^2 \leq \|\mathbf{Q}_{n,m}(\mathbf{v})\|^2 = \sum_{|\alpha| \leq n, |\beta| \leq m} |q_{\alpha, \beta}|^2 \lesssim (nm)^d \sup_{|\alpha| \leq n, |\beta| \leq m} |q_{\alpha, \beta}|^2,$$

we have

$$\|\mathbf{Q}_{m,n}(\mathbf{v})\|_{\text{op}} \lesssim C_m n^{m+d} 2^n \left( 1 + \sup_{i=1, \dots, d} \frac{|a_i - p_i|}{r_i} \right)^n. \quad (6.15)$$

for some constant  $C_m > 0$  only depending on  $m$ . Therefore, by (6.11) and (6.15), we have (6.9) in the case of  $H = H^e(\sigma, b)$ . Regarding the case of  $H^g(\sigma)$ , the argument is completely the same as above but we use  $\mathbf{v} := e^{|x-p|^2} \sigma^2 \mathbf{1}_{R(a,r)}(x) dx$  and Proposition 6.11 in the corresponding parts.  $\square$

**Remark 6.14.** For example, if the density function  $\rho$  of  $\mu$  is continuous with compact support, then such a rectangle  $R(a, r)$  always exists.

We also have the corresponding theorem to the continuous case. As the proof is completely the same as that of Theorem 6.13, we omit it.

**Theorem 6.15.** We use the same notation and assumptions as in those Corollary 3.7. Assume that  $H = H^e(\sigma, b)$  or  $H^g(\sigma)$ . Assume that  $\mu$  is compactly supported and absolutely continuous with respect to the Lebesgue measure, namely there exists a compactly supported  $\rho : \mathbb{R}^d \rightarrow \mathbb{R}_{\geq 0}$  such that  $\mu = \rho(x) dx$ . We assume that there exists a rectangle  $R(a, r) := \prod_{i=1}^d [a_i - r_i, a_i + r_i]$  for  $a_i \in \mathbb{R}$  and  $r_i \in \mathbb{R}_{>0}$  ( $i = 1, \dots, d$ ) such that  $\text{ess. inf}_{x \in R(a,r)} \rho(x) > 0$ . Let

$$\begin{aligned} B_1 &:= \sup_{x \in \text{supp}(\rho)} \|x - p\|, \\ B_2 &:= \sup_{i=1, \dots, d} \left( 1 + \frac{|a_i - p_i|}{r_i} \right). \end{aligned}$$

Then, there exists a constant  $C > 0$  independent of  $n$  such that

$$\limsup_{N \rightarrow \infty} \left\| \mathbf{A}_{F,m}^* - \widehat{\mathbf{A}}_{m,n,N} \right\| \leq \frac{C n^{m+d}}{\sqrt{(n+1)!}} \left( \frac{2B_1 B_2}{\sigma} \right)^n \quad \text{a.e.} \quad (6.16)$$



## 6.5 Explicit reconstruction error for dynamical systems

As a crucial application of JetDMD, we can reconstruct the dynamical system only from a set of discrete data on the trajectories. We actually provide the theoretical guarantee for our reconstruction method as well as the algorithms and numerical results in Section 7.3. We will use the results in this section to prove the theoretical guarantee.

First, we provide an estimate of the reconstruction error for discrete dynamical systems.

**Theorem 6.16.** Let  $H = H^c(\sigma, b)$  for  $\sigma > 0$  and  $b \in \mathbb{R}^d$ . Let  $p \in \mathbb{R}^d$ . Let  $f = (f_1, \dots, f_d) : \mathbb{R}^d \rightarrow \mathbb{R}^d$  be a map of class  $C^\infty$ . Assume that Assumptions 3.1, 3.2 for  $p$  hold. Let  $m \geq 1$  be an integer and let  $\{v_i\}_{i=1}^m$  be a basis of  $V_{p,m}$ . Let  $\mathbf{C}_{f,m}^*$  be the representation matrix of  $C_f^*|_{V_{p,m}}$  with respect to the basis. For  $i = 1, \dots, d$ , we define

$$\widehat{f}_{m,i}(x) := (\partial_{x_i} \mathbf{v}_{p,m}(b))^\top \sigma^2 \mathbf{C}_{f,m}^* \mathbf{G}_m^{-1} \mathbf{v}_{p,m}(x) + b_i. \quad (6.17)$$

Then, for any compact subset  $K \subset \mathbb{R}^d$  and  $i = 1, \dots, d$ , we have

$$\sup_{y \in K} |f_i(y) - \widehat{f}_{m,i}(y)| \leq \|f_i - b_i\|_H \frac{\sup_{y \in K} \|y - p\|^{m+1} e^{\|y-b\|^2/2\sigma^2}}{\sigma^{m+1} \sqrt{(m+1)!}}. \quad (6.18)$$

*Proof.* Since

$$C_f^* k_y(z) = k(f(y), z) = e^{(f(y)-b)^\top (z-b)/\sigma^2},$$

we have

$$f_i(y) - b_i = \sigma^2 \partial_{x_i} C_f^* k_y(x)|_{x=b} = \sigma^2 \langle C_f^* k_y, \partial_{x_i} k(x, \cdot)|_{x=b} \rangle_H.$$

On the other hand, by Proposition 3.3, we have

$$C_f^* \pi_n k_y = (v_\alpha)_{|\alpha| \leq m}^\top \mathbf{C}_{f,m}^* \mathbf{G}_m^{-1} \mathbf{v}_{p,m}(y).$$

Thus, we have

$$\sigma^2 \langle C_f^* \pi_n k_y, \partial_{x_i} k(x, \cdot)|_{x=b} \rangle_H = \widehat{f}_{m,i}(y) - b_i.$$

Since  $C_f \partial_{x_i} k(x, \cdot)|_{x=b} = \sigma^{-2}(f_i - b)$ , we have the formula (6.18) by Lemma 2.16 and Proposition 6.11.  $\square$

Next we provide a corresponding result for continuous dynamical systems as follows. We omit the proof as it is the same as the discrete case.

**Theorem 6.17.** Let  $H = H^c(\sigma, b)$  for  $\sigma > 0$  and  $b \in \mathbb{R}^d$ . Let  $p \in \mathbb{R}^d$ . Let  $F = (F_1, \dots, F_d) : \Omega \rightarrow \mathbb{R}^d$  be a map of class  $C^\infty$ . Assume that Assumptions 5.1 and 5.6 hold. Let  $m \geq 1$  be an integer and let  $\{v_i\}_{i=1}^m$  be a basis of  $V_{p,m}$ . Let  $\mathbf{A}_{F,m}^*$  be the representation matrix of  $A_F^*$  on  $V_{p,m}$ . For  $i = 1, \dots, d$ , we define

$$\widehat{F}_{m,i}(x) := (\partial_{x_i} \mathbf{v}_m(p))^\top \sigma^2 \mathbf{A}_{F,m}^* \mathbf{G}_m^{-1} \mathbf{v}_m(x) \quad (6.19)$$

Then, for any compact subset  $K \subset \mathbb{R}^d$  and  $i = 1, \dots, d$ , we have

$$\sup_{y \in K} |F_i(y) - \widehat{F}_{m,i}(y)| \leq \|F_i\|_H \frac{\sup_{y \in K} \|y - p\|^{m+1}}{\sigma^{m+1} \sqrt{(m+1)!}}. \quad (6.20)$$

Under Assumption 3.2 or 5.6, for example, under the assumption for Proposition 6.7, 6.8, or 6.9, the right hand side of (6.17) can be estimated from data as in Theorem 6.13 or 6.15.

We have another result for the reconstruction error for continuous dynamical systems using the Gaussian kernel.

**Theorem 6.18.** Let  $H = H^s(\sigma)$  for  $\sigma > 0$ . Let  $p \in \mathbb{R}^d$ . Let  $F = (F_1, \dots, F_d) : \Omega \rightarrow \mathbb{R}^d$  be a map of class  $C^\infty$ . Assume that Assumptions 5.1 and 5.6 for  $p \in \mathbb{R}^d$  hold. Let  $m \geq 1$  be an integer and let  $\{v_i\}_{i=1}^m$  be a basis of  $V_{p,m}$ . Let  $\mathbf{A}_{F,m}^*$  be the representation matrix of  $A_F^*$  on  $V_{p,m}$ . For  $i = 1, \dots, d$ , we define

$$\widehat{F}_{m,i}(x) := (\partial_{x_i} \mathbf{v}_m(x))^\top \sigma^2 \mathbf{A}_{F,m}^* \mathbf{G}_n^{-1} \mathbf{v}_m(x) \quad (6.21)$$

Then, for any compact subset  $K \subset \mathbb{R}^d$  and  $i = 1, \dots, d$ , we have

$$\sup_{y \in K} \left| F_i(y) - \widehat{F}_{m,i}(y) \right| \leq \sup_{y \in K} \|A_F \partial_{x_i} k(x, \cdot)|_{x=y}\|_H \frac{\sup_{y \in K} \|y - p\|^{m+1}}{\sigma^{m-1} \sqrt{(m+1)!}}. \quad (6.22)$$

*Proof.* Since

$$A_F^* k_y(z) = \sum_{i=1}^d F_i(y) \partial_x k(x, z)|_{x=y} = \sum_{i=1}^d F_i(y) \frac{z_i - y_i}{\sigma^2} e^{-|y-z|^2/2\sigma^2},$$

we have

$$F_i(y) = \sigma^2 \partial_{x_i} A_F^* k_y(x)|_{x=y} = \sigma^2 \langle A_F^* k_y, \partial_{x_i} k(x, \cdot)|_{x=y} \rangle_H.$$

On the other hand, by Proposition 3.3, we have

$$A_F^* \pi_n k_y = (v_\alpha)^\top_{|\alpha| \leq m} \mathbf{A}_{F,m}^* \mathbf{G}_n^{-1} \mathbf{v}_m(y).$$

Thus, we have

$$\sigma^2 \langle A_F^* \pi_n k_y, \partial_{x_i} k(x, \cdot)|_{x=y} \rangle_H = \widehat{F}_{m,i}(y).$$

Therefore, by Lemma 2.16 and Proposition 6.12, we have the formula (6.22).  $\square$

Since the right hand side of (6.21) can be estimated from data as in Theorem 6.15, our framework can effectively estimate the unknown system using only data.

## 7 Jet Dynamic Mode Decomposition

Here, we describe the details of algorithms of Jet DMD and provide several computational results.

### 7.1 Basic notation

We recall the basic notation. Let  $\Omega \subset \mathbb{R}^d$  be a connected open subset. Let  $k : \Omega \times \Omega \rightarrow \mathbb{C}$  be a positive definite kernel of class  $C^\infty$ . Let  $f = (f_1, \dots, f_d) : \Omega \rightarrow \Omega$  be a map of class  $C^\infty$ , referred to as a discrete dynamical system. Let  $F = (F_1, \dots, F_d) : \Omega \rightarrow \mathbb{R}^d$  be a map of class  $C^\infty$  and consider the ordinary differential equation  $\dot{z} = F(z)$ . We denote by  $\phi^t : \Omega \rightarrow \Omega$  the flow map at time  $t$  of the vector field defined by  $F$ , where  $\phi^t(x)$  is defined as  $z(t)$  with  $\dot{z} = F(z)$  and  $z(0) = x$ . For  $p \in \Omega$ , we define

$$V_{p,n} := \text{span}\{\partial_x^\alpha k(x, \cdot)|_{x=p} : |\alpha| \leq n\},$$

$$r_n := \dim V_{p,n}$$

We also define  $V_p := \cup_n V_{p,n}$ .

We fix a basis  $\mathcal{B}_p = \{v_{p,i}\}_{i \geq 0}$  of  $V_p$  such that the set of the first  $r_n$  vectors  $\mathcal{B}_{p,n} = \{v_{p,i}\}_{i=1}^{r_n}$  constitutes a basis of  $V_{p,n}$  for all  $n \geq 0$ . Then, we define

$$\mathbf{v}_{p,n}(x) := \left( \overline{v_{p,i}(x)} \right)_{i=1}^{r_n},$$

$$\mathbf{G}_n := (\langle v_{p,i}, v_{p,j} \rangle_H)_{i,j=1, \dots, r_n}.$$

For  $X := (x_1, \dots, x_N) \in \Omega^N$  and  $Z := (z_{ij})_{\substack{i=1, \dots, d \\ j=1, \dots, N}} \in \mathbb{R}^{d \times N}$ , we define matrices of size  $r_n \times N$  by

$$\begin{aligned} \mathbf{V}_n^X &:= (\mathbf{v}_{p,n}(x_1), \dots, \mathbf{v}_{p,n}(x_N)), \\ \mathbf{W}_n^{X,Z} &:= \sum_{i=1}^d (z_{i1} \partial_{x_i} \mathbf{v}_{p,n}(x_1), \dots, z_{iN} \partial_{x_i} \mathbf{v}_{p,n}(x_N)). \end{aligned}$$

For numerical simulation, we will consider the exponential kernel and the Gaussian kernel. We have an explicit orthogonal basis of  $V_{p,n}$  for each kernel as discussed in Section 6.

**Example 7.1** (Exponential kernel). Let  $\Omega = \mathbb{R}^d$ ,  $\sigma > 0$ , and  $b \in \mathbb{R}^d$ . Let  $k^e(x, y) := e^{(x-b)^\top (y-b)/\sigma^2}$ . The RKHS  $H^e(\sigma, b)$  associated with this kernel coincides with

$$H^e(\sigma, b) = \left\{ h|_{\mathbb{R}^d} : h \text{ is holomorphic on } \mathbb{C}^d \text{ and } \int_{\mathbb{R}^d \times \mathbb{R}^d} |h(x+yi)|^2 e^{-(\|x-b\|^2 + \|y\|^2)/\sigma^2} dx dy < \infty \right\}.$$

We fix a numbering of  $\mathbb{Z}_{\geq 0}^d$  as  $\mathbb{Z}_{\geq 0}^d = \{\alpha^{(i)}\}_{i=1}^\infty$  such that  $|\alpha^{(i)}| \leq |\alpha^{(j)}|$  if  $i \leq j$  and  $\alpha^{(i+1)} = (0, \dots, \overset{i}{1}, \dots, 0)$  for  $i = 1, \dots, d$ . We take a basis  $\{v_{p,i}^e\}_{i=1}^\infty$  of  $V_p$  as

$$v_{p,i}^e(x) := v_{p,i}^e(x; \sigma, b) := \frac{(x-p)^{\alpha^{(i)}}}{\sigma^{|\alpha^{(i)}|}} \exp\left(\frac{(p-b)^\top (2x-p-b)}{2\sigma^2}\right).$$

Then,  $\{v_{p,i}^e\}_{i=1}^\infty$  constitutes an orthogonal system. We define  $\mathbf{v}_{p,n}^e(x; \sigma) := \mathbf{v}_{p,n}(x)$  and  $\mathbf{G}_n^e := \mathbf{G}_n$  using the orthogonal system  $\{v_{p,i}^e\}_{i=1}^\infty$ . We note that  $\mathbf{G}_n^e$  is the diagonal matrix whose  $i$ -th diagonal component is  $\alpha^{(i)}$ !

**Example 7.2** (Gaussian kernel). Let  $\Omega = \mathbb{R}^d$  and  $\sigma > 0$ . Let  $k^g(x, y) := e^{-|x-y|^2/2\sigma^2}$ . The RKHS  $H^g(\sigma)$  associated with this kernel coincides with

$$H^g(\sigma) = \left\{ h|_{\mathbb{R}^d} : h \text{ is holomorphic on } \mathbb{C}^d \text{ and } \int_{\mathbb{R}^d \times \mathbb{R}^d} |h(x+yi)|^2 e^{-2\|y\|^2/\sigma^2} dx dy < \infty \right\}.$$

We fix a numbering of  $\mathbb{Z}_{\geq 0}^d$  as  $\mathbb{Z}_{\geq 0}^d = \{\alpha^{(i)}\}_{i=1}^\infty$  such that  $|\alpha^{(i)}| \leq |\alpha^{(j)}|$  if  $i \leq j$  and  $\alpha^{(i+1)} = (0, \dots, \overset{i}{1}, \dots, 0)$  for  $i = 1, \dots, d$ . We take a basis  $\{v_{p,i}^g\}_{i=1}^\infty$  of  $V_p$  as

$$v_{p,i}^g(x) := v_{p,i}^g(x; \sigma) := \frac{(x-p)^{\alpha^{(i)}}}{\sigma^{|\alpha^{(i)}|}} \exp\left(\frac{-\|x-p\|^2}{2\sigma^2}\right).$$

Then,  $\{v_{p,i}^g\}_{i=1}^\infty$  constitutes an orthogonal system. We define  $\mathbf{v}_{p,n}^g(x; \sigma) := \mathbf{v}_{p,n}(x)$  and  $\mathbf{G}_n^g := \mathbf{G}_n$  using the orthogonal system  $\{v_{p,i}^g\}_{i=1}^\infty$ . We note that  $\mathbf{G}_n^g$  is the diagonal matrix whose  $i$ -th diagonal component is  $\alpha^{(i)}$ !

## 7.2 Eigenvalues and eigenvectors of Perron–Frobenius operators and extended Koopman operators

Here, we introduce the details of the estimation algorithms of eigenvalues and eigenvectors of the Perron–Frobenius operator and the extended Koopman operator. We also provide several numerical results using the van der Pol oscillator, Duffing oscillator, and the Hénon map. We describe the algorithms in Algorithms 1, 2, 3, and 4. We provide several remarks for these algorithms and accurate convergence theorems for them as follows:

**Remark 7.3.** When  $f = \phi^{T_s}$  for some  $T_s > 0$  in Algorithm 1, using the output  $\widehat{\mathbf{C}}$ , we may define

$$\widehat{\mathbf{A}} := \frac{1}{T_s} \log \widehat{\mathbf{C}}. \quad (7.1)$$

Then,  $\widehat{\mathbf{A}}$  can provide an estimation of the generator  $A_F|_{V_{p,m}}$  by Proposition 5.5 under suitable conditions. However, generally, we need to carefully choose a branch of  $\log \widehat{\mathbf{C}}$  to get a correct approximation of the generator (see also Figure 4 below).

**Remark 7.4.** The Gaussian-Hermite quadrature (see, for example, [19, Section 3]) is more effective and faster way to compute  $\mathbf{G}_m^{ij}$  than a usual numerical integration in Algorithm 3.

Using Theorem 6.13 and Proposition 6.7, we immediately have the following theorems:

**Theorem 7.5** (Convergence of Algorithm 1). Assume that  $\Omega = \mathbb{R}^d$ . Let  $p \in \mathbb{R}^d$  be a fixed point of  $f$  and let  $k^e(x, y) = e^{-(x-p)^\top(y-p)/\sigma^2}$  for some  $\sigma > 0$ . Let  $x_1, \dots, x_N$  be i.i.d random variables of the distribution  $\rho(x)dx$  with compactly supported density function  $\rho$  such that  $\text{ess.inf}_{x \in U} \rho(x) > 0$  for some open subset  $U \subset \mathbb{R}^d$ . Assume that  $f^\alpha \in H^e(\sigma, p)$  for all  $\alpha \in \mathbb{Z}_{\geq 0}^d$ . Let  $\widehat{\mathbf{C}}_{m,n,N}$  be the output of Algorithm 1 with input  $m, n, p, X = (x_1, \dots, x_N)$ , and  $Y = (y_1, \dots, y_N)$ . Then, we have

$$\lim_{n \rightarrow \infty} \lim_{N \rightarrow \infty} \left\| \widehat{\mathbf{C}}_{m,n,N} - \mathbf{G}_m \mathbf{C}_{f,m}^* \mathbf{G}_m^{-1} \right\| = 0 \text{ a.e.}, \quad (7.2)$$

where  $\mathbf{C}_{f,m}^*$  is the representation matrix of  $C_f^*|_{V_{p,m}}$  with respect to  $\mathcal{B}_{p,m}$ .

We note that the condition  $f^\alpha \in H^e(\sigma, p)$  for all  $\alpha \in \mathbb{Z}_{\geq 0}^d$  holds for any holomorphic map on  $\mathbb{C}^d$  with exponentially growth, in particular, any polynomial map.

**Theorem 7.6** (Convergence of Algorithm 2). Assume  $\Omega = \mathbb{R}^d$  and let  $k$  be the Gaussian kernel or the exponential kernel. Let  $p \in \mathbb{R}^d$  be an equilibrium point of  $F$ . Let  $x_1, \dots, x_N$  be i.i.d random variables of the distribution  $\rho(x)dx$  with compactly supported density function  $\rho$  such that  $\text{ess.inf}_{x \in U} \rho(x) > 0$  for some open subset  $U \subset \mathbb{R}^d$ . Assume that  $p$  satisfies Assumptions 5.1 and 5.6 (see Propositions 6.9 and 6.10). Define  $\widehat{\mathbf{A}}_{m,n,N}$  as the output of Algorithm 2 with input  $m, n, p, X = (x_1, \dots, x_N)$ , and  $Y = (y_1, \dots, y_N)$ . Then, we have

$$\lim_{n \rightarrow \infty} \lim_{N \rightarrow \infty} \left\| \widehat{\mathbf{A}}_{m,n,N} - \mathbf{G}_m \mathbf{A}_{F,m}^* \mathbf{G}_m^{-1} \right\| = 0 \text{ a.e.}, \quad (7.3)$$

where  $\mathbf{A}_{F,m}^*$  is the representation matrix of  $A_F^*|_{V_{p,m}}$  with respect to  $\mathcal{B}_{p,m}$ .

---

### Algorithm 1 Estimation of Perron–Frobenius operators for discrete dynamical systems

---

**Input:** Positive integers  $m$  and  $n$  with  $m \leq n$ , a fixed point  $p \in \Omega$  of  $f$ ,  $X := (x_1, \dots, x_N) \in \Omega^N$ , and  $Y := (y_1, \dots, y_N) \in \Omega^N$  with  $N \geq r_n$ , where  $y_i = f(x_i)$ .

- 1: Construct an orthogonal basis  $\{v_{p,i}\}_{i=1}^{r_n}$  of  $V_{p,n}$  such that  $\{v_{p,i}\}_{i=1}^{r_m}$  constitutes a basis of  $V_{p,m}$ .
- 2: Define  $\mathbf{v}_{p,m} \in V_{p,n}^{r_m}$  with variable  $x$  by  $\mathbf{v}_{p,m}(x) := (\overline{v_{p,i}(x)})_{i=1}^{r_m}$ .
- 3: Define  $\mathbf{v}_{p,n} \in V_{p,n}^{r_n}$  with variable  $x$  by  $\mathbf{v}_{p,n}(x) := (\overline{v_{p,i}(x)})_{i=1}^{r_n}$ .
- 4: Construct the matrix  $\mathbf{V}_m^Y := (\mathbf{v}_{p,m}(y_1), \dots, \mathbf{v}_{p,m}(y_N))$  of size  $r_m \times N$ .
- 5: Construct the matrix  $\mathbf{V}_n^X := (\mathbf{v}_{p,n}(x_1), \dots, \mathbf{v}_{p,n}(x_N))$  of size  $r_n \times N$ .
- 6: Compute  $\mathbf{C}_0 := \mathbf{V}_m^Y (\mathbf{V}_n^X)^\dagger$ , where  $(\cdot)^\dagger$  indicates the Moore–Penrose pseudo inverse.
- 7: Extract the leading principal minor matrix  $\widehat{\mathbf{C}}$  of  $\mathbf{C}_0$  of order  $r_m$ :

$$\mathbf{C}_0 = \mathbf{V}_m^Y (\mathbf{V}_n^X)^\dagger = \begin{pmatrix} \widehat{\mathbf{C}} & * \\ & * \end{pmatrix}. \quad (7.4)$$

**Output:**  $\widehat{\mathbf{C}}$ .

---

#### 7.2.1 Van der Pol oscillators

Let  $\mu > 0$  be a positive number, and we consider the van der Pol oscillator:

$$\begin{aligned} x' &= y, \\ y' &= \mu(1 - x^2)y - x. \end{aligned} \quad (7.7)$$

---

**Algorithm 2** Estimation of the generators of Perron–Frobenius operators for continuous dynamical systems

---

- Input:** Positive integers  $m$  and  $n$  with  $m \leq n$ , a fixed point  $p \in \Omega$  of  $f$ ,  $X := (x_1, \dots, x_N) \in \Omega^N$ , and  $Y := (y_{ij})_{i,j} \in \mathbb{R}^{d \times N}$  with  $N \geq r_n$ , where  $y_{ij} = F_i(x_j)$ .
- 1: Construct an orthogonal basis  $\{v_{p,i}\}_{i=1}^{r_n}$  of  $V_{p,n}$  such that  $\{v_{p,i}\}_{i=1}^{r_m}$  constitutes a basis of  $V_{p,m}$ .
  - 2: Define  $\mathbf{v}_{p,m} \in V_{p,m}^{r_m}$  with variable  $x$  by  $\mathbf{v}_{p,m}(x) := (\overline{v_{p,i}(x)})_{i=1}^{r_m}$ .
  - 3: Define  $\mathbf{v}_{p,n} \in V_{p,n}^{r_n}$  with variable  $x$  by  $\mathbf{v}_{p,n}(x) := (\overline{v_{p,i}(x)})_{i=1}^{r_n}$ .
  - 4:  $\mathbf{W}_m^{X,Y} := \mathbf{O} \in \mathbb{C}^{r_m \times N}$ .
  - 5: **for**  $i = 1, \dots, d$  **do**
  - 6:     **for**  $j = 1, \dots, r_m$  **do**
  - 7:         Compute the derivative  $\partial_{x_i} v_{p,j}$ .
  - 8:     **end for**
  - 9:     Construct the matrix  $\mathbf{W}' := (y_{i1} \partial_{x_i} \mathbf{v}_{p,n}(x_1), \dots, y_{iN} \partial_{x_i} \mathbf{v}_{p,n}(x_N)) \in \mathbb{C}^{r_m \times N}$ .
  - 10:     Add  $\mathbf{W}'$  to  $\mathbf{W}_m^{X,Y}$ .
  - 11: **end for**
  - 12: Compute  $\mathbf{A}_0 := \mathbf{W}_m^{X,Y} (\mathbf{V}_n^X)^\dagger$ , where  $(\cdot)^\dagger$  indicates the Moore–Penrose pseudo inverse.
  - 13: Extract the the leading principal minor matrix  $\widehat{\mathbf{A}}$  of  $\mathbf{A}_0$  of order  $r_m$ :

$$\mathbf{A}_0 = (\mathbf{V}_n^X)^\dagger = \begin{pmatrix} \widehat{\mathbf{A}} & * \\ & * \end{pmatrix}. \quad (7.5)$$

**Output:**  $\widehat{\mathbf{A}}$ .

---

This dynamical system has one equilibrium point at the origin and a single limit cycle. The eigenvalues of the Jacobian matrix of the vector field are  $(\mu \pm \sqrt{\mu^2 - 4})/2$ .

Figure 3 describes the estimation of eigenvalues of the Perron–Frobenius operators  $A_F^*|_{V_{p,m}}$  of the van der Pol oscillator (7.7) for  $\mu = 1, 2$ , and 3, using Algorithm 2 with the exponential kernel  $k^e(x, y) = e^{(x-b)^\top(y-b)/\sigma^2}$  and the Gaussian kernel  $k^g(x, y) = e^{-|x-y|^2/2\sigma^2}$  with  $\sigma = 2$  and  $b = 0$ . We use  $m = 5$ ,  $n = 7$ , and  $N = 36$  samples from the uniform distribution on  $[-1, 1]^2$  for the exponential kernel, while  $m = 5$ ,  $n = 9$ , and  $N = 66$  for the Gaussian kernel. We use the exact velocities at the samples to compute  $\widehat{\mathbf{A}}$ . Basically, the exponential kernel needs less  $n$  and  $N$  than the Gaussian kernel. In the cases of  $\mu = 1, 3$ , the Hausdorff distance between the estimated eigenvalues and the true ones is less than  $10^{-9}$ , indicating that  $\widehat{\mathbf{A}}$  approximates  $A_F^*|_{V_{p,m}}$  in high precision, but for  $\mu = 2$ , the Hausdorff distance becomes greater than  $10^{-2}$ . This is due to the fact that the linear map  $A_F^*|_{V_{p,m}}$  is not diagonalizable in the case of  $\mu = 2$ , resulting in errors in the numerical computation of eigenvalues. However, as shown in Section 7.3, we demonstrate the high performance in the tasks of identification of differential equations. It indicates that the matrix  $\widehat{\mathbf{A}}$  itself provides a correct estimation of  $A_F^*|_{V_{p,m}}$ .

Figure 4 describes the estimation of eigenvalues of the Perron–Frobenius operators  $A_F^*|_{V_{p,m}}$  of the van der Pol oscillator (7.7) for  $\mu = 1$  using Algorithm 1 and the method as in Remark 7.3 with the matrix logarithm. We use the exponential kernel in the left and right figures, while the Gaussian kernel in the middle figure. In the left and middle figures, we take  $T_s = 0.5$ , and it provides fairly good approximation of the Perron–Frobenius operator. Moreover, it seems to work well although it has not been proved that  $\phi^{T_s}$  satisfies Assumption 3.2. The reason is either that  $\phi^{T_s}$  meets Assumption 3.2 or that Assumption 3.2 is too strong. On the other hand, the estimation fails if  $T_s$  is relatively large as in the right figure. The difference of the two green circles in the right figure is approximately  $2\pi$ , indicating the algorithm of the numerical computation of the matrix logarithm chooses the principal logarithm [30], that is an incorrect branch for our purpose.

Figure 5 is a collection of the approximated eigenfunctions of the extended Koopman operator  $A_F^\times$  of the van der Pol oscillator for  $\mu = 1$  and  $\mu = 3$  via Algorithm 4 using the exponential kernel  $e^{x^\top y/1.4}$ . We take  $m = 20$ ,

---

**Algorithm 3** A computational framework for estimating eigenvectors of Perron–Frobenius operators and extended Koopman operators for discrete dynamical systems

---

**Input:** positive integers  $m_1, \dots, m_r$  and  $n_1, \dots, n_r$  with  $m_i \leq n_i$  for  $i = 1, \dots, r$ , fixed points  $p_1, \dots, p_r \in \Omega$  of  $f$ ,  $X_i := (x_1^i, \dots, x_{N_i}^i) \in \Omega^{N_i}$  and  $Y_i := (y_1^i, \dots, y_{N_i}^i) \in \Omega^{N_i}$  with  $N_i \geq r_{p_i, n_i}$  and  $f(x_j^i) = y_j^i$  for  $j = 1, \dots, N_i$ .

- 1: **for**  $i = 1, \dots, r$  **do**
- 2:     Execute Algorithm 1 with inputs  $m_i, n_i, p_i, X_i$ , and  $Y_i$ , and assign the output to  $\widehat{\mathbf{C}}_i$ .
- 3:     Compute the eigenvalues  $(\gamma_i^{(1)}, \dots, \gamma_i^{(r_{m_i})})$  and eigenvectors  $(\widehat{\mathbf{w}}_i^{(1)}, \dots, \widehat{\mathbf{w}}_i^{(r_{m_i})})$  of  $\widehat{\mathbf{C}}_i$ .
- 4:     **for**  $j = 1, \dots, r$  **do**
- 5:         Compute the matrix  $\mathbf{G}^{ij} := (\langle v_{p_i, s}, v_{p_j, t} \rangle)_{s=1, \dots, r_{m_i}, t=1, \dots, r_{m_j}}$  of size  $r_{m_i} \times r_{m_j}$ , where  $v_{p_i, s}$ 's are the elements of the orthogonal basis constructed in Algorithm 1.
- 6:     **end for**
- 7:     **for**  $\ell = 1, \dots, r_{m_i}$  **do**
- 8:         Define  $\widehat{w}_i^{(\ell)}$  with variable  $x$  by  $\widehat{w}_i^{(\ell)}(x) := \mathbf{v}_{p_i, m_i}(x)^* (\mathbf{G}^{ii})^{-1} \mathbf{w}_i^{(\ell)}$ .
- 9:     **end for**
- 10:     Compute the eigenvector  $(\widehat{\mathbf{u}}_i^{(1)}, \dots, \widehat{\mathbf{u}}_i^{(r_{m_i})})$  of  $\widehat{\mathbf{C}}_i^*$  corresponding to  $(\overline{\gamma}_i^{(1)}, \dots, \overline{\gamma}_i^{(r_{m_i})})$ .
- 11: **end for**
- 12: Compute  $\mathbf{H}^{ij} \in \mathbb{C}^{r_{m_i} \times r_{m_j}}$  defined as

$$\begin{pmatrix} \mathbf{H}^{11} & \dots & \mathbf{H}^{1r} \\ \vdots & \ddots & \vdots \\ \mathbf{H}^{r1} & \dots & \mathbf{H}^{rr} \end{pmatrix} := \begin{pmatrix} \mathbf{G}^{11} & \dots & \mathbf{G}^{1r} \\ \vdots & \ddots & \vdots \\ \mathbf{G}^{r1} & \dots & \mathbf{G}^{rr} \end{pmatrix}^{-1} \begin{pmatrix} \mathbf{G}^{11} & & \mathbf{0} \\ & \ddots & \\ \mathbf{0} & & \mathbf{G}^{rr} \end{pmatrix}. \quad (7.6)$$

- 13: **for**  $i = 1, \dots, r$  **do**
- 14:     **for**  $\ell = 1, \dots, r_{m_i}$  **do**
- 15:         Define  $\widehat{u}_i^{(\ell)}$  with variable  $x$  by  $\widehat{u}_i^{(\ell)}(x) := \sum_{j=1}^r \mathbf{v}_{p_j, m}(x)^* \mathbf{H}_m^{ji} \widehat{\mathbf{u}}_i^{(\ell)}$ .
- 16:     **end for**
- 17: **end for**

**Output:**  $(\gamma_i^{(\ell)}, \widehat{w}_i^{(\ell)})$  as the pairs of the eigenvalue and the eigenvector of the Perron–Frobenius operator, and  $(\overline{\gamma}_i^{(\ell)}, \widehat{v}_i^{(\ell)})$  as those of the Koopman operator for  $i = 1, \dots, r$  and  $\ell = 1, \dots, r_{m_i}$ .

---



---

**Algorithm 4** A computational framework for estimating eigenvectors of Perron–Frobenius operators and extended Koopman operators for continuous dynamical systems

---

**Input:** positive integers  $m_1, \dots, m_r$  and  $n_1, \dots, n_r$  with  $m_i \leq n_i$  for  $i = 1, \dots, r$ , equilibrium points  $p_1, \dots, p_r \in \Omega$  of  $F$ ,  $X_i := (x_1^i, \dots, x_{N_i}^i) \in \Omega^{N_i}$  and  $Y_i := (y_1^i, \dots, y_{N_i}^i) \in \mathbb{R}^{d \times N_i}$  with  $N_i \geq r_{p_i, m_i}$  and  $F(x_j^i) = y_j^i$  for  $j = 1, \dots, N_i$ .

**Output:** the outputs of Algorithm 3 using Algorithm 2 instead of Algorithm 1 in Line 2.

---

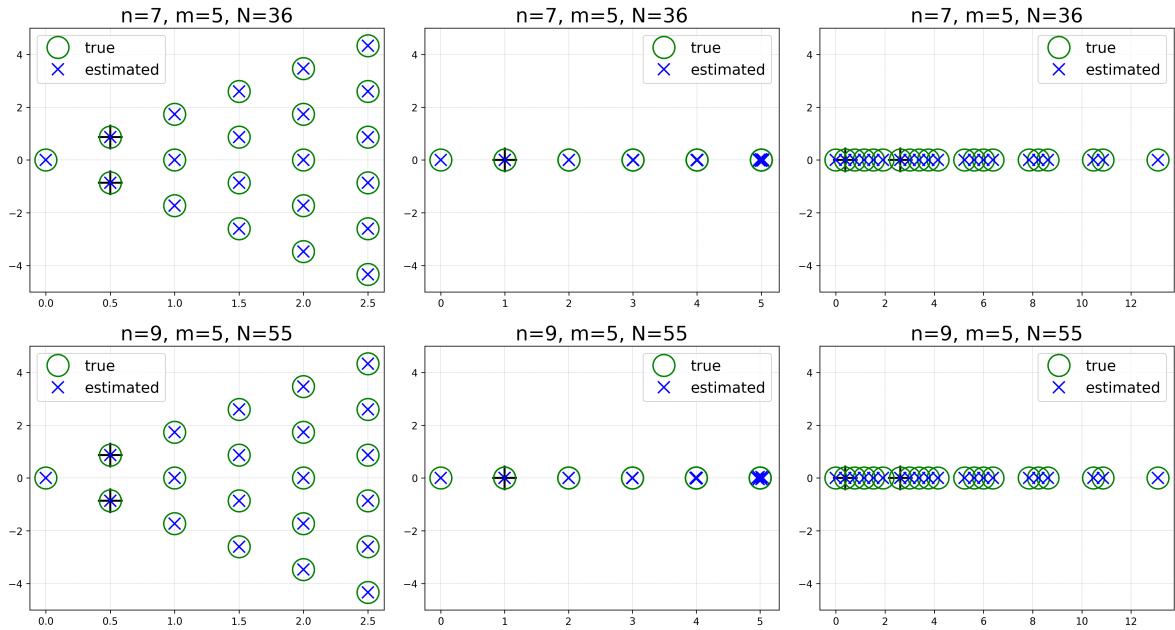


Figure 3: Estimation of eigenvalues using Algorithm 2 for van der Pol oscillators with  $\mu = 1$  (left), 2 (middle), and 3 (right). On the top row, we use the exponential kernel  $k^e(x, y) = e^{x^\top y/4}$  with  $m = 5$ ,  $n = 7$ ,  $p = (0, 0)$ ,  $N = 36$  samples from the uniform distribution on  $[-1, 1]^2$ , and the exact velocities on them. On the bottom row, we use the Gaussian kernel  $k^g(x, y) = e^{-|x-y|^2/8}$  with  $m = 5$ ,  $n = 9$ ,  $p = (0, 0)$ ,  $N = 55$  samples from the uniform distribution on  $[-1, 1]^2$ , and the exact velocities on them. The blue  $\times$ 's indicate the eigenvalues of the estimated Perron–Frobenius operator  $\hat{\mathbf{A}}$  and the green circles indicate the eigenvalues of  $A_F|_{V_{p,m}}$ . The two  $+$ 's indicate the eigenvalues of the Jacobian matrix of the vector field  $F(x, y) = (y, \mu(1-x^2)y-x)$  at  $p = (0, 0)$ .

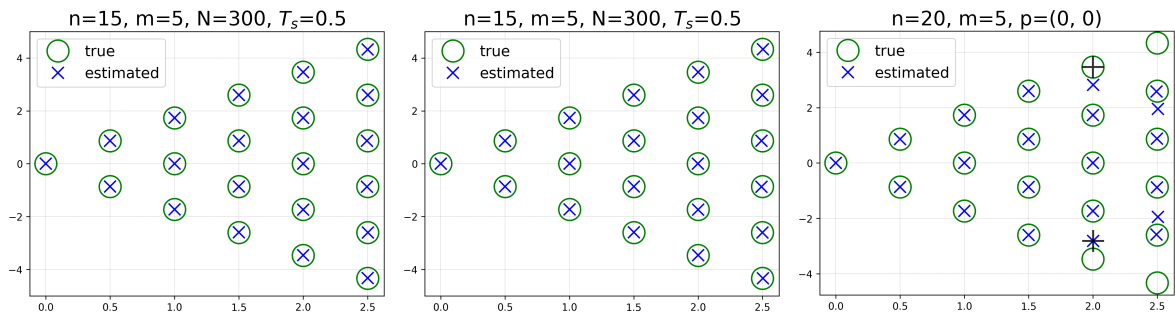


Figure 4: Estimation of eigenvalues using Algorithm 1 with the method as in Remark 7.3 for van der Pol oscillators with  $\mu = 1$ . We use the exponential kernel  $k^e(x, y) = e^{x^\top y/4}$  (left and right) and the Gaussian kernel  $k^g(x, y) = e^{-|x-y|^2/8}$  (middle). We take  $m = 5$ ,  $(n, T_s) = (15, 0.5)$  (left and middle) and  $(20, 1.0)$  (right)  $p = (0, 0)$ , and  $N = 300$  pairs of samples from the uniform distribution on  $[-1, 1]^2$  and their images under  $\phi^{T_s}$ . The blue  $\times$ 's indicate the eigenvalues of the estimated Perron–Frobenius operator  $\hat{\mathbf{A}}$  and the green circles indicate the eigenvalues of  $A_F|_{V_{p,m}}$ . The difference between the two  $+$ 's in the right figure is approximately  $2\pi$ .

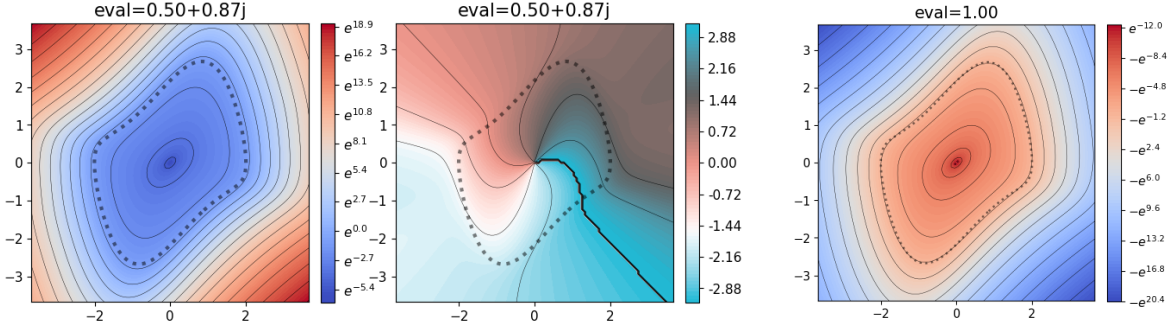


Figure 5: Approximated eigenfunction of the extended Koopman operator  $A_F^\times$  of the van der Pol oscillator for  $\mu = 3$  via Algorithm 4 using the exponential kernel  $e^{x^\top y/1.4}$  with input  $m = 20$ ,  $n = 22$ ,  $p = (0, 0)$ ,  $N = 7000$  samples from the uniform distribution on  $[-1, 1]^2$ , and the exact velocities on them. The left and middle figures are the heat map with contour lines corresponding to the absolute values and arguments of the eigenfunction for eigenvalue  $0.5 + 0.87i$ . The right figure is the heat map with contour lines corresponding to the eigenfunction for eigenvalue  $1.0$ . The dotted lines indicate the limit cycles.

$n = 24$ ,  $p = (0, 0)$ ,  $N = 7000$  samples from the uniform distribution on  $[-1, 1]^2$ , and the exact velocities on them. The left two figures are the absolute values and arguments of the eigenfunction corresponding to the eigenvalue  $0.5 + 0.87i \approx (1 + \sqrt{3}i)/2$ . The right figure is the eigenfunction corresponding to the eigenvalue  $1$ . It can be observed that the absolute value of the estimated eigenfunction increases rapidly once it exceeds the limit cycle. Similar figures are obtained in [49, 50], and our method can be considered as a data-driven version of the Taylor expansion method proposed in these articles.

Figure 6 describes the approximated eigenfunction of the extended Koopman operator  $A_F^\times$  of the van der Pol oscillator for  $\mu = 3$ , and a capability to capture a characteristic of the dynamical system. The left figure is the heat map with contour lines corresponding to the eigenfunctions of eigenvalue  $1.0$  via Algorithm 4 using the exponential kernel  $e^{x^\top y/1.4}$ . We take  $m = 16$ ,  $n = 21$ ,  $p = (0, 0)$ ,  $N = 7000$  samples from the uniform distribution on  $[-1, 1]^2$ , and the exact velocities on them. Looking at the figure on the left, unlike the case of  $\mu = 1$ , the contour lines of the eigenfunction form a distinctive inclined “S” shape around the origin, while, as shown in the middle figure, the dynamics with initial values near the origin exhibits highly skewed behavior over time. The approximated eigenfunction captures this behavior of the dynamical system around the origin.

## 7.2.2 Duffing oscillators

Here, we consider the Duffing oscillator (without external force):

$$\begin{aligned} x' &= y, \\ y' &= -\delta y - \alpha x - \beta x^3 \end{aligned} \tag{7.8}$$

only in the case of  $(\alpha, \beta, \delta) = (-1, 1, 0.5)$ . This dynamical system has two stable equilibrium points,  $(-1, 0)$ ,  $(1, 0)$ , and an unstable one  $(0, 0)$ . There exist two domains of attraction and any trajectory finally is attracted to one of the two stable equilibrium points (Figure 7).

Figure 8 describes the estimation of eigenvalues of the Perron–Frobenius operators  $A_F^*|_{V_{p,m}}$  of the Duffing oscillator (7.8) using Algorithm 2 with the exponential kernel  $k^e(x, y) = e^{-(x-b)^\top(y-b)/\sigma^2}$  with  $\sigma = 1$  and  $b = 0$ . We take  $m = 5$ ,  $n = 10$  and pick  $N = 66$  samples from the uniform distribution on  $[-2, 2]^2$ . We use the exact velocities at the samples to compute  $\hat{\mathbf{A}}$ . In each case, the Hausdorff distance between the estimated eigenvalues and the true ones is less than  $10^{-7}$ , indicating the matrix  $\hat{\mathbf{A}}$  well approximates the Perron–Frobenius operator  $A_F^*|_{V_{p,m}}$ .



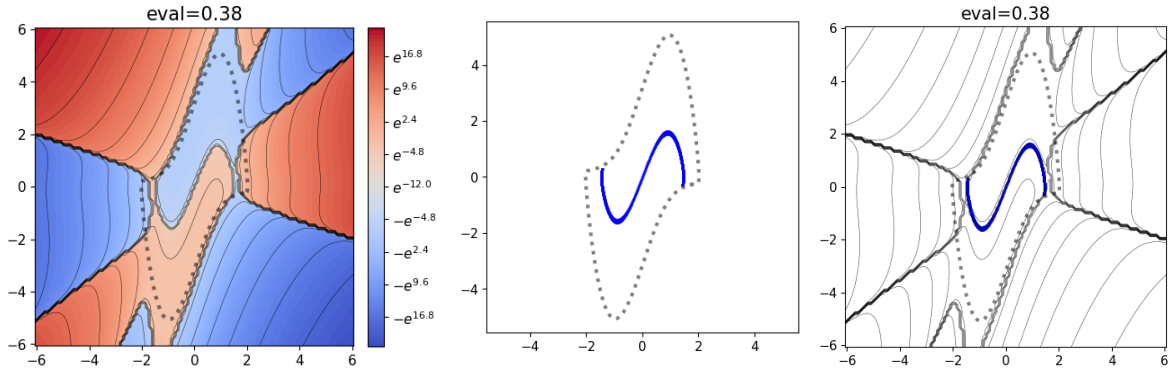


Figure 6: Estimated eigenfunction of the extended Koopman operator  $A_F^\times$  of the van der Pol oscillator for  $\mu = 3$  via Algorithm 4 using the exponential kernel  $e^{x^\top y/1.4}$  with input  $m = 16$ ,  $n = 21$ ,  $p = (0, 0)$ ,  $N = 7000$  samples from the uniform distribution on  $[-1, 1]^2$ , and the exact velocities on them. The left figure is the heat map with contour lines corresponding to the eigenfunctions of eigenvalue 0.38. The middle figure is the image of the small rectangle domain  $[-0.01, 0.01]^2$  under the flow map  $\phi^t$  at  $t = 3$ . The right figure is a combination of the middle figure and the contour lines of the left figure. The dotted lines indicate the limit cycles.

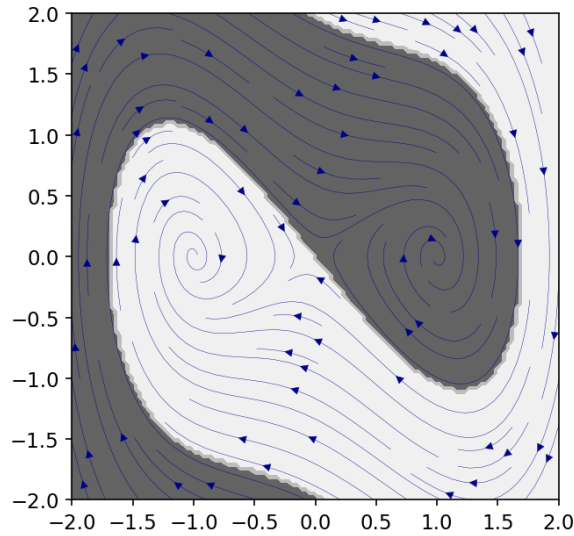


Figure 7: Two domains of attraction of the Duffing oscillator (7.8). Trajectories that start from the points within the same colored region all converge to the same equilibrium points. The black arrows indicate the streamlines along the vector field.

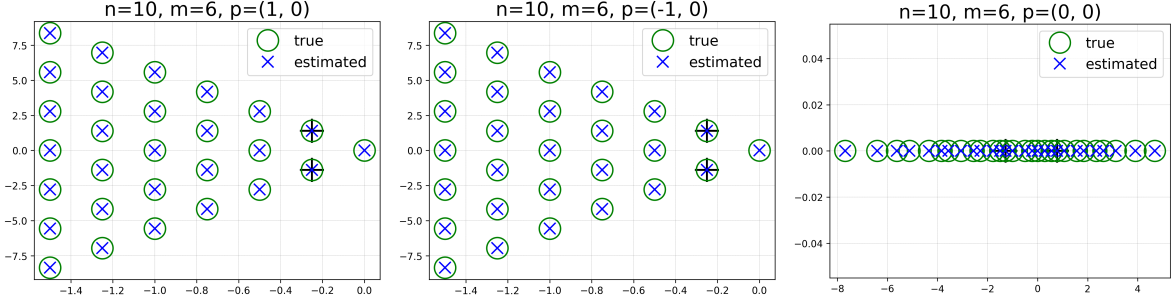


Figure 8: Estimated eigenvalues of the Perron–Frobenius operators  $A_F^*|_{V_{p,m}}$  of the Duffing oscillator (7.8) via Algorithm 4 using the exponential kernel  $e^{x^\top y}$  with input  $m = 6$ ,  $n = 10$ , the equilibrium points,  $N = 66$  samples from the uniform distribution on  $[-2, 2]^2$ , and the exact velocities on them. The figures in the left, middle, and right correspond to the eigenvalues computed using the three equilibrium points  $(1, 0)$ ,  $(-1, 0)$ ,  $(0, 0)$ , respectively. The blue  $\times$ 's indicate the eigenvalues of the estimated Perron–Frobenius operator  $\hat{\mathbf{A}}$  and the green circles indicate the eigenvalues of  $A_F|_{V_{p,m}}$ . The two  $+$ 's indicate the eigenvalues of the Jacobian matrix of the vector field  $F(x, y) = (y, -0.5y + x - x^3)$  at the equilibrium point.

Figure 9 is a collection of the approximated eigenfunctions of the Duffing oscillator (7.8). for the eigenvalues  $-0.25 + 1.39i \approx (-1 + \sqrt{31}i)/4$  (left and middle-left),  $0.78 \approx (-1 + \sqrt{17})/4$  (middle-right), and  $1.28 \approx (-1 - \sqrt{17})/4$  (right). We use the exponential kernel  $k^e(x, y) = e^{-(x-b)^\top(y-b)/\sigma^2}$  with  $\sigma = 1$  and  $b = 0$ , and take  $m_1 = 10$ ,  $n_1 = 12$ ,  $N_1 = 3000$  samples from the uniform distribution on  $[-1.5, 1.5] \times [-0.5, 0.5]$ , and the exact velocities on them as input. The left figure is the heat map with contour lines of the absolute value of the approximated eigenfunction for the eigenvalue  $(-1 + \sqrt{31}i)/4 \approx -0.25 + 1.39i$  with the equilibrium point  $(-1, 0)$ . We describe the combination of this heat map with the domain of attraction (Figure 7) on the middle-left figure, showing that the eigenfunction captures the shape of the domain of attractions around the equilibrium point  $(-1, 0)$ . The middle-right and right figures are the heat maps with contour lines of the eigenfunction for the eigenvalues  $(-1 + \sqrt{17})/4 \approx 0.78$  and  $(-1 - \sqrt{17})/4 \approx 1.28$ , respectively. The eigenfunction for the positive eigenvalue captures the attracting direction, while that of the negative eigenvalue does the repelling direction around the origin.

Figure 10 describes the approximated eigenfunctions for  $-1$  using the exponential kernel  $e^{x^\top y/\sigma^2}$  with  $\sigma = 0.5$  and  $1$ . We take two equilibrium points,  $p_1 = (-1, 0)$  and  $p_2 = (1, 0)$ . Then, we set  $m_1 = m_2 = 10$ ,  $n_1 = n_2 = 16$ , and take  $N_1 = N_2 = 7000$  samples from the uniform distribution on  $[-1.5, 1.5] \times [-0.5, 0.5]$ , and the exact velocities on them as input. Here, we draw graphs of even and odd eigenfunctions constructed as in the following procedure: first, we note that the linear operator  $C_{-1} : H \rightarrow H; h \mapsto h((-1) \times \cdot)$  induces a Hermitian unitary operator. Moreover,  $C_{-1}$  is commutative with  $A_F^*$  and satisfies  $C_{-1}(V_{p_1,n}) = V_{p_2,n}$ . Thus, for the eigenfunction  $v$  of the extended Koopman operator  $A_F^\times$  in  $V_{p_1,n}$ , the image  $C_{-1}v$  corresponds to an eigenvector for the same eigenvalue in  $V_{p_2,n}$ . Therefore, we canonically construct even and odd eigenfunctions  $v \pm C_{-1}v$  of the extended Koopman operator  $A_F^\times$ . In the case of  $\sigma = 0.5$ , two peaks appear at the two equilibrium points, while they disappear in the case of  $\sigma = 1$ . This phenomenon is caused by the computation of the inverse matrix of  $\tilde{\mathbf{G}}_m := (\mathbf{G}_m^{ij})_{i,j}$  in (7.6). In this computation, we employed the pseudo inverse of  $\tilde{\mathbf{G}}_m$  instead of its actual inverse. When  $\sigma = 1$  and  $m = 10$ , the condition number of  $\tilde{\mathbf{G}}_m$  becomes very large, thus, the smaller eigenvalues of  $\tilde{\mathbf{G}}_m$  are automatically truncated in the process of computing the pseudo inverse of  $\tilde{\mathbf{G}}_m$ . Indeed, it can be seen that peaks appear on the equilibrium points in the case of a small  $m$  with  $\sigma = 1$ , but disappear if we intentionally truncate the small eigenvalues of  $\tilde{\mathbf{G}}_m$ . While this operation of ‘‘truncating small eigenvalues’’ thought to eliminate peaks at the equilibrium points, the appearance of contour lines along the boundary of the regions of attractions is quite interesting.

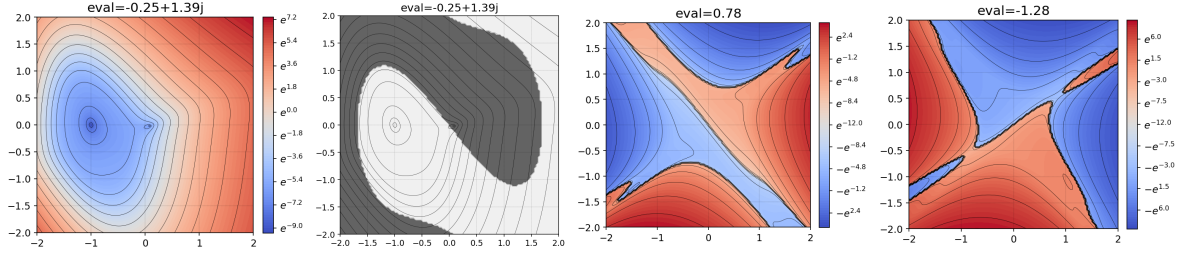


Figure 9: Estimated eigenfunction of the extended Koopman operator  $A_F^\times$  of the Duffing oscillator (7.8) via Algorithm 4 using the exponential kernel  $e^{x^\top y}$  with input  $m_1 = 10$ ,  $n_1 = 16$ ,  $p_1 = (-1, 0)$  (left and left middle),  $p_1 = (0, 0)$  (right middle and right),  $N_1 = 3000$  samples from the uniform distribution on  $[-1.5, 1.5] \times [-0.5, 0.5]$ , and the exact velocities on them. The left figure is the heat maps with contour lines corresponding to the absolute value of the eigenfunction for eigenvalue  $(-1 + \sqrt{31}i)/4$ , computed using equilibrium point  $(-1, 0)$ . The middle-left figure is a combination of the contour lines of the left figure and the domain of attraction of the dynamical system. The middle-right and right figures are the heat maps with contour lines corresponding to the eigenfunctions for eigenvalues  $(-1 + \sqrt{17})/4$  and  $(-1 - \sqrt{17})/4$ , respectively, computed using the equilibrium point  $(0, 0)$ .

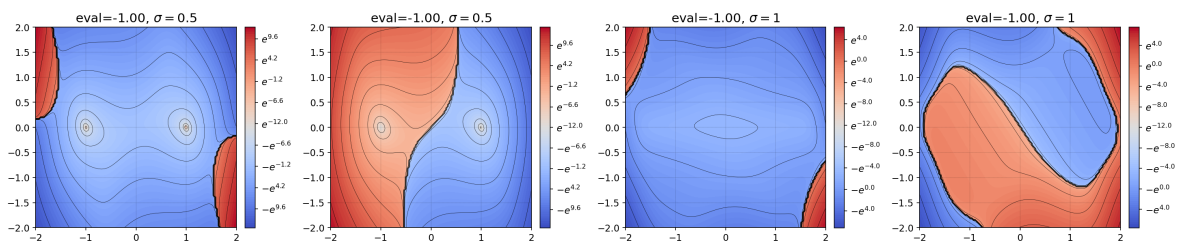


Figure 10: Estimated eigenfunctions for the eigenvalue  $-1$  of the extended Koopman operator  $A_F^\times$  of the Duffing oscillator (7.8) via Algorithm 4 using the exponential kernels  $e^{x^\top y}$  (left and middle-left) and  $e^{x^\top y/0.5}$  (right and middle-right) with input  $m_1 = m_2 = 10$ ,  $n_1 = n_2 = 16$ ,  $p_1 = (-1, 0)$ ,  $p_2 = (1, 0)$ ,  $N_1 = N_2 = 7000$  samples from the uniform distribution on  $[-1.5, 1.5] \times [-0.5, 0.5]$ , and the exact velocities on them.

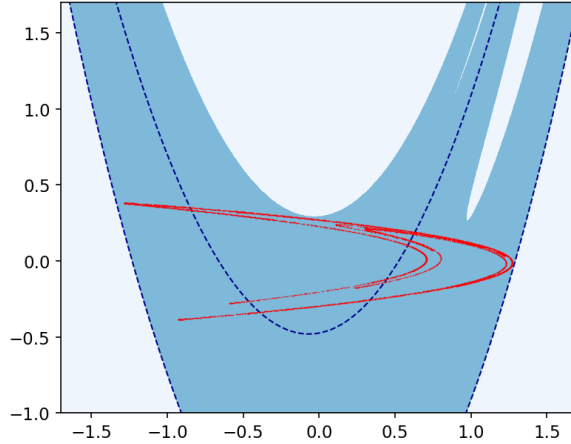


Figure 11: The attractor (red scatter plot), the domain of attraction (blue region), and the invariant manifold (dark blue dashed line) of the fixed points of the Hénon map (7.9).

### 7.2.3 Hénon maps

Here, we consider the Hénon map, the discrete dynamical system  $f : \mathbb{R}^2 \rightarrow \mathbb{R}^2$ , defined by

$$f(x, y) = (y + 1 - ax^2, bx) \quad (7.9)$$

in the case of  $a = 1.4$  and  $b = 0.3$ . This dynamical system has two fixed points

$$p = \left( \frac{b-1 \pm \sqrt{(b-1)^2 + 4a}}{2a}, \frac{b(b-1) \pm b\sqrt{(b-1)^2 + 4a}}{2a} \right). \quad (7.10)$$

Also, it has a domain of attraction and the attractor as in Figure 11.

Figure 12 describes the approximated eigenfunctions using the exponential kernel  $e^{(x-b)^\top(y-b)/\sigma^2}$  with  $\sigma = 0.6$  and  $b = 0$  with input  $m_1 = 6$ ,  $n_1 = 30$ . We take  $N_1 = 3000$  pairs of samples from the uniform distribution from  $p_1 + [-0.25, 0.25]^2$  and their images under the dynamical system  $f$ , where  $p_1$  is a fixed point defined below. For the left two figures, we use the fixed point  $p_1 \approx (0.63135448, 0.18940634)$ . The eigenvalues are estimated with enough precision (the Hausdorff distance between approximated eigenvalues and the true ones is less than  $10^{-5}$ ). For the right two figures, we take another fixed point  $p_1 \approx (-1.13135448, -0.33940634)$ . In this case, the Hausdorff distance between approximated eigenvalues and the true ones is less than approximately  $1.3796 \times 10^{-3}$ , and the accuracy of the estimation is a little less than the case.

Basically, the vanishing region of the eigenfunctions captures the several characteristic features of the dynamical system, for example, some parts of invariant manifold and the attractor. Our framework shows that the estimated eigenfunctions actually approximate those of  $C_f^\times$ . The study of the mathematical properties of these eigenfunctions of  $C_f^\times$  is a crucial research task for the future.

## 7.3 Data-driven reconstruction of dynamical systems

Here, we assume  $\Omega = \mathbb{R}^d$ . As an application of JetDMD, we propose a method to reconstruct the original dynamical system from finite discrete data on trajectories of the dynamical system. We show the performance of the reconstruction using the van der Pol oscillator and the Lorenz system.

We describe the data-driven reconstruction algorithms in Algorithms 5, 6, and 7. Moreover, combining Theorems 6.16 and 7.5, we have accurate convergence results for these algorithms as follows:

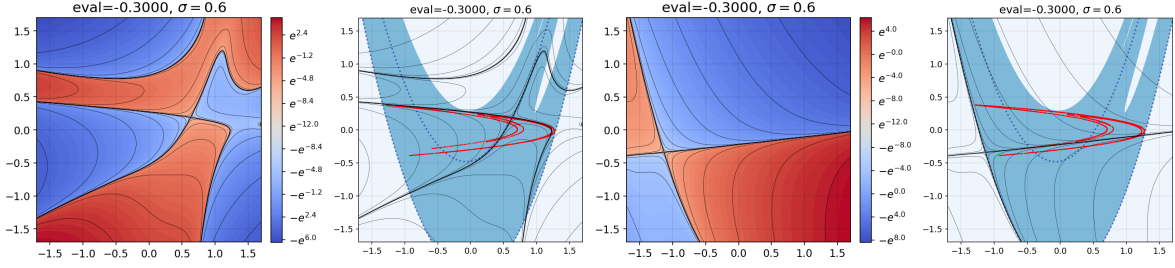


Figure 12: Estimated eigenfunctions for eigenvalue 0.3 of the extended Koopman operator  $C_f^\times$  of the Hénon map (7.9) via Algorithm 3 using the exponential kernel  $e^{x^\top y/0.6}$  with input  $m_1 = 6$ ,  $n_1 = 30$ ,  $p_1 \approx (0.63135448, 0.18940634)$  (left and middle-left) and  $(-1.13135448, -0.33940634)$  (right and middle-right),  $N_1 = 3000$  pairs of the samples from the uniform distribution on  $p_1 + [-0.25, 0.25]^2$  and the images under  $f$ . The middle-left and right figures are the combination of the corresponding heat maps with Figure 11.

**Theorem 7.7** (Convergence of Algorithm 5). Let  $\sigma > 0$ . Let  $k^e(x, y) = e^{-(x-p)^\top(y-p)/\sigma^2}$ . Let  $x_1, \dots, x_N$  are i.i.d random variables of the distribution with compactly supported density function  $\rho$  such that  $\text{ess.inf}_{x \in U} \rho(x) > 0$  for some open subset  $U \subset \mathbb{R}^d$ . Let  $x_0, y_0 \in \mathbb{R}^d$  such that  $y_0 = f(x_0)$ . Assume that  $f^\alpha \in H^e(\sigma, \rho)$  for all  $\alpha \in \mathbb{Z}_{\geq 0}^d$ . Define  $\widehat{f}_{m,n,N}$  as the output of Algorithm 5 with input  $k = k^e$ ,  $\sigma$ ,  $m$ ,  $n$ ,  $(x_0, y_0)$ ,  $X = (x_1, \dots, x_N)$ , and  $Y = (y_1, \dots, y_N)$ . Then, for any compact set  $K \subset \mathbb{R}^d$ , we have

$$\lim_{m \rightarrow \infty} \lim_{n \rightarrow \infty} \limsup_{N \rightarrow \infty} \sup_{y \in K} \|f(y) - \widehat{f}_{m,n,N}(y)\| = 0 \quad \text{a.e.}$$

Combining Theorem 7.6 with Theorems 6.17 and 6.18, we have

**Theorem 7.8** (Convergence of Algorithm 6). Let  $\sigma > 0$ . Let  $k$  be the exponential kernel or the Gaussian kernel. Let  $x_1, \dots, x_N$  are i.i.d random variables of the distribution with compactly supported density function  $\rho$  such that  $\text{ess.inf}_{x \in U} \rho(x) > 0$  for some open subset  $U \subset \mathbb{R}^d$ . Let  $x_0, y_0 \in \mathbb{R}^d$  such that  $y_0 = F(x_0)$  and assume that  $x_0$  satisfies Assumptions 5.1 and 5.6 (see Propositions 6.9 and 6.10). Define  $\widehat{F}_{m,n,N}$  as the output of Algorithm 6 with input  $k$ ,  $\sigma$ ,  $m$ ,  $n$ ,  $(x_0, y_0)$ ,  $X = (x_1, \dots, x_N)$ , and  $Y = (y_1, \dots, y_N)$ . Then, for any compact set  $K \subset \mathbb{R}^d$ , we have

$$\lim_{m \rightarrow \infty} \lim_{n \rightarrow \infty} \limsup_{N \rightarrow \infty} \sup_{y \in K} \|F(y) - \widehat{F}_{m,n,N}(y)\| = 0 \quad \text{a.e.}$$

**Theorem 7.9** (Convergence of Algorithm 7). Let  $\sigma > 0$ . Let  $T_s > 0$  and  $f := \phi^{T_s}$ . Let  $x_1, \dots, x_N$  are i.i.d random variables of the distribution with compactly supported density function  $\rho$  such that  $\text{ess.inf}_{x \in U} \rho(x) > 0$  for some open subset  $U \subset \mathbb{R}^d$ . Let  $x_0, y_0 \in \mathbb{R}^d$  such that  $y_0 = f(x_0)$  and let  $k^e(x, y) = e^{-(x-x_0)^\top(y-x_0)/\sigma^2}$ . Assume  $f^\alpha \in H^e(\sigma, \rho)$  for all  $\alpha \in \mathbb{Z}_{\geq 0}^d$ . Define  $\widehat{F}_{m,n,N}$  as the output of Algorithm 7 with input  $k = k^e$ ,  $\sigma$ ,  $m$ ,  $n$ ,  $(x_0, y_0)$ ,  $X = (x_1, \dots, x_N)$ , and  $Y = (y_1, \dots, y_N)$ . Then, for any compact set  $K \subset \mathbb{R}^d$ , we have

$$\lim_{m \rightarrow \infty} \lim_{n \rightarrow \infty} \limsup_{N \rightarrow \infty} \sup_{y \in K} \|F(y) - \widehat{F}_{m,n,N}(y)\| = 0 \quad \text{a.e.}$$

Theorem 7.9 guarantees that, under Assumption 3.2, namely, analytically favorable properties of the dynamical system, the original vector field can be reconstructed from finite data even if the sampling period remains long. This significantly improves [48, Theorem 1].

<sup>1</sup>We will use the exponential kernel as the input  $k$  in Algorithm 5 when we perform the numerical simulations in Sections 7.3.1 and 7.3.2

<sup>2</sup>We will use the exponential kernel or the Gaussian kernel as the input  $k$  according to the choice of (1) or (2), respectively, in Algorithm 6 when we perform the numerical simulations in Sections 7.3.1 and 7.3.2.

---

**Algorithm 5** A computational framework for data-driven reconstruction of discrete dynamical systems

---

**Input:** a positive definite kernel<sup>1</sup> $k$ , a positive number  $\sigma > 0$ , positive integers  $m$  and  $n$  with  $m \leq n$ , a pair of points  $(x_0, y_0) \in \Omega^2$  with  $y_0 = f(x_0)$ , and  $X := (x_1, \dots, x_N), Y := (y_1, \dots, y_N) \in \Omega^N$  such that  $y_i = f(x_i)$  with  $N \geq r_n$ .

- 1: Set  $\tilde{Y} := (y_1 - y_0 + x_0, \dots, y_N - y_0 + x_0) \in \Omega^N$ .
- 2: Compute  $\hat{\mathbf{C}}$  by Algorithm 1 using  $k$  with input  $m, n, p = x_0, X$ , and  $Y$ .
- 3: **for**  $i = 1, \dots, d$  **do**
- 4: Define  $\hat{f}_i$  with variable  $x$  by the  $(i + 1)$ -th component of

$$\sigma^2 \mathbf{G}_m^{-1} \hat{\mathbf{C}} \mathbf{G}_m (\mathbf{G}_m^e)^{-1} \mathbf{v}_{x_0, m}^e(x; \sigma) + y_0.$$

5: **end for**

**Output:**  $\hat{f} := (\hat{f}_1, \dots, \hat{f}_d)$ .

---

**Algorithm 6** A computational framework for data-driven reconstruction of continuous dynamical systems

---

**Input:** a positive definite kernel<sup>2</sup> $k$ , a positive number  $\sigma > 0$ , positive integers  $m$  and  $n$  with  $m \leq n$ , a pair of points  $(x_0, y_0) \in \Omega \times \mathbb{R}^d$  with  $y_0 = F(x_0)$ , and  $X := (x_1, \dots, x_N) \in \Omega$  and  $Y := (y_1, \dots, y_N) \in \mathbb{R}^{d \times N}$  with  $y_i = F(x_i)$ .

- 1: Set  $\tilde{Y} := (y_1 - y_0, \dots, y_N - y_0) \in \Omega^N$ .
- 2: Compute  $\hat{\mathbf{A}}$  by Algorithm 2 using  $k$  with input  $m, n, p = x_0, X$ , and  $Y$ .
- 3: **for**  $i = 1, \dots, d$  **do**
- 4: Define  $\hat{F}_i$  with variable  $x$  as either of

- (1) the  $(i + 1)$ -th component of  $\sigma^2 \mathbf{G}_m^{-1} \hat{\mathbf{A}} \mathbf{G}_m (\mathbf{G}_m^e)^{-1} \mathbf{v}_{x_0, m}^e(x; \sigma) + y_0$ ,

- (2)  $(\partial_{x_i} \mathbf{v}_{x_0, m}^g(x; \sigma))^\top \sigma^2 \mathbf{G}_m^{-1} \hat{\mathbf{A}} \mathbf{G}_m (\mathbf{G}_m^g)^{-1} \mathbf{v}_{x_0, m}^g(x; \sigma) + y_0$ .

5: **end for**

**Output:**  $\hat{F} := (\hat{F}_1, \dots, \hat{F}_d)$ .

---

**Algorithm 7** A computational framework for data-driven reconstruction of continuous dynamical systems with knowledge of the location of equilibrium points

---

- 1: a positive definite kernel<sup>3</sup> $k$ , a positive number  $\sigma > 0$ , positive integers  $m$  and  $n$  with  $m \leq n$ , an equilibrium point  $p \in \Omega$  of  $F$ , and  $X := (x_1, \dots, x_N), Y := (y_1, \dots, y_N) \in \Omega^N$  such that  $y_i = \phi^{T_s}(x_i)$  for a fixed  $T_s > 0$  for  $i = 1, \dots, N$ .

- 2: Compute  $\hat{\mathbf{C}}$  by Algorithm 1 using  $k$  with input  $m, n, p, X$ , and  $Y$ .
- 3: Choosing an appropriate brunch of matrix logarithm, compute  $\hat{\mathbf{A}}$  by  $\hat{\mathbf{A}} := \frac{1}{T_s} \log \hat{\mathbf{C}}$ .

- 4: **for**  $i = 1, \dots, d$  **do**
- 5: Define  $\hat{F}_i$  with variable  $x$  as either of

- (1) the  $(i + 1)$ -th component of  $\sigma^2 \mathbf{G}_m^{-1} \hat{\mathbf{A}} \mathbf{G}_m (\mathbf{G}_m^e)^{-1} \mathbf{v}_{x_0, m}^e(x; \sigma) + y_0$ ,

- (2)  $(\partial_{x_i} \mathbf{v}_{x_0, m}^g(x; \sigma))^\top \sigma^2 \mathbf{G}_m^{-1} \hat{\mathbf{A}} \mathbf{G}_m (\mathbf{G}_m^g)^{-1} \mathbf{v}_{x_0, m}^g(x; \sigma) + y_0$ .

6: **end for**

**Output:**  $\hat{F} := (\hat{F}_1, \dots, \hat{F}_d)$ .

---

### 7.3.1 Van der Pol oscillator

Figure 13 describes the data-driven reconstruction of the van der Pol oscillator (7.7) for  $\mu = 1, 2$ , and 3 using Algorithm 6 with the exponential kernel and the Gaussian kernel. We set  $m = 5$  and  $n = 7$ . We take  $M = 100$  samples  $x_1^{(0)}, \dots, x_M^{(0)}$  from the uniform distribution on  $[0, 1]^2$ , and define

$$x_i^{(j)} := \phi^{0.01j}(x_i^{(0)}),$$

for  $i = 1, 2, \dots, M$  and  $j = 1, 2, 3, 4$ . Then, using the finite difference method [20], we define

$$\begin{aligned} y_i^{(0)} &:= -\frac{25}{12}x_i^{(0)} + 4x_i^{(1)} - 3x_i^{(2)} + \frac{4}{3}x_i^{(3)} - \frac{1}{4}x_i^{(4)}, \\ y_i^{(1)} &:= -\frac{1}{4}x_i^{(0)} - \frac{5}{6}x_i^{(1)} + \frac{3}{2}x_i^{(2)} - \frac{1}{2}x_i^{(3)} + \frac{1}{12}x_i^{(4)} \\ y_i^{(2)} &:= \frac{1}{12}x_i^{(4)} - \frac{2}{3}x_i^{(3)} + \frac{2}{3}x_i^{(1)} - \frac{1}{12}x_i^{(0)}, \\ y_i^{(3)} &:= \frac{1}{4}x_i^{(4)} + \frac{5}{6}x_i^{(3)} - \frac{3}{2}x_i^{(2)} + \frac{1}{2}x_i^{(1)} - \frac{1}{12}x_i^{(0)}, \\ y_i^{(4)} &:= \frac{25}{12}x_i^{(4)} - 4x_i^{(3)} + 3x_i^{(2)} - \frac{4}{3}x_i^{(1)} + \frac{1}{4}x_i^{(0)}. \end{aligned}$$

for  $i = 1, \dots, M$  as approximations of the velocities  $F(x_i^{(0)}), F(x_i^{(1)}), \dots, F(x_i^{(4)})$ . Then, we define  $X := (x_i^{(j)})_{i=1, \dots, M, j=0, \dots, 4}$  and  $Y := (y_i^{(j)})_{i=1, \dots, M, j=0, \dots, 4}$  (thus,  $N = 540$ ). We set  $x_0$  as an element of  $\{x_i^{(j)}\}_{i=1, \dots, M, j=0, \dots, 4}$  closest to the mean of  $\{x_i^{(j)}\}_{i=1, \dots, M, j=0, \dots, 4}$ , and define  $y_0$  as the element of  $\{y_i^{(j)}\}_{i=1, \dots, M, j=0, \dots, 4}$  corresponding to  $x_0$ . Basically, the both kernels have the similar performance and reconstruct the original system with certain accuracy. However, when we use the Gaussian kernel, each component of the reconstructed system  $\widehat{F} = (\widehat{F}_1, \dots, \widehat{F}_d)$  is rapidly decaying, and we cannot predict the trajectory with an initial point far from the point  $x_0$ . We also note that the reconstruction algorithm works well in the case of  $\mu = 2$ , where we cannot judge whether the approximation works or not as long as we observe the computational result of the eigenvalues since the Perron–Frobenius operator  $A_F|_{V_{p,n}}$  is not diagonalizable and the computation of the eigenvalues gets computationally unstable as mentioned in Section 7.2.1.

Figure 14 describes the performance of Algorithm 7 for the van der Pol oscillator (7.7) for  $\mu = 1$ . We take common inputs  $m = 3$  and  $\sigma = 1$ . On the left figure, we set  $n = 6$ ,  $p = (0, 0)$ , and  $T_s = 0.5$ , and take 15 collections  $\{(x_i, x_i^+, x_i^{++})\}_{i=1}^{15}$  of snapshots at time 0,  $T_s$ ,  $2T_s$  of 15 trajectories with initial points sampled from the uniform distribution on  $[-1, 1]^2$ , namely  $x_i$ 's are the initial values and  $x_i^+ = \phi^{T_s}(x_i)$  and  $x_i^{++} = \phi^{2T_s}(x_i)$  hold. We set  $X := (x_1, \dots, x_{15}, x_1^+, \dots, x_{15}^+)$  and  $Y := (x_1^+, \dots, x_{15}^+, x_1^{++}, \dots, x_{15}^{++})$ . On the middle figure, we set  $n = 12$ ,  $p = (0, 0)$ ,  $T_s = 1.0$ , and take 50 pairs of data  $\{(x_i, x_i^+)\}_{i=1}^{50}$  with  $x_i^+ = \phi^{T_s}(x_i)$ . We set  $n = 20$ ,  $T_s = 0.5$ , and take 2000 pairs of data  $\{(x_i, x_i^+)\}_{i=1}^{2000}$  with  $x_i^+ = \phi^{T_s}(x_i)$  in the right figure. The sampling period is longer than the cases in Figure 13, our method has still high accuracy of reconstruction. This algorithm basically has significantly better performance than above algorithms. However, it seems to be essential to know the position of the equilibrium point in advance. In fact, if we take  $p = (0.5, 0.5)$ , non-equilibrium point, as in the right figure of Figure 14, the reconstructed system is distorted, and it is hard to correct it.

### 7.3.2 The Lorenz system

Here, we consider the Lorenz equation defined by

$$\begin{aligned} x' &= 10(y - x), \\ y' &= x(28 - z) - y, \\ z' &= xy - \frac{8}{3}z. \end{aligned} \tag{7.11}$$

<sup>3</sup>We will use the exponential kernel in Algorithm 7 as the input  $k$  when we perform the numerical simulations in Sections 7.3.1 and 7.3.2.

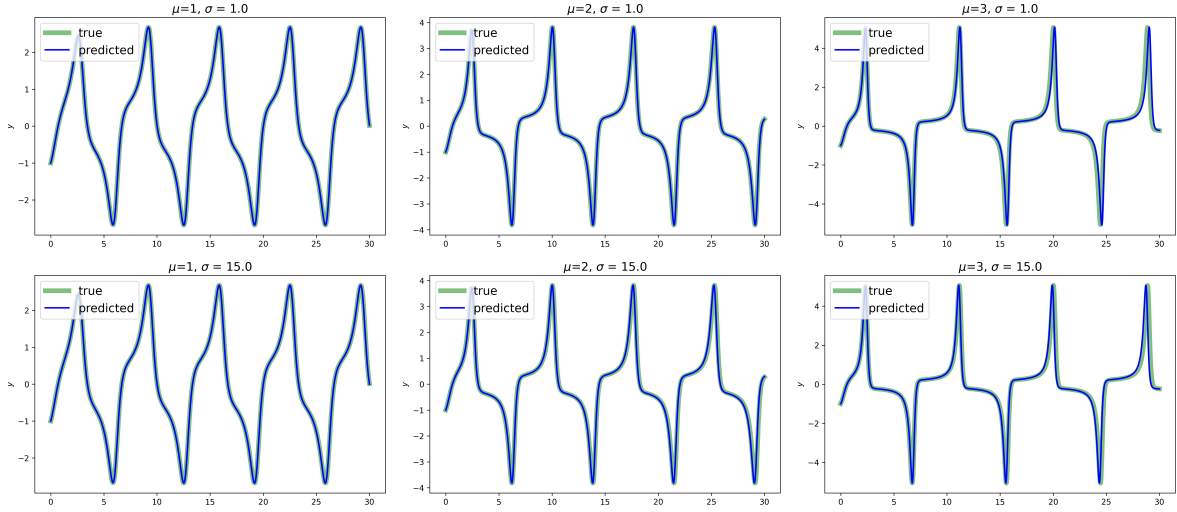


Figure 13: Data-driven reconstruction of the van der Pol oscillator (7.7) for  $\mu = 1$  (left), 2 (middle), 3 (right) using Algorithm 6 with the exponential kernel  $e^{x^\top y}$  (top row) and the Gaussian kernel  $e^{|x-y|^2/15^2}$  (bottom row) with input  $m = 5, n = 7$ . The data is composed of 100 collections of 5 snapshots at times  $0, 0.01, 0.02, \dots, 0.04$  of a trajectory with an initial point sampled from the uniform distribution on  $[0, 1]^2$  and the velocities at these points in the collections, computed using the finite difference method. The blue thin curves are the graphs of  $y$ -axis of the the predicted trajectories and green thick curves are that of true ones. The initial point for each curve is  $(-1, -1) \in \mathbb{R}^2$ .

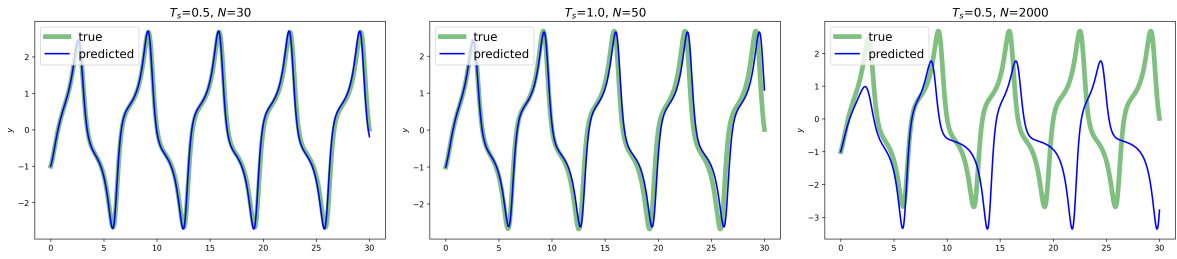


Figure 14: Data-driven reconstruction of the van der Pol oscillator (7.7) for  $\mu = 1$  using Algorithm 7 with input  $k(x, y) = e^{x^\top y}$ ,  $\sigma = 1$ ,  $m = 3$ , and  $n = 6$  (left),  $n = 12$  (middle), or  $n = 20$  (right). The data is composed of  $N$  pairs of data  $(x_i, y_i)$  with  $y_i = \phi^{T_s}(x_i)$  (see the text for more details), where  $(T_s, N) = (0.5, 30)$  (left),  $(1.0, 50)$  (middle), and  $(0.5, 2000)$  (right). We take  $p$  as the origin  $(0, 0)$  for the left and middle figures, but take  $p = (0.5, 0.5)$  for the right figure.



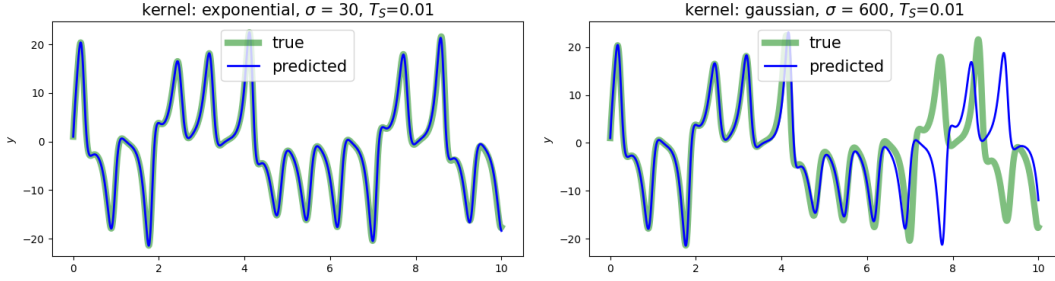


Figure 15: Data-driven reconstruction of the Lorenz attractor (7.11) using Algorithm 6 with the exponential kernel of  $\sigma = 30$  (left) and the Gaussian kernel of  $\sigma = 600$  (right) with input  $(m, n) = (2, 4)$  (left) and  $(2, 5)$  (right). The data is composed of 50 collections of 10 snapshots at times  $0, 0.01, 0.02, \dots, 0.09$  of trajectories with initial points sampled from the uniform distribution on  $[-10, 10]^3$  and the velocities at these points in the collections, computed using the finite difference method of order 10. The blue thin curves are the graphs of  $y$ -axis of the predicted trajectories and green thick curves are that of true ones. The initial point for each curve is  $(10, 1, 10) \in \mathbb{R}^3$ .

Figure 15 describes the performance of Algorithm 6 for the Lorenz system (7.11). We take  $M = 50$  samples  $x_1^{(0)}, \dots, x_M^{(0)}$  from the uniform distribution on  $[-10, 10]^3$ , and define

$$x_i^{(j)} := \phi^{0.01j}(x_i^{(0)}),$$

for  $i = 1, 2, \dots, M$  and  $j = 1, \dots, 9$ . Then, using the finite difference method [20] of order 10, there exist rational numbers  $c_k^{ij}$  ( $k = 1, \dots, 9$ ) such that

$$y_i^{(j)} := \frac{1}{0.01} \sum_{k=0}^9 c_k^{ij} x_i^{(j)}$$

provides suitable approximations of the velocities  $F(x_i^{(j)})$ . Then, we set  $X := (x_i^{(j)})_{i=1, \dots, M, j=0, \dots, 9}$  and  $Y := (y_i^{(j)})_{i=1, \dots, M, j=0, \dots, 9}$  (thus  $N = 500$ ). We set  $x_0$  as an element of  $\{x_i^{(j)}\}_{i=1, \dots, M, j=0, \dots, 9}$  closest to the mean of  $\{x_i^{(j)}\}_{i=1, \dots, M, j=0, \dots, 9}$ , and  $y_0$  as an element of  $\{y_i^{(j)}\}_{i=1, \dots, M, j=0, \dots, 9}$  corresponding to  $x_0$ . On the left figure, we use the exponential kernel, and take  $m = 2$ ,  $n = 4$ , and  $\sigma = 30$ , while on the right figure, we use the Gaussian kernel, and take  $m = 2$ ,  $n = 5$ , and  $\sigma = 600$ .

Figure 16 describes the performance of Algorithm 7 for the Lorenz system (7.11). We set  $p = (0, 0, 0)$  as the equilibrium point. On the left figure, we set  $\sigma = 80$ ,  $m = 4$ ,  $n = 11$ , and  $T_s = 0.033$ , and take 20 collections  $\{(x_i^{(0)}, \dots, x_i^{(15)})\}_{i=1}^{20}$  of snapshots at times  $0, T_s, \dots, 15T_s$  of trajectories with initial points sampled from the uniform distribution on  $[-20, 20]^3$ , namely  $x_i^{(j)} = \phi^{jT_s}(x_i^{(0)})$  holds. We set  $X = (x_1^{(0)}, \dots, x_{20}^{(0)}, x_1^{(1)}, \dots, x_{20}^{(14)})$  and  $Y = (x_1^{(1)}, \dots, x_{20}^{(1)}, x_1^{(2)}, \dots, x_{20}^{(15)})$ . On the right figure, we set  $\sigma = 20$ ,  $m = 2$ ,  $n = 10$ , and  $T_s = 0.1$ . We take 300 samples  $\{x_i\}_{i=1}^{300}$  from the uniform distribution  $[-10, 10]^3$ , and define  $y_i = \phi^{T_s}(x_i)$ . Even in highly complex and chaotic system like the Lorenz system, we see that the original system can be reconstructed from data with a small numbers of samples with relatively long sampling periods, similar to the case with the van der Pol oscillator.

**Remark 7.10.** On the left figures of Figure 14 and Figure 16, we use the same data as in [48], and our method also has the same or better performance than the lifting method proposed in [48]. Our approaches approximate the operators using the space of the intrinsic observables in RKHS defined via the jets, independent of data, and this constitutes an essential difference from their lifting method.

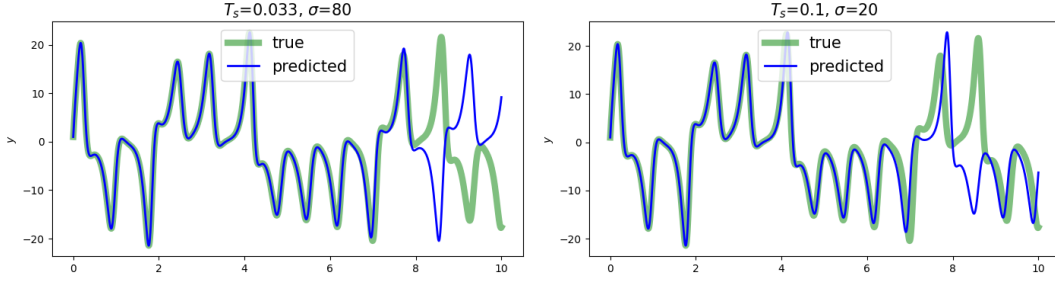


Figure 16: Data-driven reconstruction of the Lorenz attractor (7.11) using Algorithm 7 with the exponential kernel of  $\sigma = 80$  (left) and  $\sigma = 20$  (right) with input  $(m, n) = (4, 11)$  (left) and  $(2, 10)$  (right). The  $N = 300$  pairs  $(x_i, y_i)$  ( $i = 1, \dots, N$ ) are in the form of  $y_i = \phi^{T_s}(x_i)$  (see the text for more details), where  $T_s = 0.033$  (left) and  $0.1$  (right). The blue thin curves are the graphs of  $y$ -axis of the predicted trajectories and green thick curves are that of true ones. The initial point for each curve is  $(10, 1, 10) \in \mathbb{R}^3$ .

#### 7.4 Relation among Jet DMD, Extended DMD, and Kernel DMD

The matrix  $\mathbf{V}_n^Y(\mathbf{V}_n^X)^\dagger$  appearing on the left-hand side of (7.4) in Algorithm 1 coincides with the transpose of the matrix that appears in EDMD [77] using  $\{v_{p,\alpha}\}_{|\alpha| \leq n}$  as the observable functions. In the framework EDMD, they regard the matrix  $\mathbf{V}_n^Y(\mathbf{V}_n^X)^\dagger$  as the correct approximation of the Koopman operator. However, as shown in Theorem 3.5, this matrix will not correctly approximate the operator (see the discussion after Theorem 3.5). Therefore, JetDMD provides an appropriate refinement of EDMD. While JetDMD involves only a very simple procedure of truncation to a leading principal submatrix of the matrix  $\mathbf{V}_n^Y(\mathbf{V}_n^X)^\dagger$ , it enables a clear depiction of the eigenvalues as in Figure 1 in Section 1.

When the positive definite kernel  $k(x, y)$  is the exponential kernel  $e^{x^\top y}$  and the dynamical system has a fixed point at origin, it corresponds to the EDMD with the monomials. According to the Stone–Weierstrass theorem, any continuous function can be approximated with polynomials on a compact set with arbitrary precision, providing a certain theoretical justification to the use of polynomials. However, in the context of JetDMD, the polynomials appear much more naturally and canonically through a process involving the jets and the RKHS as in Section 2. Furthermore, by considering rigged Hilbert space, the Koopman operator approximated by JetDMD can be clearly understood as an approximation of the extended Koopman operator explained in Section 4.

We also provide a remark on the relation between JetDMD and the Kernel DMD (KDMD) [38, 78]. We impose the condition that  $r_n = \dim V_{p,n}$  is less than or equal to the number  $N$  of samples in the framework of JetDMD, but the matrix  $\mathbf{V}_n^Y(\mathbf{V}_n^X)^\dagger$  itself may be considered on the opposite case, namely the case of  $r_n > N$ . In this case, the eigenvalues of  $\mathbf{V}_n^Y(\mathbf{V}_n^X)^\dagger$  approximately correspond to those computed by KDMD. In fact, assume that  $r_n > N$  and  $\mathbf{V}_n^X$  is a full column rank matrix. By [26], we have

$$(\mathbf{V}_n^X)^\dagger \mathbf{G}_n^{1/2} = (\mathbf{G}_n^{-1/2} \mathbf{V}_n^X)^\dagger = ((\mathbf{V}_n^X)^* \mathbf{G}_n^{-1} \mathbf{V}_n^X)^{-1} (\mathbf{V}_n^X)^* \mathbf{G}_n^{-1/2}.$$

Thus, we have

$$(\mathbf{V}_n^X)^\dagger \mathbf{V}_n^Y = ((\mathbf{V}_n^X)^* \mathbf{G}_n^{-1} \mathbf{V}_n^X)^{-1} (\mathbf{V}_n^X)^* \mathbf{G}_n^{-1} \mathbf{V}_n^Y.$$

By Proposition 3.4, we see that

$$(\mathbf{V}_n^X)^* \mathbf{G}_n^{-1} \mathbf{V}_n^Y = \left( \overline{\langle \pi_n k_{x_i}, \pi_n k_{y_j} \rangle_H} \right)_{i,j=1,\dots,N} \xrightarrow[n \rightarrow \infty]{} (k(y_i, x_j))_{i,j=1,\dots,N}.$$

By [32, Theorem 1.3.22.], the nonzero eigenvalues of  $\mathbf{V}_n^Y(\mathbf{V}_n^X)^\dagger$  coincide with those of  $(\mathbf{V}_n^X)^\dagger \mathbf{V}_n^Y$ . Therefore, we conclude that the computation of the eigenvalues of  $\mathbf{V}_n^Y(\mathbf{V}_n^X)^\dagger$  is essentially equivalent to that of  $(k(x_i, x_j))_{i,j=1,\dots,N}^{-1} (k(y_i, x_j))_{i,j=1,\dots,N}$ , that is the objective matrix of the KDMD.

## 8 Conclusion

This paper introduces a novel approach to estimating the Koopman operator on the RKHS, through the development of the JetDMD. In the context of data analysis, the  $L^2$ -space has been the central stage for Koopman analysis, originated from Koopman’s work. The Koopman operator on RKHS and its application in data analysis are relatively new fields. Through this paper, we intend to show that the RKHS is also quite promising venue for developing the theory of the Koopman operator. In fact, we present accurate convergence results, backing the performance of JetDMD for RKHSs for two positive definite kernels, the exponential kernel and Gaussian kernel. We also show that some existing methods, such as EDMD with monomials, is considered within the framework of RKHS. Furthermore, we delve into the spectral analysis of Koopman operator. More precisely, we introduce the notion of the extended Koopman operator in the framework of the rigged Hilbert space to achieve the deeper understanding of the “Koopman eigenfunctions”, leading to a promising method to analyze the spectrum of the Koopman operator.

Although we only consider the the exponential kernel and Gaussian kernel, exploring the performance and properties of JetDMDs with other kernels is also quite an important challenge. This paper also clarifies to which the “Koopman eigenfunction” belongs by regarding it as an eigenvector of the extended Koopman operator. However, the definition of the extended Koopman operator is rather abstract, and its theoretical interpretation still is needed to be explored. Additionally, elucidating the relationship between the eigenvectors of the extended Koopman operator and the dynamical systems is also a significant problem since the former must capture some important characteristics of dynamical system although it is not an eigenfunction in the usual sense.

In conclusion, we believe that this paper significantly advances the study of Koopman operators on RKHSs. We hope the ideas and methodologies presented in this paper will serve as a foundation for further development of Koopman operators.

## References

- [1] Ian Abraham and Todd D. Murphey. Active learning of dynamics for data-driven control using Koopman operators. *IEEE Transactions on Robotics*, 35(5):1071–1083, 2019.
- [2] Mustaffa Alfatlawi and Vaibhav Srivastava. An incremental approach to online dynamic mode decomposition for time-varying systems with applications to eeg data modeling. *Journal of Computational Dynamics*, 7(2):209–241, 2020.
- [3] N. Aronszajn. Theory of reproducing kernels. *Transactions of the American Mathematical Society*, 68(3):337–404, 1950.
- [4] Erik Berger, Mark Sastuba, David Vogt, Bernhard Jung, and Heni Ben Amor. Estimation of perturbations in robotic behavior using dynamic mode decomposition. *Advanced Robotics*, 29(5):331–343, 2015.
- [5] Petar Bevanda, Max Beier, Armin Lederer, Stefan Georg Sosnowski, Eyke Hüllermeier, and Sandra Hirche. Koopman kernel regression. In *Thirty-seventh Conference on Neural Information Processing Systems*, 2023.
- [6] A. Bohm, A. Böhm, M. Gadella, and J.D. Dollard. *Dirac Kets, Gamow Vectors, and Gel’fand Triplets: The Rigged Hilbert Space Formulation of Quantum Mechanics : Lectures in Mathematical Physics at the University of Texas at Austin*. Lecture notes in physics. Springer-Verlag, 1989.
- [7] Armand Borel. *Linear algebraic groups*, volume 126 of *Graduate Texts in Mathematics*. Springer-Verlag, New York, second edition, 1991.
- [8] Daniel Bruder, Xun Fu, R. Brent Gillespie, C. David Remy, and Ram Vasudevan. Koopman-based control of a soft continuum manipulator under variable loading conditions. *IEEE Robotics and Automation Letters*, 6(4):6852–6859, 2021.

- [9] Daniel Bruder, Brent Gillespie, C. David Remy, and Ram Vasudevan. Modeling and control of soft robots using the Koopman operator and model predictive control. In *Proceedings of Robotics: Science and Systems*, Freiburg/Breisgau, Germany, June 2019.
- [10] Bingni W. Brunton, Lise A. Johnson, Jeffrey G. Ojemann, and J. Nathan Kutz. Extracting spatial–temporal coherent patterns in large-scale neural recordings using dynamic mode decomposition. *Journal of Neuroscience Methods*, 258:1–15, 2016.
- [11] Steven L. Brunton, Marko Budišić, Eurika Kaiser, and J. Nathan Kutz. Modern Koopman theory for dynamical systems. *SIAM Review*, 64(2):229–340, 2022.
- [12] Brent J. Carswell, Barbara D. MacCluer, and Alex Schuster. Composition operators on the Fock space. *Acta Scientiarum Mathematicarum*, 69(3-4):871–887, 2003.
- [13] Hayato Chiba. A spectral theory of linear operators on rigged Hilbert spaces under analyticity conditions. *Advances in Mathematics*, 273:324–379, 2015.
- [14] Hayato Chiba, Masahiro Ikeda, and Isao Ishikawa. Generalized eigenvalues of the Perron–Frobenius operators of symbolic dynamical systems. *SIAM Journal on Applied Dynamical Systems*, 22(4):2825–2855, 2023.
- [15] Matthew J. Colbrook, Lorna J. Ayton, and Máté Szőke. Residual dynamic mode decomposition: robust and verified Koopmanism. *Journal of Fluid Mechanics*, 955:A21, 2023.
- [16] Matthew J. Colbrook and Alex Townsend. Rigorous data-driven computation of spectral properties of Koopman operators for dynamical systems. *Communications on Pure and Applied Mathematics*, 77(1):221–283, 2024.
- [17] Carl C. Cowen and Barbara D. Maccluer. *Composition Operators on Spaces of Analytic Functions*. CRC Press, Boca Raton, 1995.
- [18] Suddhasattwa Das and Dimitrios Giannakis. Koopman spectra in reproducing kernel Hilbert spaces. *Applied and Computational Harmonic Analysis*, 49(2):573–607, 2020.
- [19] Philip J. Davis and Philip Rabinowitz. *Methods of numerical integration*. Dover Publications, Inc., Mineola, NY, 2007. Corrected reprint of the second (1984) edition.
- [20] Bengt Fornberg. Generation of finite difference formulas on arbitrarily spaced grids. *Mathematics of Computation*, 51(184):699–706, 1988.
- [21] Keisuke Fujii and Yoshinobu Kawahara. Dynamic mode decomposition in vector-valued reproducing kernel Hilbert spaces for extracting dynamical structure among observables. *Neural Networks*, 117:94–103, 2019.
- [22] I.M. Gel’fand and G.E. Shilov. *Generalized Functions, Volume 2: Spaces of Fundamental and Generalized Functions*. AMS Chelsea Publishing. American Mathematical Society, 2016.
- [23] I.M. Gel’fand and N.Y. Vilenkin. *Generalized Functions: Applications of Harmonic Analysis*. Generalized functions. Elsevier Science, 2014.
- [24] Dimitrios Giannakis, Yuka Hashimoto, Masahiro Ikeda, Isao Ishikawa, and Joanna Slawinska. Koopman spectral analysis of skew-product dynamics on Hilbert  $C^*$ -modules. *arXiv: 2307.08965*, 2023.
- [25] Dimitrios Giannakis, Anastasiya Kolchinskaya, Dmitry Krasnov, and Jörg Schumacher. Koopman analysis of the long-term evolution in a turbulent convection cell. *Journal of Fluid Mechanics*, 847:735–767, 2018.
- [26] T. N. E. Greville. Note on the generalized inverse of a matrix product. *SIAM Review*, 8(4):518–521, 1966.
- [27] Yuka Hashimoto, Isao Ishikawa, Masahiro Ikeda, Fuyuta Komura, Takeshi Katsura, and Yoshinobu Kawahara. Reproducing kernel Hilbert  $C^*$ -module and kernel mean embeddings. *Journal of Machine Learning Research*, 22(267):1–56, 2021.

- [28] Yuka Hashimoto, Isao Ishikawa, Masahiro Ikeda, Yoichi Matsuo, and Yoshinobu Kawahara. Krylov subspace method for nonlinear dynamical systems with random noise. *Journal of Machine Learning Research*, 21(172):1–29, 2020.
- [29] Yuka Hashimoto, Sho Sonoda, Isao Ishikawa, Atsushi Nitanda, and Taiji Suzuki. Koopman-based generalization bound: New aspect for full-rank weights. In *The Twelfth International Conference on Learning Representations*, 2024.
- [30] Nicholas J. Higham. *Functions of Matrices*. Society for Industrial and Applied Mathematics, 2008.
- [31] Thomas Hofmann, Bernhard Schölkopf, and Alexander J. Smola. Kernel methods in machine learning. *The Annals of Statistics*, 36(3):1171 – 1220, 2008.
- [32] Roger A. Horn and Charles R. Johnson. *Matrix analysis*. Cambridge University Press, Cambridge, second edition, 2013.
- [33] Masahiro Ikeda, Isao Ishikawa, and Yoshihiro Sawano. Boundedness of composition operators on reproducing kernel Hilbert spaces with analytic positive definite functions. *Journal of Mathematical Analysis and Applications*, 511(1):126048, 2022.
- [34] Masahiro Ikeda, Isao Ishikawa, and Corbinian Schlosser. Koopman and Perron–Frobenius operators on reproducing kernel Banach spaces. *Chaos: An Interdisciplinary Journal of Nonlinear Science*, 32(12):123143, 12 2022.
- [35] Masahiro Ikeda, Isao Ishikawa, and Koichi Taniguchi. Boundedness of composition operators on higher order besov spaces in one dimension. *Mathematische Annalen*, May 2023.
- [36] Isao Ishikawa. Bounded composition operators on functional quasi-banach spaces and stability of dynamical systems. *Advances in Mathematics*, 424:109048, 2023.
- [37] A. A. Kaptanoglu, K. D. Morgan, C. J. Hansen, and S. L. Brunton. Characterizing magnetized plasmas with dynamic mode decomposition. *Physics of Plasmas*, 27(3):032108, 03 2020.
- [38] Yoshinobu Kawahara. Dynamic mode decomposition with reproducing kernels for Koopman spectral analysis. In D. Lee, M. Sugiyama, U. Luxburg, I. Guyon, and R. Garnett, editors, *Advances in Neural Information Processing Systems*, volume 29. Curran Associates, Inc., 2016.
- [39] Stefan Klus, Feliks Nüske, and Sebastian Peitz. Koopman analysis of quantum systems. *Journal of Physics A: Mathematical and Theoretical*, 55(31):314002, jul 2022.
- [40] Stefan Klus, Ingmar Schuster, and Krikamol Muandet. Eigendecompositions of transfer operators in reproducing kernel Hilbert spaces. *Journal of Nonlinear Science*, 30(1):283–315, Feb 2020.
- [41] Ivan Kolář, Peter W. Michor, and Jan Slovák. *Natural operations in differential geometry*. Springer-Verlag, Berlin, 1993.
- [42] Hikosaburo Komatsu. Projective and injective limits of weakly compact sequences of locally convex spaces. *Journal of the Mathematical Society of Japan*, 19(3):366 – 383, 1967.
- [43] B. O. Koopman. Hamiltonian systems and transformation in Hilbert space. *Proc. Natl. Acad. Sci. USA*, 17(5):315318, 1931.
- [44] Milan Korda and Igor Mezić. On convergence of extended dynamic mode decomposition to the Koopman operator. *Journal of Nonlinear Science*, 28(2):687–710, Apr 2018.
- [45] Vladimir R Kostic, Karim Lounici, Pietro Novelli, and massimiliano pontil. Sharp spectral rates for Koopman operator learning. In *Thirty-seventh Conference on Neural Information Processing Systems*, 2023.
- [46] Jordan Mann and J. Nathan Kutz. Dynamic mode decomposition for financial trading strategies. *Quantitative Finance*, 16(11):1643–1655, 2016.

- [47] A. Martineau. Sur la topologie des espaces de fonctions holomorphes. *Mathematische Annalen*, 163:62–88, 1966.
- [48] Alexandre Mauroy and Jorge Goncalves. Koopman-based lifting techniques for nonlinear systems identification. *IEEE Transactions on Automatic Control*, 65(6):2550–2565, 2020.
- [49] Alexandre Mauroy and Igor Mezić. A spectral operator-theoretic framework for global stability. In *52nd IEEE Conference on Decision and Control*, pages 5234–5239, 2013.
- [50] Alexandre Mauroy and Igor Mezić. Global stability analysis using the eigenfunctions of the Koopman operator. *IEEE Transactions on Automatic Control*, 61(11):3356–3369, Nov 2016.
- [51] Giacomo Meanti, Antoine Chatalic, Vladimir R Kostic, Pietro Novelli, Massimiliano Pontil, and Lorenzo Rosasco. Estimating Koopman operators with sketching to provably learn large scale dynamical systems. In *Thirty-seventh Conference on Neural Information Processing Systems*, 2023.
- [52] Igor Mezić. Spectral properties of dynamical systems, model reduction and decompositions. *Nonlinear Dynamics*, 41(1):309–325, Aug 2005.
- [53] Igor Mezić. Analysis of fluid flows via spectral properties of the Koopman operator. *Annual Review of Fluid Mechanics*, 45(1):357–378, 2013.
- [54] Igor Mezić. Spectrum of the Koopman operator, spectral expansions in functional spaces, and state-space geometry. *Journal of Nonlinear Science*, 30(5):2091–2145, Oct 2020.
- [55] Igor Mezić and Andrzej Banaszuk. Comparison of systems with complex behavior. *Physica D: Nonlinear Phenomena*, 197(1):101–133, 2004.
- [56] Krikamol Muandet, Kenji Fukumizu, Bharath Sriperumbudur, and Bernhard Schölkopf. Kernel mean embedding of distributions: A review and beyond. *Foundations and Trends® in Machine Learning*, 10(1-2):1–141, 2017.
- [57] Juan A. Navarro González and Juan B. Sancho de Salas.  *$C^\infty$ -differentiable spaces*, volume 1824 of *Lecture Notes in Mathematics*. Springer-Verlag, Berlin, 2003.
- [58] Eric A. Nordgren. Composition operators. *Canadian Journal of Mathematics*, 20:442–449, 1968.
- [59] Motoya Ohnishi, Isao Ishikawa, Kendall Lowrey, Masahiro Ikeda, Sham Kakade, and Yoshinobu Kawahara. Koopman spectrum nonlinear regulator and provably efficient online learning. *arXiv: 2106.15775*, 2021.
- [60] Joshua L. Proctor and Philip A. Eckhoff. Discovering dynamic patterns from infectious disease data using dynamic mode decomposition. *International Health*, 7(2):139–145, 02 2015.
- [61] Clarence W. Rowley, Igor Mezić, Shervin Bagheri, Philipp Schlatter, and Dan S. Henningson. Spectral analysis of nonlinear flows. *Journal of Fluid Mechanics*, 641:115–127, 2009.
- [62] John V. Ryff. Subordinate  $H^p$  functions. *Duke Mathematical Journal*, 33(2):347 – 354, 1966.
- [63] Saburo Saitoh and Yoshihiro Sawano. *Theory of reproducing kernels and applications*, volume 44 of *Developments in Mathematics*. Springer, Singapore, 2016.
- [64] Peter J. Schmid. Dynamic mode decomposition of experimental data. In *Eighth International Symposium on Particle Image Velocimetry (PIV09)*, August 2009.
- [65] Peter J. Schmid. Dynamic mode decomposition of numerical and experimental data. *Journal of Fluid Mechanics*, 656:5–28, 2010.
- [66] Peter J. Schmid. Dynamic mode decomposition and its variants. *Annual Review of Fluid Mechanics*, 54(1):225–254, 2022.
- [67] Julia Slipantschuk, Oscar F. Bandtlow, and Wolfram Just. Dynamic mode decomposition for analytic maps. *Communications in Nonlinear Science and Numerical Simulation*, 84:105179, 2020.

- [68] Jan Stochel and Jerzy Bartłomiej Stochel. Composition operators on Hilbert spaces of entire functions with analytic symbols. *Journal of Mathematical Analysis and Applications*, 454(2):1019–1066, 2017.
- [69] Yoshihiko Susuki and Igor Mezic. Nonlinear Koopman modes and coherency identification of coupled swing dynamics. *IEEE Transactions on Power Systems*, 26(4):1894–1904, 2011.
- [70] Yoshihiko Susuki, Igor Mezić, and Takashi Hikihara. Coherent swing instability of power grids. *Journal of Nonlinear Science*, 21(3):403–439, Jun 2011.
- [71] Gábor Szegő. *Orthogonal polynomials*, volume Vol. XXIII of *American Mathematical Society Colloquium Publications*. American Mathematical Society, Providence, RI, fourth edition, 1975.
- [72] Naoya Takeishi, Keisuke Fujii, Koh Takeuchi, and Yoshinobu Kawahara. Discriminant dynamic mode decomposition for labeled spatiotemporal data collections. *SIAM Journal on Applied Dynamical Systems*, 21(2):1030–1058, 2022.
- [73] Naoya Takeishi and Yoshinobu Kawahara. Learning dynamics models with stable invariant sets. *Proceedings of the AAAI Conference on Artificial Intelligence*, 35(11):9782–9790, May 2021.
- [74] Naoya Takeishi, Yoshinobu Kawahara, and Takehisa Yairi. Learning koopman invariant subspaces for dynamic mode decomposition. In I. Guyon, U. Von Luxburg, S. Bengio, H. Wallach, R. Fergus, S. Vishwanathan, and R. Garnett, editors, *Advances in Neural Information Processing Systems*, volume 30. Curran Associates, Inc., 2017.
- [75] Naoya Takeishi, Yoshinobu Kawahara, and Takehisa Yairi. Subspace dynamic mode decomposition for stochastic koopman analysis. *Physical Review E*, 96(3):033310, Sep 2017.
- [76] Roy Taylor, J. Nathan Kutz, Kyle Morgan, and Brian A. Nelson. Dynamic mode decomposition for plasma diagnostics and validation. *Review of Scientific Instruments*, 89(5):053501, 05 2018.
- [77] Matthew O. Williams, Ioannis G. Kevrekidis, and Clarence W. Rowley. A data-driven approximation of the Koopman operator: Extending dynamic mode decomposition. *Journal of Nonlinear Science*, 25(6):1307–1346, Dec 2015.
- [78] Matthew O. Williams, Clarence W. Rowley, and Ioannis G. Kevrekidis. A kernel-based method for data-driven koopman spectral analysis. *Journal of Computational Dynamics*, 2(2):247–265, 2015.
- [79] Kôzaku Yosida. *Functional analysis*, volume 123 of *Grundlehren der Mathematischen Wissenschaften*. Springer-Verlag, Berlin-New York, sixth edition, 1980.
- [80] Kahe Zhu. *Operator theory in Function spaces: second edition*, volume 138. Mathematical Surveys and Monographs, 2007.
- [81] Kehe Zhu. *Analysis on Fock spaces*, volume 263 of *Graduate Texts in Mathematics*. Springer, New York, 2012.